

Industria Textilă

ISSN 1222-5347 (49-96)

2/2010

Revistă cotate ISI și inclusă în Master Journal List a Institutului pentru Știința Informării din Philadelphia – S.U.A., începând cu vol. 58, nr. 1/2007/

ISI rated magazine, included in the ISI Master Journal List of the Institute of Science Information, Philadelphia, USA, starting with vol. 58, no. 1/2007

Editată în 6 nr./an, indexată și recenzată în:/

Edited in 6 issues per year, indexed and abstracted in:

Science Citation Index Expanded (SciSearch®), Materials Science Citation Index®, Journal Citation Reports/Science Edition, World Textile Abstracts, Chemical Abstracts, VINITI

COLEGIUL DE REDACȚIE:

Dr. ing. EMILIA VISILEANU
cerc. șt. pr. I – EDITOR

Institutul Național de Cercetare-Dezvoltare
pentru Textile și Pielărie – București

Prof. dr. ing. CRIȘAN POPESCU

Institutul German de Cercetare a Lăinii – Aachen

Cerc. șt. pr. I ERIC BOUDON

Institutul Francez de Textile-Îmbrăcăminte –
Paris

Prof. dr. ing. DUMITRU LIUȚE
Universitatea Tehnică Gh. Asachi – Iași

Prof. dr. ing. AURELIA GRIGORIU
Universitatea Tehnică Gh. Asachi – Iași

Prof. dr. ing. COSTEA BUDULAN
Universitatea Tehnică Gh. Asachi – Iași

Prof. dr. ing. VALERIA GRIBINCEA
Universitatea Tehnică Gh. Asachi – Iași

Ing. VASILE MIRCIU

director general adjunct

Direcția Generală Politici Industriale –
Ministerul Economiei și Comerțului

Ing. VASILE PĂTRÂNIOIU – consilier
Ministerul Economiei și Comerțului

Dr. ing. ION PIRNA – cerc. șt. pr. I
Institutul Național de Cercetare-Dezvoltare
pentru Mașini Agricole – București

Prof. dr. ing. EROL MURAD

Universitatea Politehnică – București

Dr. ing. MIHAELA IORDĂNESCU

cerc. șt. pr. I – RENAR

Conf. dr. CRIȘAN ALBU

Academia de Studii Economice – București

Dr. ing. CARMEN GHITULEASA

cerc. șt. pr. II

Institutul Național de Cercetare-Dezvoltare
pentru Textile și Pielărie – București

Prof. ing. ARISTIDE DODU

cerc. șt. pr. gr. I

Membu de onoare al Academiei
de Științe Tehnice din România

Ec. AURELIENȚIU POPESCU

președinte executiv FEPAIUS

Prof. univ. dr. MARGARETA FLORESCU

Academia de Studii Economice – București

Conf. univ. dr. ing.

LUCIAN CONSTANTIN HANGANU

Universitatea Tehnică Gh. Asachi – Iași

HUI ZHANG, LIMIN ZHANG

Modificări structurale ale fibrelor de cânepă tratate cu chitosan și BTCA 51–56

RIZA ATAV, ABBAS YURDAKUL

Utilizarea dendrimerilor pentru optimizarea capacității de vopsire
a fibrelor de mohair și Angora la temperaturi scăzute 57–61

HÜSEYİN GAZI ORTLEK

Materiale de ecranare tip rețea ce oferă protecție electromagnetică 62–65

FAMING WANG, SHANYUAN WANG

Caracterizarea mărimii porilor la fibrele PET microporoase
cu structură tip fagure, prin utilizarea tehnicilor de prelucrare
a imaginii 66–69

**ALINA POPESCU, AURELIA GRIGORIU, CARMEN ZAHARIA,
RODICA MUREȘAN, AUGUSTIN MUREȘAN**

Modelarea matematică și optimizarea procesului tehnologic
de biocurățare a materialelor textile din bumbac 70–80

LUCICA CIOARĂ, IOAN CIOARĂ, DOINA TOMA

Relația structură-proprietăți pentru țesături antistatice,
destinate echipamentelor de protecție 81–85

**ȘTEFANIA GAVRILIU, MAGDALENA LUNGU, ELENA ENESCU,
LIANA GAVRILIU**

Nanopulbere compozită pentru textile antibacteriene 86–90

**CIPRIAN MURARIU, MARTA HARNAGEA, FLORENTINA HARNAGEA,
ROMEN BUTNARU, ALINA MURARIU**

Noi materiale biocompozite bazate pe celuloză regenerată,
utilizate la confecționarea branșurilor destinate diabeticilor 91–96

Industria textilă în lume

56, 61

Note economice

69

Recunoscută în România, în domeniul științelor ingineresti, de către
Consiliul Național al Cercetării Științifice din Învățământul Superior
(C.N.C.S.I.S.), în grupa A /

Acknowledged in Romania, in the engineering sciences domain,
by the National Council of the Scientific Research from the Higher Education
(CNCSIS), in group A

HUI ZHANG, LIMIN ZHANG	Structural changes of hemp fibres modified with chitosan and BTCA	Strukturelle Modifizierungen der Hanffaser veredelt mit Chitosan und BTCA	51
RIZA ATAV ABBAS YURDAKUL	The use of dendrimers to obtain low temperature dyeability on mohair and Angora fibers	Die Anwendung der Dendrimere für die Kapazitätsoptimierung der Mohair und Angore- Faserfärbung bei niedrigen Temperaturen	57
HÜSEYİN GAZI ORTLEK	Net curtain fabrics offering electromagnetic shielding	Netzabschirmungsmaterialien für den elektromagnetischen Schutz	62
FAMING WANG, SHANYUAN WANG	Characterization on pore size of honeycomb-patterned micro-porous PET fibers using image processing techniques	Die Charakterisierung der Porengröße bei den mikroporösen PET-Faser mit Wabenstruktur, durch Benutzung von Bildbearbeitungstechniken	66
ALINA POPESCU AURELIA GRIGORIU CARMEN ZAHARIA RODICA MUREȘAN AUGUSTIN MUREȘAN	Mathematical modelling and the technological process optimization for the bio-scouring of the cotton textile materials	Die mathematische Modellierung und die Optimierung des technologischen Prozesses für Bioreinigung der Baumwolltextilmaterialien	70
LUCICA CIOARĂ IOAN CIOARĂ DOINA TOMA	Structure-properties relationship of the antistatic woven fabrics for protective equipment application	Die Beziehung Struktur-Eigenschaften für antistatische Gewebe bestimmt der Protektionsanzüge	81
ȘTEFANIA GAVRILIU MAGDALENA LUNGU ELENA ENESCU LIANA GAVRILIU	Composite nanopowder for antibacterial textiles	Nanopulververbundstoffe für antibakterielle Textilien	86
CIPRIAN MURARIU MARTA HARNAGEA FLORENTINA HARNAGEA ROMEN BUTNARU ALINA MURARIU	New bio-composite materials based on regenerated cellulose used in making insoles for the diabetic foot	Neue Bioverbundwerkstoffe aus regenerierten Zellulose für die Herstellung von Einlagen für Diabetiker	91
INDUSTRIA TEXTILĂ ÎN LUME	Textile industry in the world	Die Textilindustrie in der Welt	56, 61
NOTE ECONOMICHE	Economic notes	Ökonomische Hinweise	69

ERATĂ/ERRATUM

For the paper, *Neuroprotective and consequent neurorehabilitative outcomes, in elderly with severe brain conditions, treated with neurotrophics: Actovegin and/or Cerebrolysin*, authors Onose G., Chedreanu D., Mihăescu A., Spircu T., Popescu C., Angheliescu A., Mardare D. C., Onose L., Mirea, A., Haras, M., Spînu, A., Andone, I., Popescu, C., published in *Proceedings from the national conference of neurosurgery and neurorehabilitation*, ISSN 2067-2322, pp. 161–167, the correct bibliography is the following one:

- [1] Onose, G. *Recuperare, Medicină Fizică și Balneoclimatologie*. Editura Medicală, vol. I, București, 2008
- [2] Onose, G. et al. *Neuroprotective and consequent neurorehabilitative clinical outcomes, in patients treated with the pleiotropic drug Cerebrolysin*. In: *Journal of Medicine and Life*, 2009, vol. II, issue 4, pp. 350–360
- [3] Blackman, S. *A matter of life and cell death: solidifying PARPōs role in DNA repair and apoptosis*. In: *The Scientist*, Philadelphia, 2005, 19: 22–23
- [4] Mureșanu, D. *Neuroprotection and neuroplasticity – two aspects of continuous process, genetically regulated and powered by neurotrophic factors*. Communication at the 6th AMN Congress, April 2008, Cluj-Napoca, Romania
- [5] Anderer, P., Saletu, B., Semlitsch, H. V., Pascual-Marqui, R. D. *Electrical sources of P300 event-related brain potentials by low resolution electromagnetic tomography. Effects of nootropic therapy in age-associated memory impairment*. In: *Neuropsychobiology*, 1998, 37: 28–35
- [6] Ziegler, D., Rathmann, W., Dickhaus, T. et al. KORA Study Group. *Prevalence of polyneuropathy in pre-diabetes and diabetes is associated with abdominal obesity and macroangiopathy: the MONICA/KORA Augsburg Surveys S2 and S3*. In: *Diabetes Care* 2008, 31: 464–469
- [7] Ziegler, D. et al. *Treatment of symptomatic polyneuropathy with Actovegin in type 2 diabetic patients*. In: *Diabetes Care*, August 2009, 32: 1479–1484
- [8] Apfel, S.C. et al. *Adhoc panel on endpoints for diabetic neuropathy trials. Positive neuropathic sensory symptoms as endpoints in diabetic neuropathy trials*. In: *Journal of Neurological Sciences*, 2001, 189: 3–5

REZUMAT – ABSTRACT – INHALTSANGABE

Modificări structurale ale fibrelor de cânepă tratate cu chitosan și BTCA

Scopul lucrării îl constituie modificarea fibrelor de cânepă cu ajutorul acidului butanetetracarboxilic (BTCA) și a chitosanului, cu o greutate moleculară mai mică de 10 000 și un grad de deacetilare de 90%, în vederea îmbunătățirii capacității de vopsire. Modificările structurale ale fibrelor de cânepă au fost caracterizate prin intermediul microscopiei electronice de scanare (SEM), spectroscopiei în infraroșu cu transformare Fourier (FT-IR), termogravimetriei (TG), calorimetriei diferențiale cu scanare (DSC) și difracției de raze X (XRD). Au fost studiate atât proprietățile de rezistență la alungire și la încovoiere, cât și gradul de alb ale materialului textil din cânepă, înainte și după tratare. Rezultatele au demonstrat că, în comparație cu fibra de cânepă netratată, rezistența termică a fibrei de cânepă tratată cu chitosan s-a îmbunătățit, iar procentul masei reziduale a crescut în intervalul de temperatură 25–550°C. De asemenea, a crescut gradul de cristalizare și, respectiv, cel de orientare. În cazul tratării cu chitosan a materialului din cânepă, s-a constatat o înrăutățire a rigidității și a rezistenței la alungire. Cuvinte-cheie: fibră de cânepă, structură, chitosan, BTCA

Structural changes of hemp fibres modified with chitosan and BTCA

The aim of this paper is to modify the hemp fibre with butanetetracarboxylic acid (BTCA) and chitosan of molecular weight less than 10,000 and degree of deacetylation 90%, to improve the dyeing ability. The structural changes in hemp fibres were characterized by scanning electron microscopy (SEM), Fourier transform Infrared spectroscopy (FT-IR), thermogravimetry (TG), differential scanning calorimetry (DSC) and X-ray diffraction (XRD). The tensile and bending properties, as well as whiteness of the hemp fabric were also studied before and after treatment. The results showed that, compared with the untreated hemp fibre, the thermal stability of chitosan treated hemp fibre was improved, and the percent residual weights increased in the range of temperature 25–550°C. The degrees of crystallization and orientation increased for chitosan treated hemp fabric, while the flexural stiffness and tensile properties became worse.

Key-words: hemp fibre, structure, chitosan, BTCA

Strukturelle Modifizierungen der Hanffaser veredelt mit Chitosan und BTCA

Der Zweck dieser Arbeit besteht in der Modifizierung der Hanffaser mit Hilfe der Butanetetracarbonsäure (BTCA) und Chitosan mit einem Molekulargewicht kleiner als 10.000 und einem Deacetylierungsgrad von 90%, im Sinne der Verbesserung der Farbeigenschaften. Die strukturelle Modifizierungen der Hanffaser wurden charakterisiert mit Hilfe der Elektronenmikroskopie mit Bildaufnahme (SEM), der Infrarot-Spektroskopie mit Fourier-Transformation (FT-IR), der Thermogravimetrie (TG), der differentiellen Kalorimetrie mit Bildaufnahme (DSC) und der X-Strahlendiffraktion (XRD). Es wurden sowohl die Eigenschaften bei Dehnung und Biegung, als auch der Weissgrad des Hanftextilmaterials, vor und nach der Veredelung untersucht. Die Ergebnisse zeigten, dass sich der thermische Widerstand der Hanffaser behandelt mit Chitosan im Vergleich zur unbehandelten Hanffaser verbesserte und der Prozent der Restmasse im Temperaturintervall 25–550°C wuchs. Gleichfalls ist der Kristallisationsgrad gestiegen und entsprechend, der Orientierungsgrad. Im Falle der Behandlung mit Chitosan wurde eine Verschlechterung der Steifheit- und der Dehnungseigenschaften bemerkt.

Schlüsselwörter: Hanffaser, Struktur, Chitosan, BTCA

With the ever growing concern of ecological and environmental sustainable development for textiles, hemp has recently been undergoing a revival worldwide as a fast growing natural source of bast fibres. In Chinese raw hemp bast, there is 57.01% cellulose, 17.84% hemicellulose, 5.80% pectin, 7.31% lignin, 1.96% ester wax, 10.08% water-soluble matter and a small amount of ash in the fibres [1]. Differences in the chemical composition data may be caused by the species and the test methods used. Because of the presence of some non-cellulosic substances in raw hemp bast, it was difficult for hemp fibre to obtain a high added-value fabric with comfort and good appearance [2]. Previous investigations were focused mainly on understanding the behavior so that to remove the non-cellulosic substances in the bast fibres [3, 4]. Although the chemical and mechanical processings of hemp fibres were effective for non-cellulosic substance removing, the damage done to fibre cellulose could not be avoided completely.

On the other hand, chitosan has a great potential for a wide range of uses due to its hydrophilicity, biodegradability, biocompatibility, antimicrobial activity, non-toxicity, and versatile chemical and physical properties [5]. It can be used for textile wet processing, including dyeing, printing, durable press and antistatic finishing and so on [6–10]. Studies showed that chitosan could react with cellulose by using a cross-linking reaction

of the poly-carboxylic acid [11–13]. To the author's knowledge, the structure of hemp fibre modified with 1, 2, 3, 4-butanetetracarboxylic acid (BTCA) and chitosan had been lacking. To maximize the exploitation of hemp fibre for clothing textile fabrics, a more complete understanding of its structure is required. In the present work, the structural changes in hemp fibres modified with BTCA and chitosan of molecular weight below 10,000 and degree of deacetylation 90% is described. The properties of the hemp fabric before and after treatment were also investigated.

EXPERIMENTAL PART

Materials

Bleached 100% hemp fabric (plain weave, the linear densities of warp and weft are identical, 14 tex, numbers of ends and picks are identical, 220 per 10 cm, the weight per unit area is 182 g/m²), was obtained from Zhejiang Lihui Dyeing and Finishing Co. Ltd.

The chemicals used in this study are in the analytical reagent grade and include 1, 2, 3, 4-butanetetracarboxylic acid (C₈H₁₀O₈), sodium hypophosphite monohydrate (NaH₂PO₂·H₂O), and triethanolamine (C₆H₁₅O₃N).

The wetting agent JFC was provided by Shijiazhuang HaiSeng Chemical Co. Ltd. Chitosan with 90% deacetylation degree, which was supplied by Qingdao

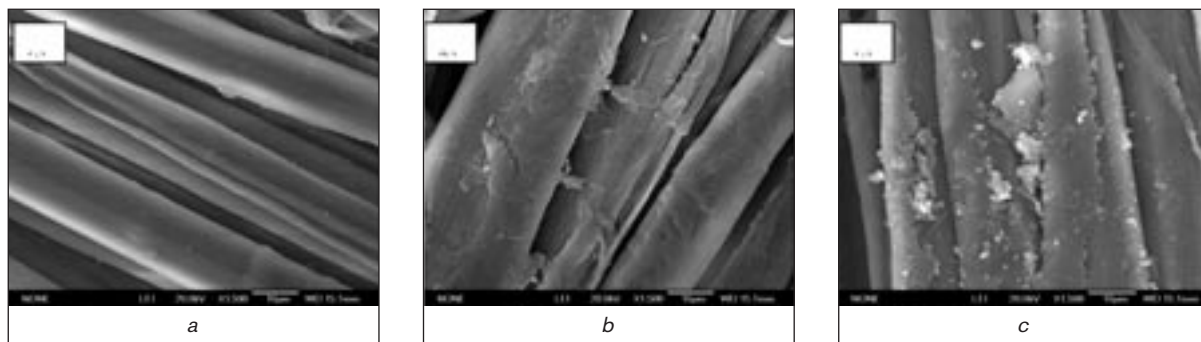


Fig. 1. SEM photographs of hemp fibres:
a, b – untreated hemp fibre; c – hemp fibre modified with chitosan and BTCA

Hepe Biotechnology Co. Ltd., was degraded to further obtain the molecular weight below 10,000, under references 14 and 15.

Hemp fabric treatment

First, 1.8% of degraded chitosan was dissolved in 6% BTCA solution at room temperature, followed by the addition of 7% sodium hypophosphite monohydrate and 0.2% wetting agent, which was mixed to make the chitosan processing solution.

Second, hemp fabric was impregnated in chitosan processing solution at 85°C, for 30 minutes, and a 30:1 liquor ratio; then, it was padded twice to a 100% wet pickup. The padded fabric was further dried at 95°C, for 150 seconds, and cured at 140°C, for 60 seconds. Finally, the sample was washed thoroughly at 80°C, for 10 minutes, neutralized with a sodium hydroxide concentration of 0.1 M, again cold washed and dried in air.

Testing methods

Scanning electron microscopy

Dry samples of hemp fibres were mounted, before and after treatment, on SEM stubs and sputter coated with platinum before examination in a JSM-6700F field scanning electron microscope. Photographs of the samples with surface characteristics were taken randomly.

FT-IR spectrometry

The hemp fibre samples were examined in KBr pellets, obtained by pressing the materials pulverized at 1% concentration. The FT-IR spectrophotometer was a Nicolet Nexus 870 model, and the spectra were collected with the aid of the OMNIC software. The wavenumbers were in the range of 400 cm⁻¹ – 4 000 cm⁻¹.

TG and DSC analysis

Thermogravimetric analyses were determined on the samples before and after treatment, using a TGA/SDTA851e thermal gravimetric and differential scanning calorimetry analysis (TG-DTA) instrument. Percentage weight change versus temperature was evaluated at 10°C/minute, heating rates with a nitrogen flush rate of 30 ml/minute, over the range of 25–550°C. The onset and endset decomposing temperatures and the percent residual weight were obtained according to ASTM E474-80. DSC analyses were performed in a Sapphire apparatus equipped with a DSC 20 cell purged with nitrogen of 30 ml/minute. The temperature program was set in the range from 25°C to 550°C, at a heating rate of 10°C/minute.

XRD analysis

The X-ray diffraction patterns of hemp fibres were collected by a Shimadzu diffractometer (Model XRD-7000S, Cu K α radiation and graphite filter at 40 kV and 40 mA, $\lambda = 1.540562 \text{ \AA}$), before and after treatment, in the 2θ ranging from 5° to 40° at a continuous scan speed of 6.0 degrees/minute. The apparent crystallite size of the sample was determined using the Scherrer formula. The degree of crystallinity was calculated using Jade 5.0 software. The sample degree of orientation was also measured, using the above instrument (40 kV, 30 mA) in the range of 0–360° at a 60 degrees/minute scanning speed, and calculated by (1).

$$\text{Orientation} = \frac{360^\circ - \sum wi}{360^\circ} \cdot 100 \quad (1)$$

where:

wi is the full width at half maximum, FWHM (°).

Measurement of fabric tensile properties

Tensile properties of the samples were carried out on an Instron 5565 electromechanical test system (Instron Japan Co. Ltd.), according to GB3923-1997. The initial gauge length was 10 cm and the width was 5 cm. The testing rate was 100 mm/minute, and the pre-tension was 4.9 N. Ten samples per treatment set were tested and the breaking load and tensile strain averaged.

Measurement of fabric bending properties

The flexural rigidities of hemp fabric before and after treatment were evaluated using the LLY-01B electrical fabric stiffness tester according to GB/T18318-2001. The length of the sample was 15 cm and the width 2 cm. The bending angle was set on 45°. Values reported represented the averages of at least five measurements.

Fabric whiteness testing

Whiteness indices of hemp fabric before and after treatment were measured using the SBD-1 digital whiteness meter, according to GB/T9338-1988, taking the average of five readings.

RESULTS AND DISCUSSION

Fibre surface morphology

The surface of the bleached hemp fibre was relatively smooth and clean, under the SEM investigation. Fibre bundles were arranged in the axis of the fibre, onto whose surface a number of tiny linear grooves were dispersed (fig. 1a). Besides many small crevices and

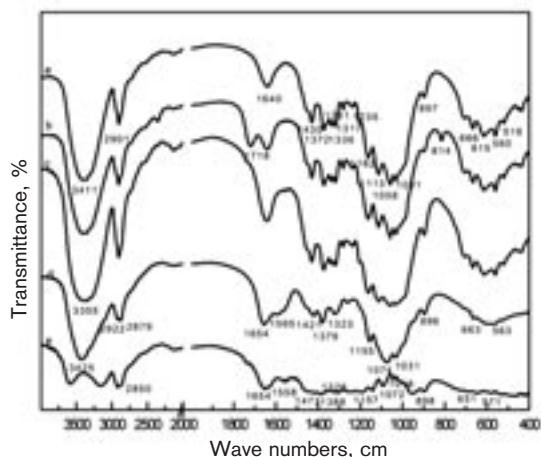


Fig. 2. FT-IR spectra of the samples: a – untreated hemp fibre; b – unwashed hemp fibre treated with chitosan and BTCA; c – hemp fibre washed with 0.1 mol NaOH solution; d – chitosan; e – subtract spectrum of c and a

pores distributed between hemp fibres, some debris and other non-fibrous impurities could be found, such as the polypectate, which was not degummed completely (fig. 1b). After being treated with chitosan, the fibre surfaces were coated in a layer of substances and the openings were filled with chitosan. Some white particles could be seen, which might be the effect of chitosan absorbed on the fiber surfaces (fig. 1c).

FT-IR analysis

The spectra of hemp fibres, before and after treatments, were presented in figure 2. The spectrum of chitosan, 90% deacetylation degree, was also given. It could be seen that, as compared to the untreated hemp fibre (line a), peaks at $1\ 718\ \text{cm}^{-1}$ and $814\ \text{cm}^{-1}$ were observed for the chitosan-treated but unwashed hemp fibre (line b), and then disappeared when the sample was treated with 0.1 M alkali solution (line c). Except the broadening of peak at $3\ 355\ \text{cm}^{-1}$ (N-H stretching), there was no other significant change. Thus, the subtract of c and a (line e) was analyzed. Compared with the spectrum of chitosan (line d), two peaks were formed, due to the separation of band at $3\ 425\ \text{cm}^{-1}$, and the peak at $1\ 654\ \text{cm}^{-1}$ (amide I band) was intensified. The peaks at $1\ 595\ \text{cm}^{-1}$ (amide II band) and $1\ 421\ \text{cm}^{-1}$ (CH_2 bending and CH_3 deformation) of chitosan were absent. Instead, the new absorption bands at $1\ 558\ \text{cm}^{-1}$ and $1\ 473\ \text{cm}^{-1}$ were identified.

The peaks at $2\ 879\ \text{cm}^{-1}$ (CH_2 asymmetrical stretching), $1\ 379\ \text{cm}^{-1}$ (C-H bending and CH_2 symmetrical deformation), $1\ 323\ \text{cm}^{-1}$ (amide III band) and $896\ \text{cm}^{-1}$ (β -D-glucopyranoside band) shifted to $2\ 850\ \text{cm}^{-1}$, $1\ 388\ \text{cm}^{-1}$, $1\ 326\ \text{cm}^{-1}$ and $898\ \text{cm}^{-1}$, respectively. At the same time, the peaks at $1\ 155\ \text{cm}^{-1}$, $1\ 074\ \text{cm}^{-1}$ and $1\ 031\ \text{cm}^{-1}$ were also shifted, which could be assigned to asymmetrical and symmetric stretching vibrations of $-\text{COO}^-$ anion group. Therefore, this suggested that the chemical modification induced in hemp fibres by chitosan treatment was confirmed.

TG and DSC analyses

The effect of chitosan treatment was distinctly observed in the hemp fibres thermograms run at a heating rate of $10^\circ\text{C}/\text{minute}$, as depicted in figure 3. It was clear from TG curves (figure 3a) that the weight change could be divided into two temperature regions, namely: from 219.8°C to 346.3°C , with a weight loss of 73.4%, and from 385.3°C to 505.4°C , with a weight loss of 90.0% to initial weight. But for the chitosan treated hemp fibre, there was only one temperature region, that is: from 215.6°C to 414.8°C , with a weight loss of 79.7%.

Differences in remains left in the crucible at the end of the TG runs had shown that the substance of treated fibre was larger than that of the untreated fibre. As the temperature increased, a gradual degradation occurred, which included de-polymerization, hydrolysis, dehydration and decarboxylation [16]. These occurrences then lead to the decomposition of the fibres. It was obvious from the DSC curves (figure 3b) that the small endothermal peaks at 54.2°C , for the untreated fibre, and 49.8°C , for the chitosan treated fibre, were attributed to the dehydration of absorbed water. The maximum endothermal temperature was shifted from 364.3°C to 373.3°C , creating a more thermally stable fabric when hemp fabric was treated with chitosan and BTCA. This indicated the decrease in amorphous cellulose for the chitosan treated hemp fibre [17].

In order to investigate the chemical reaction among hemp fibre, chitosan, and BTCA, we took hemp fibre, chitosan, sodium hypophosphite with or without BTCA in equative mass and then mixed them. The DSC curves were illustrated in figure 4a. It was obvious that hemp fibre could not react with chitosan without BTCA. The endothermal peak at 147.8°C indicated that the chemical reaction, which catalyzed by sodium

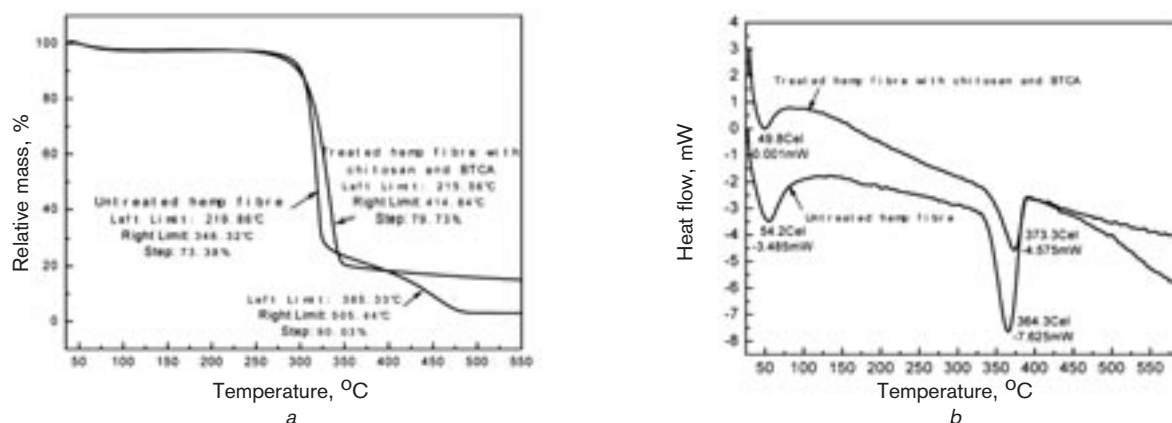


Fig. 3. TG and DSC curves of hemp fibres: a – TG curve; b – DSC curve

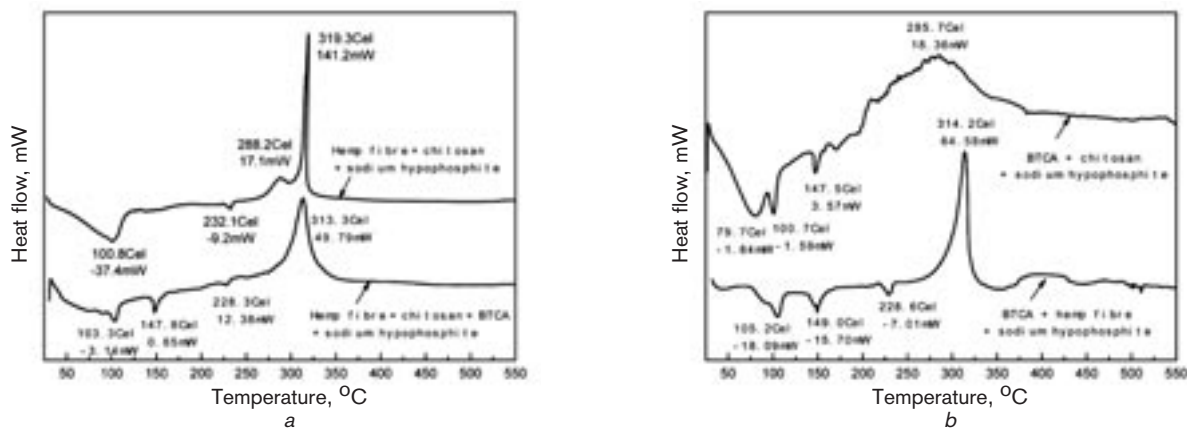


Fig. 4. DSC curves of hemp fibre, chitosan, BTCA and sodium hypophosphite

hypophosphite, occurred among hemp fibre, chitosan and BTCA. To further verify the reaction temperature among hemp fibre, chitosan and BTCA, we mixed sodium hypophosphite, BTCA and hemp fibre (or chitosan) following the above method. The DSC curves were shown in figure 4b. It was evident that BTCA reacted with chitosan and hemp fibre at the temperature of 147.5°C and, respectively, 149.0°C, which was very close to the curing temperature 140°C. Combining figure 4a with figure 4b, it was concluded that the endothermic peaks at 100.8°C (fig. 4a), 79.7°C and 100.7°C (fig. 4b), were ascribed to the dehydration of absorbed water. The endothermic peaks at 232.1°C, 228.3°C (fig. 4a) and 228.6°C (fig. 4b), were attributed to the pyrolysis of sodium hypophosphite. BTCA reacted with hemp fibre at the temperature of 103.3°C (fig. 4a), or 105.2°C (fig. 4b). The exothermic peaks at 313.3°C (fig. 4a), 314.2°C and 285.7°C (fig. 4b) were caused by the chemical reaction between BTCA and hemp fibre, BTCA and chitosan, respectively. The small exothermic peaks at 288.2°C and 319.3°C (fig. 4a), resulted from the action between hemp fibre and sodium hypophosphite. Therefore, chitosan was grafted onto hemp fibre through BTCA.

XRD analysis

The hemp fibre diffraction patterns, before and after treatment, were exhibited in figure 5. Table 1 shows the corresponding fine structures and the degree of crystallization. The results indicated that cellulose I and II, crystal forms of hemp fibre before and after treatment,

did not change. From the XRD pattern of untreated hemp fibre (degummed and bleached), the four diffraction peaks at $2\theta = 14.50^\circ$, 16.10° , 22.21° and 33.81° were characteristic for hemp fibre and corresponding to (101), (002) and (040) reflections, respectively. When hemp fibre was treated with chitosan and BTCA, the corresponding diffraction peaks 2θ and the inter-planar spacings had no distinct change. The FWHM increased, but the crystal size decreased. Calculation of the percentages of the crystalline fraction showed that the degree of crystallization increased from 63.3% to 70.8%. The amorphous fractions might be dissolved after treatment, which resulted in the increase of ordered fraction.

The hemp fibre orientation patterns, before and after treatment, were given in figure 6. Table 2 showed the corresponding angle, FWHM and orientation. The results indicated that, when hemp fibres were treated with chitosan and BTCA, the characteristic peaks shifted from 34.67° and 119.97° to 38.87° and 131.12° , and the degree of orientation increased from 62.4% to 84.6%.

Tensile properties analyses

The tensile properties of hemp fabric before and after treatments, as reflected by the breaking load, tensile strain and initial modulus, were reported in table 3. It was found that, compared with those in the untreated hemp sample, drops in breaking load and initial modulus in both warp and weft directions were 17% and, respectively, 5.6%. The corresponding reductions in tensile strain were 14.4% and 1.6%. This was due to the fact that BTCA present in chitosan processing solution acted as the hydrolyzation catalyst, which

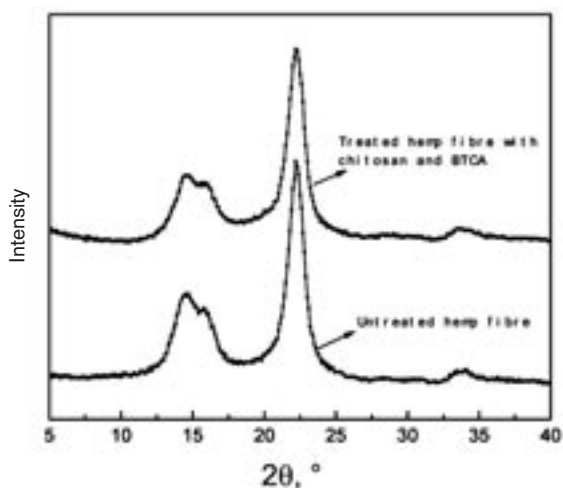


Fig. 5. X-ray diffractions of hemp fibres

Table 1

X-RAY DIFFRACTION OF HEMP FIBRES					
Sample	Characteristic peaks $2\theta, ^\circ$	Interplanar spacing, nm	FWHM, $^\circ$	Size of crystal grain, nm	Crystallization, %
Untreated hemp fibre	14.50	0.6104	1.897	4.221	63.3
	16.10	0.5501	1.414	5.694	
	22.21	0.4000	1.384	5.872	
	33.81	0.2649	1.779	4.670	
Hemp fibre treated with chitosan and BTCA	14.60	0.6062	1.966	4.072	70.8
	15.60	0.5676	2.564	3.118	
	22.19	0.4003	1.487	5.460	
	33.91	0.2641	1.975	4.203	

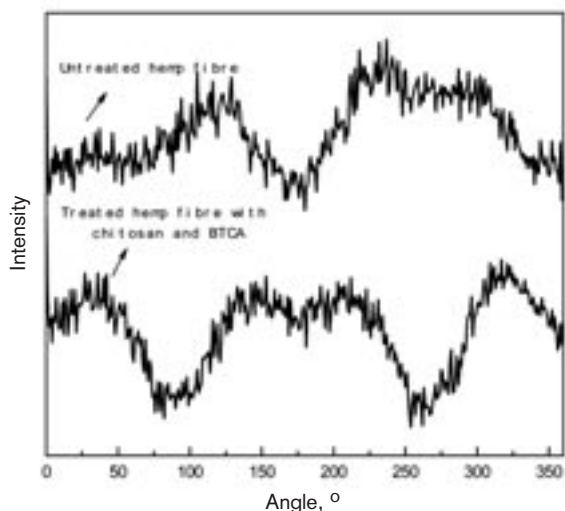


Fig. 6. Orientation curves of the samples

catalyzed the hydrolyzation of cellulose and chitosan. The non-fibrous materials, i.e. lignin, pectin, hemicellulose etc. remaining in the fibre, were probably damaged owing to the high curing temperature. The chemical cross-linkage mostly occurred in the amorphous region or in the surface of the crystal region. The interfacial forces between the crystal region and the amorphous region were changed. Under the non-homogeneous grafting condition, the distribution of branched chains was non-uniform and the lengths of the chains were different from each other [18]. Thus the movements of the macromolecular chains were restricted, resulting in the internal stress concentration phenomenon. Therefore, the tensile properties of the chitosan treated fabric became worse.

Bending properties analyses

As table 4 shows, changes took place in bending length, bending rigidity and bending modulus, which were related to the softness of hemp fabric. It was clear that, compared to the untreated hemp sample, the bending rigidity and bending modulus of the chitosan treated hemp sample increased to some extent. This was mainly due to the chemical cross-linkage between hemp fibre, chitosan and BTCA.

Table 2

ORIENTATION OF HEMP FIBRES			
Sample	Angle, °	FWHM, °	Orientation, %
Untreated hemp fibre	34.67	20.667	62.4
	119.97	46.944	
Hemp fibre treated with chitosan and BTCA	38.87	10.229	84.6
	131.12	17.580	84.6

BIBLIOGRAPHY

- [1] Zhang, J. C., Zhang, H., Zhang, H. P., Guo, Y. H. *The Development of Chinese Hemp*. Changcheng Press, Beijing, 2006, p. 229
- [2] Wang, J., Ramaswamy, G. N. *Effects of chemical processing on hemp and kenaf dyeing properties*. In: AATCC Review, 2005, vol. 5, issue 3, p. 21
- [3] Buschle, D. G., Fanter, C., Loth, F. *Structural changes in hemp fibers as a result of enzymatic hydrolysis with mixed enzyme systems*. In: Textile Research Journal, 1999, vol. 69, issue 4, p. 244
- [4] Wang, H. M., Postle, R., Kessler, R. W., Kessler, W. *Removing pectin and lignin during chemical processing of hemp for textile applications*. In: Textile Research Journal, 2003, vol. 73, issue 8, p. 664
- [5] Majeti N. V. R. K. *A review of chitin and chitosan applications*. In: , 2000, vol. 46, issue 1, p. 1
- [6] Hasebe, Y., Kuwahara, K., Tokunaga, S. *Chitosan hybrid deodorant agent for finishing textiles*. In: AATCC Review, 2001, vol. 1, issue 11, p. 23

Table 3

TENSILE PROPERTIES OF THE HEMP FABRIC				
Test targets	Untreated hemp fabric		Hemp fibre treated with chitosan and BTCA	
	warp	weft	warp	weft
Breaking load, N	1008.31	1075.34	836.49	1015.06
Tensile strain, %	18.48	23.10	15.81	22.72
Initial modulus, Mpa	20.17	21.51	16.73	20.30

Table 4

STIFFNESS PROPERTIES OF THE HEMP FABRIC						
Sample	Bending length, cm		Bending rigidity, mgf · cm		Bending modulus, kgf · cm ⁻²	
	warp	weft	warp	weft	warp	weft
Untreated hemp fabric	3.59	3.30	842.48	654.36	281.32	218.50
Hemp fibre treated with chitosan and BTCA	3.76	3.78	985.19	1000.99	215.45	218.91

Fabric whiteness analysis

The whiteness of the untreated hemp sample was about 71.9%. After being treated with chitosan and BTCA, the whiteness decreased to 65.7%. This was due to the decomposing of poly-carboxylic acid during the high temperature curing. When 2.5% of triethanolamine (TEA) was added to the processing solution, a comparable whiteness (69.2%) to that of the untreated fabric was obtained. TEA could swell hemp fibres further, which facilitated the process solution to penetrate into hemp fibre.

CONCLUSIONS

In this work, hemp fabric was treated using BTCA and chitosan of molecular weight below 10,000 and degree of deacetylation 90%, and then was investigated by means of SEM, FT-IR, TG, DSC and XRD. The tensile and stiffness properties, as well as whiteness were also measured. It was found that, compared to the untreated hemp fibre, the fibre surfaces were covered with a thin layer of chitosan. The thermal stability of treated hemp fibre was changed, and the temperature at the maximum endothermic peak increased. Hemp fibre reacted with chitosan by BTCA acting as a bridge. The size of crystal grain decreased, and the degrees of crystallization and orientation increased. The tensile and stiffness properties, as well as whiteness of treated hemp fabric degraded, but not too much.

- [7] Wu, L. L., Yu, J. Y. *Anti-bacterial and crease resistant finish of cotton fabric with poly-carboxylic acid and chitin*. In: Dyeing and Finishing, 2001, vol. 27, issue 11, p. 8
- [8] Chen, J. Y., Liu, G. F. *Study on the chemical modification of chitosan and the antibiotic activity of its finishing fabric*. In: Journal of Functional Polymers, 2002, vol. 15, issue 2, p. 194
- [9] Xu., Y. H., Zhu, S. W., Huang, C., Wang, H., Yang, P. S. *Integrating properties of chitosan with cotton knitted fabric*. In: Journal of Anhui Agricultural University, 2005, vol. 32, issue 2, p. 250
- [10] Wang, J. G., Wang, Y. L., Ge, M. Q., Gan, Y. J., Chen, D. S. In: *Research on antimicrobial finishing of cotton fabrics with a citric acid and chitosan*. In: Journal of Textile Research, 2006, vol. 27, issue 1, p. 89
- [11] Wang, L., Li, Z. *Analyses and studies on reaction mechanism of poly-carboxylic acids with cellulosic fibers*. In: Journal of Textile Research, 2000, vol. 21, issue 1, p.18
- [12] Xu, X. H., Wang, X. Q. *Cross-linking modification of butane-tetra-carboxylic acid on viscose fibers*. In: Journal of Cellulose Science and Technology, 2008, vol. 16, issue 2, p. 6
- [13] Hua, W. S., Gu, S. L., Gu, Y. X., Pan, C., Rui, X. S. *Application of butane-tetra-carboxylic acid on textile finishing*. In: Textile Auxiliaries, 2008, vol. 25, issue 8, p. 5
- [14] Zhang, F., Yin, J. M., Ding, L. J. *Study on the degradation of chitosan with H₂O₂ under the ultrasonic*. In: Polymer Materials Science & Engineering, 2004, vol. 20, issue 1, p. 221
- [15] Li, J., Du, Y. M., Yao, P. J. Wei, Y. A. *Prediction and control of de-polymerization of chitosan by sonolysis and degradation kinetics*. In: Acta Polymerica Sinica, 2007, issue 5, p. 401
- [16] Peters, R., Still, R. *Applied Fibre Science*. Academic Press, London, 1979, p. 321
- [17] Mwaikambo, L. *Plant-based resources for sustainable composites*. PhD thesis, Department of Engineering and Applied Science, University of Bath, 2002
- [18] Miyake, H., Nagura, M. *Molecular weight dependence of tensile properties of ramie and linen fibers*. In: Textile Research Journal, 2001, vol. 71, issue 7, p. 645

Authors:

HUI ZHANG
LIMIN ZHANG

School of Textile & Materials
Xi'an Polytechnic University
Xi'an Shaanxi 710048, China
e-mail: hzhangw532@xpu.edu.cn

INDUSTRIA TEXTILĂ ÎN LUME

BENEFICIILE ÎNCORPORĂRII OXIDULUI DE ZINC ÎN FIBRA LYOCELL

Compania **Smartfiber AG** – Rudolstadt/Germania, în colaborare cu **Institutul Thuringian de Cercetare pentru Textile și Mase Plastice (TITK)**, au elaborat o nouă fibră scurtă din lyocell, **Smartcell Sensitive**, cu oxid de zinc integrat, ce conferă proprietăți antibacteriene și de reducere a mirosurilor neplăcute, fiind recomandată pentru așternuturi, stofe de mobilă și covoare, mai ales în cazul persoanelor cu alergii, neurodermatite sau psoriazis. Cu Smartcell Sensitive, metabolismul bacteriilor este întrerupt de așa-numitul „efect oligodinamic“, care reduce dezvoltarea acestora și producerea mirosurilor neplăcute.

Această fibră poate fi vopsită în orice culoare, inclusiv alb, și utilizată în amestecuri cu lână. După cum subliniază compania, în procesul de producere se folosește o materie primă biogenă, prietenoasă mediului, 100% biodegradabilă, care conduce la economisirea resurselor. **Smartcell Sensitive** este certificată conform standardului Eco-Tex 100, ca produs clasa I (produse pentru copii). De altfel, oxidul de zinc pur, farmaceutic, provenit din zincul metalic utilizat, întrunește cerințele de puritate ale DAB 10 și alte altor reglementări internaționale privind prepararea produselor farmaceutice.

Smarttextiles and nanotechnology,
martie 2010, p. 10

FIRE DE NAILON DIN BOABE DE RICIN

Compania franceză **Condamin Prodon** a dezvoltat o nouă gamă de fire de înaltă performanță, obținute din biopolimeri derivați din plante de ricin. Aceste plante provin din Africa și Asia – din semințe modificate genetic, cultivate pe terenuri care nu se pretează agriculturii și care nu necesită irigarea – și reprezintă o biomasă regenerabilă 100%.

Noii biopolimeri **Greenfil** au fost elaborați de **Sofila** – societatea-mamă a firmei Condamin, în parteneriat cu compania de produse chimice **Arkema**, care a furnizat poliamida Rilsan 11 pentru fabricarea firelor. Aceștia au fost încorporați în țesături, care au fost prezentate în cadrul târgului **Prèmiere Vision 2009**. În prezent, noile materiale sunt disponibile pe piață și se află în curs de testare sub marca franceză de tricotaje **Dim**. Rilsan nu reprezintă o tehnologie nouă, polimerul fiind utilizat în industria de mase plastice încă din anul 1942. În domeniul îmbrăcăminte, Rilsan a fost folosit la accesorii de plastic ale acesteia, de exemplu la sutiene. El este produs din boabe de ricin, având bune proprietăți termice, fizico-chimice și mecanice. Elementul de noutate constă în faptul că Rilsan este utilizat, pentru prima dată, în producerea firelor din nailon la scară industrială.

Compania oferă fire cu finețea de 22, 44 și 78 dtex, obținute prin filare cu jet de aer sau prin torsionare cu jet de aer, fire de nailon texturate sau laminate cu profil rotund și cu un luciu deosebit.

Informații de presă. Condamin Prodon, februarie 2010

The use of dendrimers to obtain low temperature dyeability on mohair and Angora fibers

RIZA ATAV

ABBAS YURDAKUL

REZUMAT – ABSTRACT – INHALTSANGABE

Utilizarea dendrimerilor pentru optimizarea capacității de vopsire a fibrelor de mohair și Angora la temperaturi scăzute

Dendrimerii sunt macromolecule cu o arhitectură 3D regulată și puternic ramificată. Scopul lucrării îl constituie îmbunătățirea capacității de vopsire a fibrelor de mohair și Angora prin folosirea dendrimerilor și evaluarea posibilității de vopsire a acestor fibre la temperaturi scăzute. Potrivit rezultatelor experimentării, s-a constatat că fibrele de mohair și Angora, pe care s-a aplicat dendrimerul, pot fi vopsite în culori mai închise decât fibrele netratate și, în special, în cazul vopsirii fibrelor de mohair cu coloranți reactivi, s-a constatat faptul că fibrele pe care s-a aplicat un dendrimer pot fi vopsite la temperaturi mai mici sau în intervale de timp reduse, fără vreo diminuare a calității culorii.

Cuvinte-cheie: dendrimer, mohair, Angora, vopsire

The use of dendrimers to obtain low temperature dyeability on mohair and Angora fibers

Dendrimers are macromolecules with a regular and highly branched three-dimensional architecture. In this study, the aim was to improve the dyeability of mohair and Angora fibers via dendrimer application and to assess the potential of low temperature dyeability of these fibers. According to the experimental results, it was found that dendrimer applied mohair and Angora fibers could be dyed darker than the un-treated fibers and, especially in dyeing mohair fibers with reactive dyes, it was determined that it is possible to dye dendrimer applied fibers at lower temperatures or shorter times, without causing any decrease in color yield.

Key-words: dendrimer, mohair, Angora, dyeing

Die Anwendung der Dendrimere für die Kapazitätsoptimierung der Mohair und Angora- Faserfärbung bei niedrigen Temperaturen

Die Dendrimere sind Makromoleküle mit einer regelmässigen und einer stark verzweigter 3D-Architektur. Der Zweck dieser Arbeit besteht in der Verbesserung der Färbungskapazität der Mohair- und Angorafaser durch die Benutzung der Dendrimere und die Bewertung der Möglichkeiten der Färbung dieser Fasern bei niedrigen Temperaturen. Gemäss den Ergebnissen der Versuche wurde ermittelt, dass die Mohair- und Angorafasern mit einer dunkleren Farbe als die unbehandelten Faser gefärbt werden können und insbesondere im Falle der Färbung von Mohairfaser mit Reaktivfarbstoffen, die Faser, welche mit Dendrimere behandelt wurden, bei niedrigeren Temperaturen oder in reduzierten Zeitintervallen gefärbt werden können, ohne eine Verminderung der Farbqualität.

Schlüsselwörter: Dendrimer, Mohair, Angora, Färbung

Most synthetic and naturally occurring macromolecules have a simple linear structure. Over the last 20 years, polymer chemistry has created a number of non-linear variations on this simple polymer structure. The introduction of a large number of branches during the polymer's synthesis leads to a macromolecule with many end groups [1]. Dendrimers consist of three major components: core, branches, and end-groups [2]. Many of the dendrimer chemical and physical properties, such as state of aggregation, reactivity, stability and solubility are closely related to the nature of the end groups. Thus, it is possible to tailor the dendrimer's properties by appropriate chemical modification of the end groups. Between the dendrimer's branches, there is room for guest molecules. Guests can be, for example, simple solvents, but it is possible for the dendrimer to take up larger species as well. The nature of the host-guest interaction is varied. Ionic (acid/base), donor-acceptor, Van der Waals and hydrogen bonding interactions are known. The large-scale availability of dendritic macromolecules has opened the road towards a broad scale of new applications, both with scientific and industrial relevance [1].

Burkinshaw et al. (2000) have treated the cotton with a derivative of Am₁₆decanamide₈, an example of the Astramol™ (DSM) range of dendrimers. On this line, the aim of the study is to determine the effect of dendrimers on cotton dyeability with reactive dyes. Fabrics, which were both treated with dendrimers, and un-treated, were dyed in the presence and absence of electrolyte and alkali at different pH. The cotton fabric

that had been pretreated with a dendrimer displayed markedly enhanced color strength with reactive dyes, even when dyeing had been carried out in the absence of both electrolyte and alkali [3].

Burkinshaw et al (2002) have demonstrated that the incorporation of hyper-branched polymer into polypropylene, prior to fiber spinning, markedly enhances the dyeability of polypropylene with C.I. Disperse Blue 56. The observed enhancement of dye-uptake was attributed to the introduction of polar groups provided by the stearate-modified hyper-branched polymer [4].

Yiyun and Jiepin (2005) have synthesized polyamidoamine dendrimers from ethylenediamine and methyl acrylate and demonstrated their effectiveness in decolorizing wastewater containing Acid Fuchsin and Methyl Blue. The effect of variables, such as initial pH, quantity and generation of dendrimer, have been investigated. The experimental results show that, under suitable conditions, polyamidoamine dendrimers can be highly effective as de-colorants [5].

In this study, the aim was to improve the dyeability of mohair and Angora fibers via dendrimer application, according to its determination, and assess the potential for low temperature dyeability of these fibers.

MATERIAL AND METHOD

In these experiments, mohair fibers (Angora goat) – fineness 31.47 micron, and Angora fibers – fineness 16.82 micron were used. All the experiments were carried out by using soft mill water. For this study, a

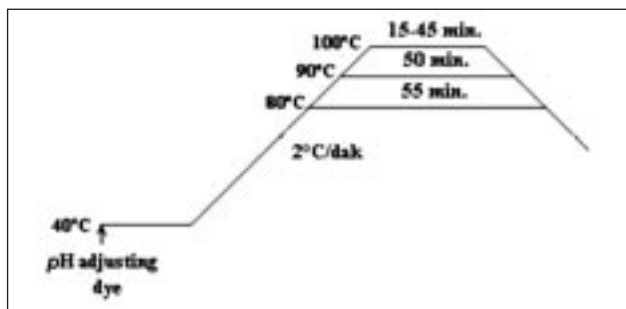


Fig. 1. Dyeing procedure

commercial dendrimer product was used. It is a cationic hyper-branched self-orientation of a star-shaped branched polymer (so-called dendrimer).

For treatment optimization of dendrimer application, fibers were treated at different pH, concentrations, times and temperatures. The pH was adjusted to 4.7 and 9, and the concentration was set at 2% and 5%. During these experiments, time was 30 minute, and temperature 50°C. The dendrimer application treatment time was also set at 30, 45 and 60 minutes. During these experiments, pH was 4 and concentration was 2%. After the optimization of the pH, concentration and time, the effect of temperature (50-70-90°C) was studied at pH 4, concentration 2% and time 30 minutes. After dendrimer applications, the samples were dyed with reactive dye (Realan Blue RC), in 1% depth, at 80°C (figures 2 and 3), to determine the effect of dendrimer application on mohair and Angora fibers dye exhaustion. Color yield values – K/S – of samples dyed were measured by Minolta 3600d spectral photometer (D65/10°). After determining the optimal dendrimer application conditions for fiber dyeability increase, Fourier Transform Infrared spectroscopy (FTIR) measurement of the fibers treated with dendrimers at optimum conditions was carried out with a Perkin Emler Spectrum 100, in order to observe the changes in the functional groups of the fiber.

After determining the optimum dendrimer application condition for fiber dyeability increase, dyeing properties were tested for dendrimer-applied mohair and Angora fibers, at various dye classes and different temperatures.

Dyeing procedures

Dyeing procedures were carried out in 1:30 liquor ratio, in a 3% dyeing depth, according to the graph given in figure 1. For milling acid dye (Telon Blue M-RLW) and 1:2 metal complex dye (Isolan Dark Blue 2S-GL), dyeing pH has been chosen as 6 (with CH₃COOH). For the reactive dye (Realan Blue RC), dyeing pH has been chosen as 5 (with CH₃COOH). In order to prevent affecting the dyeing properties of fibers, the usage of auxiliaries (equalizing agent etc.) or salts has been avoided. As can be seen from figure 1, dyeings were carried out at three different temperatures (100, 90 and 80°C), where the total dyeing time was constant (90 minute). Furthermore, at 100°C, dyeing time was chosen as 15 and 45 minute. After dyeing, the liquor was cooled down and the fibers were taken out. Then, samples dyed were rinsed with cold (5 minutes) – warm (5 minutes at 50°C) – cold (5 minutes) water,

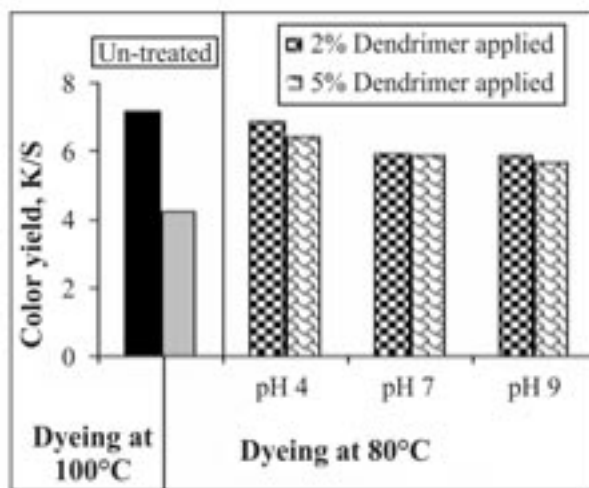


Fig. 2. Effect of dendrimer application pH and concentration (30 minute at 50°C) on the color yield of mohair fibers during dyeing with 1% Realan Blue RC

respectively, and dried. All experiments were carried out in Termal HT type dyeing machine.

Color yield, K/S, and CIELab values of samples dyed were measured with Minolta 3600d spectral photometer (D65/10°). Washing fastness tests were also carried out according to the ISO 105 C06 standard.

RESULTS AND DISCUSSION

Treatment optimization for dendrimer application

The results of experiments carried out to determine the pH and concentration effect during dendrimer application are given in figures 2 and 3.

As can be seen in figures 2 and 3, the color yield of dendrimer applied mohair and Angora fibers decreased with the pH rise. It means that dendrimer application efficiency decreases in the neutral and basic pH, when compared to the acidic pH. According to these results, it can be concluded that, for dendrimer application, the optimal pH is 4. When the effect of dendrimer concentration is examined, it can be said that this is not very significant, reason for which it can be chosen as 2%. However, it is not recommended to use it at lower concentrations, because level distribution of dendrimers on the fiber surface cannot be obtained.

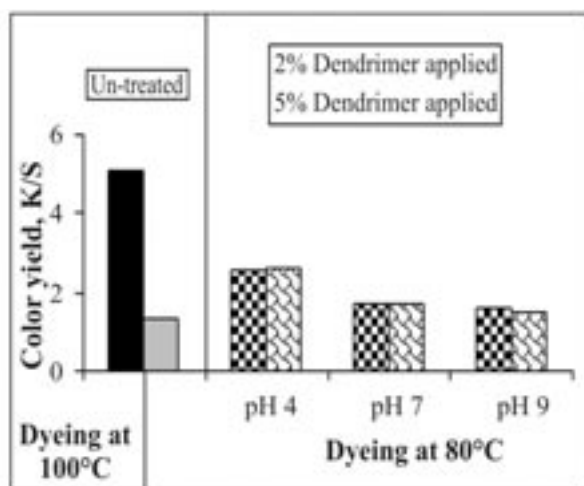


Fig. 3. Effect of dendrimer application pH and concentration (30 minute at 50°C) on the color yield of Angora fibers during dyeing with 1% Realan Blue RC

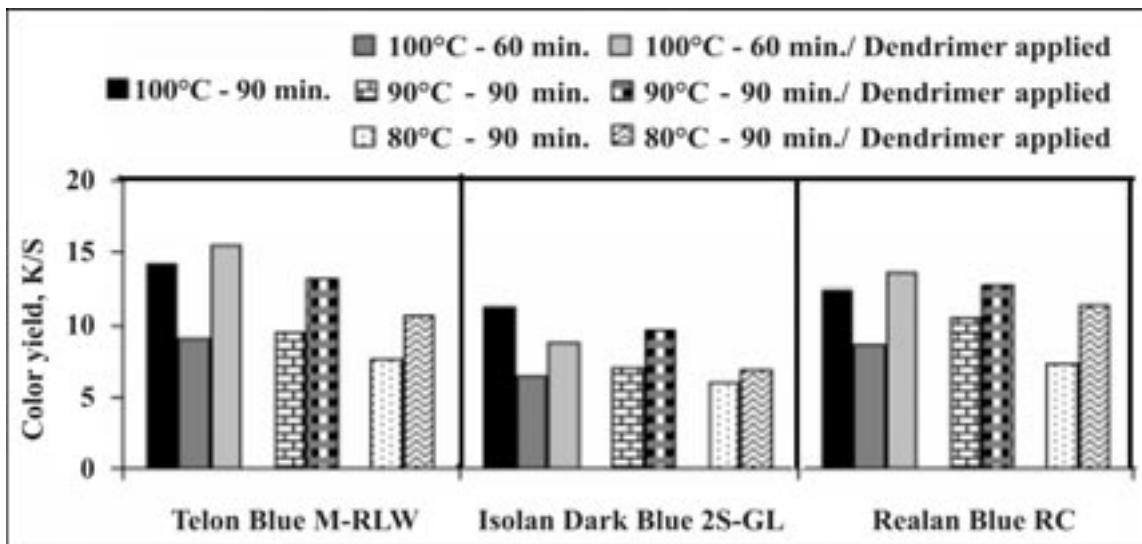


Fig. 4. Color yield values of mohair fibers un-treated and dendrimer applied (at optimum conditions)

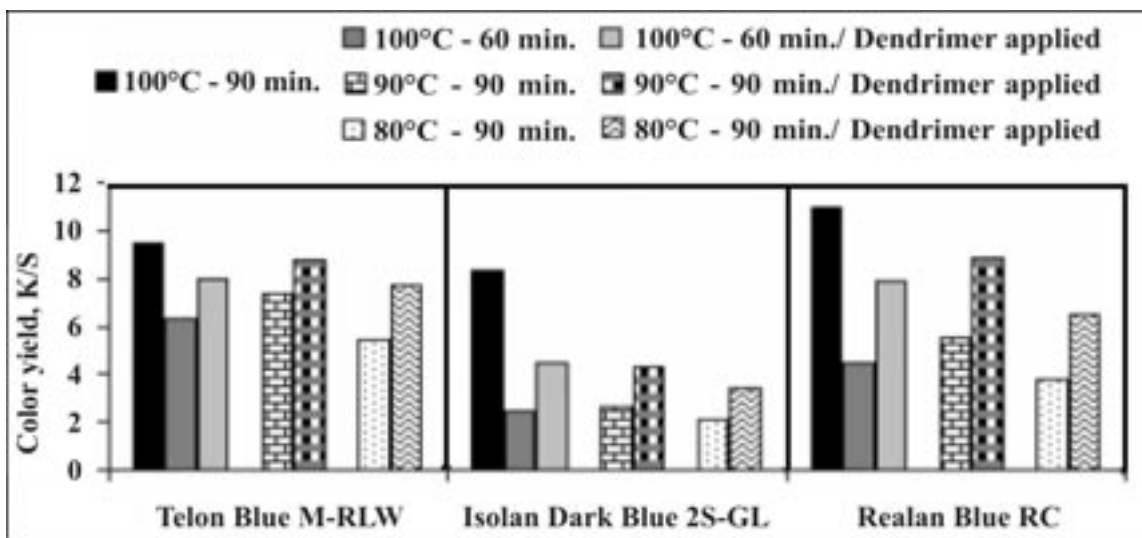


Fig. 5. Color yield values of Angora fibers un-treated and dendrimer applied (at optimum conditions)

Furthermore, the effect of time (30-45-60 minutes) and temperature (50-70-90°C) was also searched, but it was determined that these parameters did not have a significant effect, and optimum conditions were determined as 30 minutes and 50°C.

To demonstrate the changes in the functional groups of mohair and Angora fibers, surface FTIR spectroscopy was used, because significant changes in the chemical composition of fibers were expected. The band at $3\ 270\text{--}3\ 290\ \text{cm}^{-1}$ was attributed to the --OH stretching vibrations. Dendrimer applied mohair and Angora fibers showed a reduction and shifting of the peak position in --OH stretching absorbance. Bands for amide I ($1\ 620\text{--}1\ 640\ \text{cm}^{-1}$), amide II ($1\ 510\text{--}1\ 530\ \text{cm}^{-1}$) and amide III ($1\ 230\text{--}1\ 240\ \text{cm}^{-1}$) were also noticed in the spectrum. However, after dendrimer application, the transmittance values of these bands increased and showed a shifting of the peak position. Furthermore, band for the C-H single bond ($2\ 910\text{--}2\ 930\ \text{cm}^{-1}$) of dendrimer applied mohair and Angora fibers also showed a reduction and shifting of the peak position. These results represent the reason of a significant

improvement in the dyeability of the dendrimer-applied fibers.

Effect of the dendrimer application on the dyeability of fibers with various dye classes

Color yields of dendrimer applied at optimum conditions and of the un-treated fibers, which were dyed at various temperatures and times, are given in figure 4–5. In the figures, it can be seen that dendrimer applied fibers dyed darker than the un-treated fibers and that, as determined, especially in dyeing mohair fibers with reactive dyes, it is possible to dye dendrimer-applied fibers at lower temperatures or shorter times, without causing any decrease in the color yield.

The affectivity of dendrimer added in improving the dyeing process can be explained in terms of pH behavior of the constituent amine groups. At acidic pH , the amine groups of the dendrimer are protonated. The ensuing local high positive charge density should act as a primary point of the attraction for the anionic dye molecules, such as the acid, 1:2 metal complex and reactive dyes [3].

Table 1

CIELAB VALUES OF MOHAIR FIBERS UN-TREATED AND DENDRIMER APPLIED (AT OPTIMUM CONDITIONS)						
Dye	Total dyeing time	L	a	b	c	H
Telon Blue M-RLW	100°C – 90 min.	34.89	1.41	-36.96	36.98	272.18
	100°C – 60 min.	39.44	-1.81	-32.49	32.54	266.81
	100°C – 60 min./Dendrimer applied	33.20	2.61	-37.10	37.19	274.03
	90°C – 90 min.	40.17	-0.40	-35.74	35.74	269.36
	90°C – 90 min./Dendrimer applied	36.78	2.68	-39.92	40.01	273.85
	80°C – 90 min.	41.16	-3.06	-30.36	30.51	264.25
Isolan Dark Blue 2S-GL	100°C – 90 min.	28.67	-1.51	-13.30	13.39	263.52
	100°C – 60 min.	36.46	-2.71	-13.02	13.29	258.24
	100°C – 60 min./Dendrimer applied	31.84	-1.99	-12.74	12.90	261.14
	90°C – 90 min.	34.96	-2.31	-12.85	13.05	259.80
	90°C – 90 min./Dendrimer applied	30.46	-1.64	-13.03	13.22	262.82
	80°C – 90 min.	36.89	-1.94	-11.63	1.79	260.52
Realan Blue RC	80°C – 90 min./Dendrimer applied	35.78	-2.64	-12.12	12.40	257.71
	100°C – 90 min.	32.86	-0.93	-31.17	31.18	268.29
	100°C – 60 min.	36.97	-2.05	-29.59	29.68	266.03
	100°C – 60 min./Dendrimer applied	31.62	0.04	-31.71	31.71	270.07
	90°C – 90 min.	35.20	-1.83	-31.12	31.17	266.63
	90°C – 90 min./Dendrimer applied	33.27	0.01	-31.18	31.18	270.02
Realan Blue RC	80°C – 90 min.	39.09	-2.85	-28.45	28.59	264.29
	80°C – 90 min./Dendrimer applied	33.85	-0.61	-32.46	32.47	268.92

Table 2

CIELAB VALUES OF ANGORA FIBERS UN-TREATED AND DENDRIMER APPLIED (AT OPTIMUM CONDITIONS)						
Dye	Total dyeing time	L	a	b	c	H
Telon Blue M-RLW	100°C – 90 min.	42.68	3.23	-44.71	44.83	274.13
	100°C – 60 min.	48.05	0.60	-40.63	40.64	270.85
	100°C – 60 min./Dendrimer applied	44.98	2.12	-43.80	43.58	272.77
	90°C – 90 min.	45.41	1.60	-42.65	42.68	272.15
	90°C – 90 min./Dendrimer applied	43.49	2.98	-44.14	44.24	273.87
	80°C – 90 min.	48.37	-0.11	-39.17	39.17	269.84
Isolan Dark Blue 2S-GL	80°C – 90 min./Dendrimer applied	45.90	2.40	-43.40	43.47	273.16
	100°C – 90 min.	33.06	-0.38	-16.19	16.20	268.64
	100°C – 60 min.	49.53	-1.25	-12.71	12.77	264.38
	100°C – 60 min./Dendrimer applied	41.76	-1.39	-15.36	15.43	264.85
	90°C – 90 min.	49.25	-1.30	-14.57	14.63	264.89
	90°C – 90 min./Dendrimer applied	42.87	-1.47	-16.79	16.85	265.00
Realan Blue RC	80°C – 90 min.	50.45	-1.57	-13.59	13.68	263.39
	80°C – 90 min./Dendrimer applied	45.86	-1.65	-15.39	15.48	263.90
	100°C – 90 min.	38.00	-0.87	-39.40	39.41	268.74
	100°C – 60 min.	48.64	-4.49	-33.97	34.27	262.47
	100°C – 60 min./Dendrimer applied	41.88	-2.36	-37.75	37.82	266.43
	90°C – 90 min.	46.37	-3.71	-36.20	36.39	264.16
Realan Blue RC	90°C – 90 min./Dendrimer applied	40.38	-1.49	-38.56	38.58	267.79
	80°C – 90 min.	50.99	-4.29	-34.16	34.43	262.85
	80°C – 90 min./Dendrimer applied	43.89	-2.98	-36.13	36.26	265.28

Table 3

WASHING FASTNESS TEST RESULTS OF MOHAIR AND ANGORA FIBERS UN-TREATED AND DENDRIMER APPLIED (AT OPTIMUM CONDITIONS) DYED WITH REACTIVE DYE								
Dye	Fibers	Total dyeing time	Washing fastness					
			WO	PAC	PES	PA	CO	CA
Realan Blue RC	Mohair	100°C – 90 min.	5	5	5	5	4-5	5
		100°C – 60 min./Dendrimer applied	5	5	5	5	4-5	5
		90°C – 90 min./Dendrimer applied	5	5	5	5	4-5	5
		80°C – 90 min./Dendrimer applied	5	5	5	5	4-5	5
	Angora	100°C – 90 min.	5	5	5	5	4-5	5
		100°C – 60 min./Dendrimer applied	5	5	5	5	4-5	5
		90°C – 90 min./Dendrimer applied	5	5	5	5	4-5	5
		80°C – 90 min./Dendrimer applied	5	5	5	5	4-5	5

Furthermore, taking into consideration that dyeing pH is 5, there should be some un-protonated amine groups and they can serve as highly reactive nucleophilic sites for the reactive dyes.

CIELab values of fibers dyed (untreated and dendrimer applied) are illustrated in table 1 and 2. When table 1 and 2 are examined, it is seen that, generally, the differences in a^* and b^* values of the color obtained in the un-treated and dendrimer applied fibers are smaller. If L values are examined, it can be seen that these are higher for the un-treated fibers. L value is the lightness-darkness value and its increase shows that the color gets lighter. From this perspective, the results obtained are parallel with the K/S values. When table 3 is

examined, it can be seen that there is no negative effect of dendrimers on the washing fastnesses.

CONCLUSION

In this investigation, dendrimer is suggested for improving mohair and Angora fibers dyeability. According to the experimental results, it can be concluded that, dendrimer application will increase the dye-uptake of mohair and Angora fibers and will give chance to carry out low temperature dyeings, especially for mohair fibers dyeing with reactive dyes.

ACKNOWLEDGEMENTS

This study was carried out at Ege University Textile Engineering Laboratories. We would like to express our gratitude to all those who gave us the possibility to complete this study.

BIBLIOGRAPHY

- [1] Froehling, P.E. *Dendrimer and Dyes – A review*. In: Dyes and Pigments, 2001, vol. 48, p.187
- [2] Burkinshaw, S.M., Mignanelli, M., Froehling, P.E., Bide, M.J. *The use of dendrimers to modify the dyeing behavior of reactive dyes on cotton*. In: Dyes and Pigments, 2000, vol. 47, p. 259
- [3] Burkinshaw, S.M., Mignanelli, M., Froehling, P.E. *The effect of hyper-branched polymers on the dyeing of polypropylene fibers*. In: Dyes and Pigments, 2002, vol. 53, p. 229
- [4] Yiyun, C., Jiepin, Y. *Effect of polyamidoamine dendrimers in de-coloring triarylmethane dye effluent*. In: Coloration Technology, 2005, vol. 121, issue 2, p.72
- [5] Atav, Riza and Yurdakul, Abbas. *Comparison of dyeing characteristics of luxury fiber (mohair and Angora) with wool*. In: Industria Textilă, 2009, vol. 60, issue 4, p. 187

Authors:

RIZA ATAV

Department of Textile Engineering,
Namık Kemal University, Çorlu-Tekirdağ
59860 Turkey

E-mail: rizaatav@corlu.ege.edu.tr

ABBAS YURDAKUL

Department of Textile Engineering
Ege University – Bornova
Izmir, Turkey

INDUSTRIA TEXTILĂ ÎN LUME

COVER MULTISTRATIFICAT PURE MOSS

Compania **Bayer MaterialScience**, în colaborare cu **Kymo GmbH**, din Karlsruhe – Germania, a creat o nouă inovație în domeniul materialelor de acoperire a pardoselii, și anume un covor vâscoelastic, din spumă poliuretanică și un material textil special, ce oferă senzația mersului pe un mușchi moale.

Datorită designului inovator, avangardist, **Kymo** a devenit unul dintre producătorii de top ai acoperitoarelor de pardoseli destinate locuințelor, sau spațiilor publice și comerciale.

Kymo a prezentat primul covor vâscoelastic, *Pure Moss*, la Salonul produselor destinate amenajărilor interioare, *IMM Cologne*. Noul concept se bazează pe o structură multistratificată: un strat superior din tricot bielastic, cu textură moale de pluș înalt, care face ca structura spumei să cedeze numai sub presiunea tălpii, nu și în zonele adiacente; un strat poliuretanic vâscoelastic, care – fiind foarte moale – permite cufundarea

piciorului, iar, sub el, o spumă din material poliuretanic reciclat, care oprește compresia la o adâncime specifică, prevenind comprimarea totală a întregii structurii și un strat inferior dintr-un material subțire de consolidare, ce conferă stabilitate întregii structurii și rezistență la rupere.

Principiul modular permite controlul asupra unor proprietăți mecanice ale straturilor poliuretanică, precum modulul de duritate-elasticitate. Proprietățile vâscoelastice ale noului covor oferă un nivel ridicat de confort și reduc tensiunea exercitată asupra încheieturilor și membrilor, făcându-le adecvate diverselor aplicații: articole pentru sport, casă, spații de lucru publice și comerciale, dar și spații destinate copiilor mici și vârstnicilor, fizioterapie etc. În plus, conținutul mare de spumă poliuretanică oferă covoarelor excelente proprietăți termoizolatoare, atenuază impactul și, în consecință, propagația zgomotului.

Smarttextiles and nanotechnology,
martie 2010, p. 10

Net curtain fabrics offering electromagnetic shielding

HÜSEYİN GAZI ORTLEK

REZUMAT – ABSTRACT – INHALTSANGABE

Materiale de ecranare tip rețea ce oferă protecție electromagnetică

Lucrarea prezintă un studiu preliminar al dezvoltării unui material de ecranare tip rețea, destinat prevenirii emanației de informații secrete prin emisia nedorită de energie electromagnetică radiată de surse interne ale unor edificii speciale, cum sunt cele militare, guvernamentale, bancare etc. Rezultatele experimentale indică faptul că performanța materialelor de ecranare tip rețea privind EMSE poate fi îmbunătățită prin combinarea structurii hibride a firului cu valoarea și caracteristicile parametrilor firelor metalice.

Cuvinte-cheie: protecție electromagnetică, rețea metalică, fire hibride, material de ecranare tip rețea

Net curtain fabrics offering electromagnetic shielding

This paper presents a preliminary study for the development of the net curtain fabric meant to prevent the emanation of secret information from the unwanted emission of electromagnetic energy radiated by internal sources of some special buildings such as military, government, banks, etc. The experimental results indicate that the EMSE performance of net curtain fabrics could be tailored by a combination of hybrid yarn structure, the amount and the characteristics of metal wire parameters.

Key-words: electromagnetic shielding, metal grid, hybrid yarns, net curtain fabric

Netzabschirmungsmaterialien für den elektromagnetischen Schutz

Die Arbeit stellt eine Vorstudie vor, der Entwicklung eines Netzabschirmungsmaterialies für den Schutz der Emanation von Geheiminformationen durch die unerwünschte elektromagnetische Energiestrahlung aus internen Quellen spezieller Gebäude, wie die Militärischen Gebäude, Regierungsgebäude, Bankgebäude usw. Die experimentellen Ergebnisse zeigen die Tatsache, dass die Leistung der Netzabschirmungsmaterialien betreff EMSE verbessert werden können durch die Kombination der hybriden Struktur des Garnes mit der Summe und die Eigenschaften der Parameter der Metallgarne.

Schlüsselwörter: elektromagnetischen Schutz, metallisches Netz, Hybridgarne, Netzabschirmungsmaterialien

The usage of electrical and electronic equipments has grown rapidly with the development of science and technology. Many devices used in our daily life, such as cell phones, computers, microwave ovens, televisions, printers, modems working with different frequency and different power produce electromagnetic (EM) fields. The EM fields have led to important problems such as electromagnetic interference (EMI) of electronic devices and health issues. In the future, it is likely to become more severe with the development of information technology as well as electronic devices [1–3].

EM energy is the only form of energy that can be used effectively to transmit signals over long distances, in free space, under controlled conditions. Even though most of the transmissions are achieved under controlled conditions, the transmitted energy that may create an interference phenomenon affects the performance of many electronic devices. The most common type of EMI occurs in the radio frequency (RF) range of the EM spectrum, from 10^4 to 10^{12} Hz. The EMI problem is becoming more critical, due to the smaller size and faster operating speeds of electronic devices, which make it more difficult to manage the EM pollution they create. Increased device frequencies cause proportionally decreased wavelengths that can pass through very small holes and slits of equipment cabinets. Consequently, regulations on the EM wave emission of electronic products are getting stricter around the world [4].

Furthermore, when a high frequency electromagnetic wave gets into an organism, it vibrates molecules to give out heat [5]. The network of veins within high-risk organs, such as eyes, could be weakened because this

heat cannot be easily dissipated [6]. Moreover, it brings on abnormal chemical activities to produce cancer cells and increases the possibility of leukemia and other cancers [5]. There is an ongoing controversy worldwide about the potential health hazards associated with the exposure to electromagnetic fields [4]. Believing that prevention is better than cure, a great deal of effort is needed for the development of electromagnetic shielding materials.

Traditionally, shielding techniques are based on the use of stiff metallic materials with well-known electromagnetic properties [7]. Shields made of metal are expensive, heavy and not always convenient or sometimes even entirely unsuitable for application. Some special textiles, which are integrated with metallic materials, can be used as a shielding material. One advantage of shields made of textiles is their lightness and considerably lower cost, in comparison with shields made of metal sheets or wire mesh [8].

The development of textiles that have electromagnetic shielding properties originated in the military industry and moved gradually to civilian industries [5].

In recent years, a number of investigations have been carried out on electromagnetic wave resistant textiles. Roh, J. S. et al. [5] and Su, C. I. & Chern, J. T. [6] studied the EMSE of fabrics that have different constructions and are made of several kinds of composite yarns. Lai, K. et al. [8] examined the electromagnetic shielding effectiveness, using metal coating films and a vacuum evaporation deposition technique, with the woven fabrics made of metal/polyester (PET) filaments. Koprowska et al. [7] and Aniolczyk et al. [8] examined new shielding nonwoven textiles that were produced by electrically conductive fibers, Nitril-Static®.

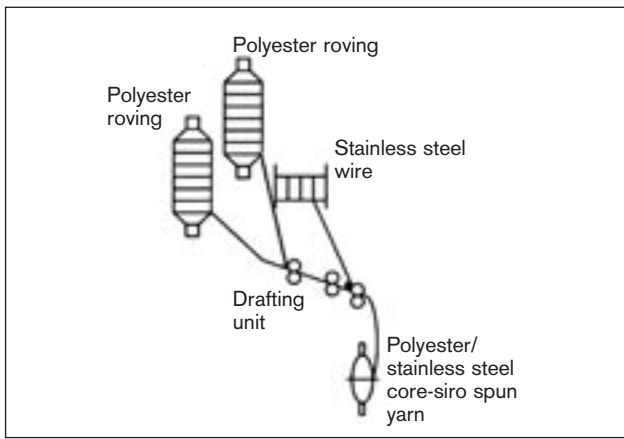


Fig. 1. Core-siro spun spinning mechanism

Cheng, K. B. et al. [9, 10] have studied the production methods of woven and knitted fabrics meant for electromagnetic shielding applications; their methods include the production of different kinds of blended yarns containing stainless steel (SS) and PET staple fibers. In another paper, Cheng, K. B. et al. [11] showed a fabrication method for conductive fabrics, which knitted from stiff copper wires and glass fibers, in an uncommingled yarn form, reinforced polypropylene for electromagnetic shielding. Kim, T. and Chung, D. D. L. [12] compared mats and fabrics made of bare carbon fibers, metal-coated carbon fibers and metal-coated polymer fibers.

Today's information theft is a serious threat to government security and high profile business. Electronic equipments used in office, such as wireless networks, laptops, cellular phones, computer monitors and keyboards release electromagnetic fields that are intercepted and decoded by high-tech criminals. The primary objective of this research work is to develop a net curtain fabric to strengthen the weak points of some special buildings in order to prevent the emanation of secret information from the unwanted emission of electromagnetic energy radiated by internal sources.

MATERIALS AND METHODS

Hybrid yarns used in the construction of curtain fabrics were produced with commercially available metal wires, PET staple fibers and PET filaments. AISI 316 L type SS wire, 0.035 mm in diameter (70 denier), and silver

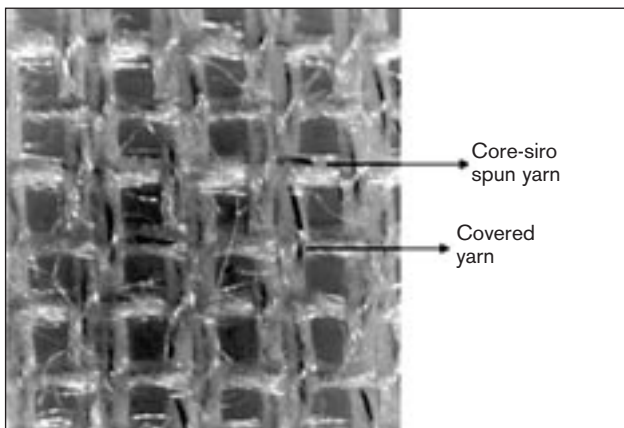


Fig. 3. The fabric samples coded AB at the magnification of 25 X

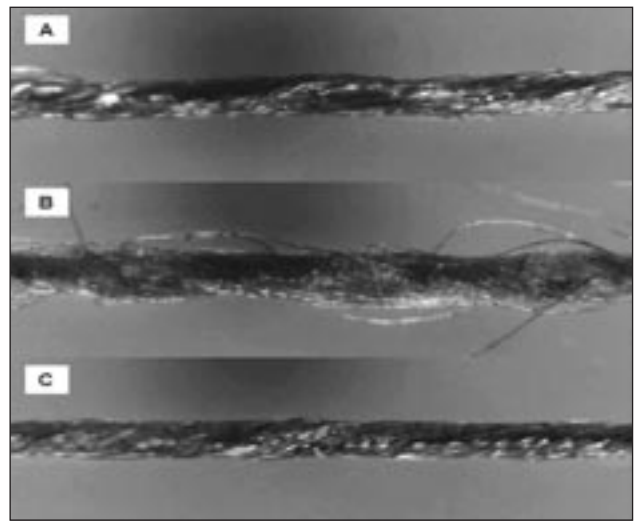


Fig. 2. Longitudinal views of hybrid yarns at the magnification of 45 X

plated copper wire (Cu/Ag) of 0.059 mm (173 denier) were used as conductive part of hybrid yarns. The SS wire has a 8.0 kg/dm^3 density and $785 \Omega/\text{m}$ DC resistance, whereas the Cu/Ag wire has a density of 8.9 kg/dm^3 and a DC resistance of $3.72 \Omega/\text{m}$. The codes, composition and characteristics of the hybrid yarns are listed in table 1. Hybrid yarns coded A and C are produced by the hollow spindle covering technique, whereas hybrid yarns coded B are produced by core-siro spun spinning technique.

The production system of hybrid yarns coded B is illustrated in figure 1. Two polyester rovings of 4086 denier linear density were adapted as cover materials, whereas 70 denier SS wire was used as core material. The longitudinal views of hybrid yarns coded A, B and, respectively, C are given in figure 2.

Since, Su, C. I. and Chern, J. T. stated in their study that 1/1 plain weave fabric type shows the optimum EMSE, the net curtain fabric samples were produced in a 1/1 plain weave, on an automatic rapier weaving machine. All fabric samples had 32 ends/cm warp and 22 picks/cm weft densities. Hybrid yarns coded A were used as warp yarns for all samples. For the sake of simplicity, fabric samples were classified according to the following general form: first letter stands for warp yarn type and second letter stands for weft yarn type. For example when producing fabric sample coded AC,

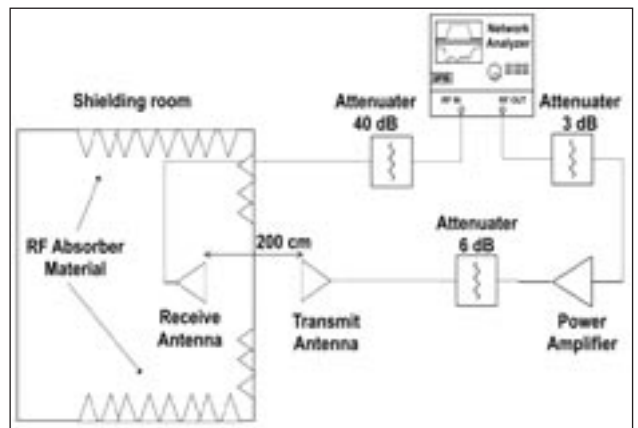


Fig. 4. Schematic diagram of the EMSE test setup

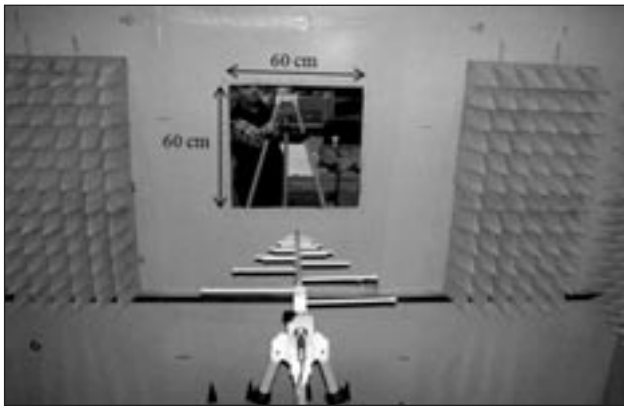


Fig. 5. Test area in the shielding room

the hybrid yarn coded *A* was used as warp yarn, whereas hybrid yarn coded *C* was used as weft yarn. During the weaving process, it was observed that the cover part of hybrid warp yarns was scraped, when the reed was pushed to the weft. To solve this problem, two warp yarns were passed into the same teeth on the reed, as can be seen in figure 3.

The EMSE of the fabric samples was measured according to IEEE Standard 299-1997 [13]. A schematic diagram of the test setup is shown in figure 4. The electromagnetic frequency range, comprising the lower frequency limit of electromagnetic radiated emissions, can be swept from 0.030 GHz to 2.5 GHz.

The opening on the wall of the shielding room is in the shape of a 60 cm square (fig. 5). Measurements were performed by using the horizontal polarization of antennas. For different frequency ranges, the different antennas, such as bi-conical, log-periodic and horn, were used.

The definition of shielding effectiveness is as follows: $EMSE [dB] = 20 \log (E_1 / E_2)$, where the value of the electric field component E_1 is measured without the fabric samples, whilst E_2 is measured with the fabric samples at the opening on the shielding room.

RESULTS AND DISCUSSION

The EMSE values of the fabric samples with the incident frequency ranging from 30 MHz to 2.5 GHz are given in figure 6, 7 and 8. All kinds of fabric samples were obviously frequency dependent and showed a

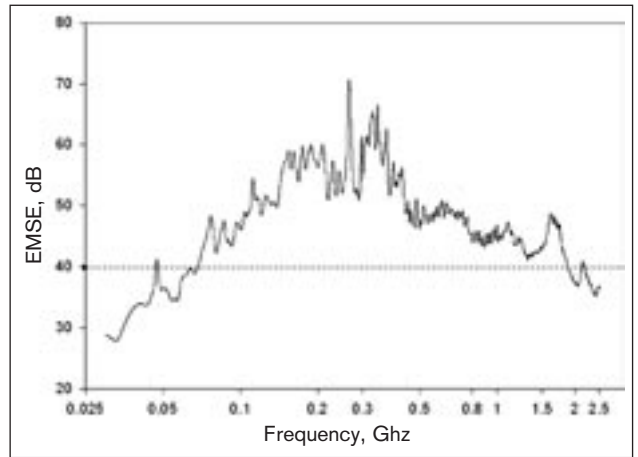


Fig. 6. EMSE values of sample *AA*

similar trend. The overall EMSE of fabric samples initially increases as the frequency increases, and then declines. We have emphasized on the graphics the 40 dB lines, since many practical EMI problems related with the unwanted emissions can be solved by an EMSE value of 40 dB.

As it can be seen in figure 6, the EMSE values of the *AA* fabric are above 40 dB, from 68.6 MHz to 1.88 GHz. The EMSE value of the *AA* fabric reached 70.65 dB at 266 MHz. The EMSE values of the *AB* fabric were found above 40 dB from 46.5 MHz to 2.25 GHz, as seen in figure 7. The maximum EMSE value of *AB* fabric was found 70.08 dB at 307 MHz. The frequency range of the *AB* fabric samples, in which the EMSE is higher than 40 dB, is wider than that of the *AA* fabric samples. This result is attributed to the fact that *AB* fabric has a larger amount of SS wire than the *AA* fabric.

The fabric *AC* displays an EMSE above 40 dB from 54.12 MHz to 2.41 GHz, even though the EMSE decreases to 38.05 dB between 62.50 MHz and 67.35 MHz (fig. 8). The maximum EMSE value of the *AC* fabric was found 72.1 dB at 370 MHz.

The *AC* fabric shows higher EMSE properties than other fabric samples, in respect to the range of frequency in which the EMSE value of fabrics exceeds 40 dB. This result is due mainly to the type and the highest rate of metal wire used for the production of *AC* fabric samples (table 1).

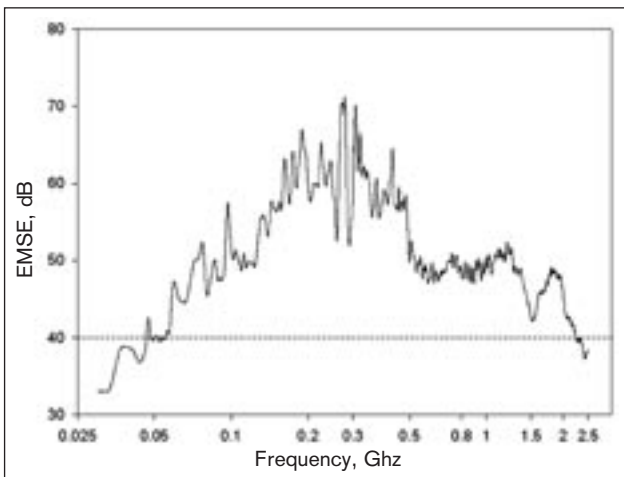


Fig. 7. EMSE values of sample *AB*

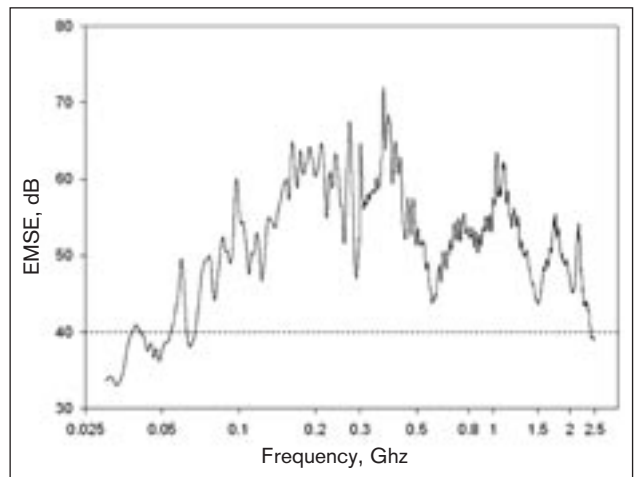


Fig. 8. EMSE values of sample *AC*

Table 1

CHARACTERISTICS OF THE HYBRID YARNS					
Yarn code	Yarn type	PET	Metal wire	Composition, %	Linear density, denier
A	Covered yarn	150d48f continuous filament	SS	PET: SS (63-37)	240
B	Core-siro spun yarn	1.44 denier 38 mm staple fiber	SS	PET: SS (60-40)	220
C	Covered yarn	150d48f continuous filament	Cu/Ag	PET: Cu/Ag (44-56)	343

Although all the fabric samples have the same weft and warp densities, the grid openness of the AC fabric is lower than that of other fabric samples, since the linear density of Cu/Ag, used for the production of hybrid yarns coded C, is higher than that of the SS wire. Roh et al. stated that the longer openings caused the overall shielding effectiveness to drop, for the fabrics with the same warp openings [3]. The lower grid openness of the AC fabrics is also one of the reasons for the higher EMSE properties of the AC fabrics.

CONCLUSIONS

In this study, we have developed three types of net curtain fabrics offering EMSE properties. It has been shown that the EMSE performance of the fabric can be tailored in a number of ways, such as grid openness, varying hybrid yarn structure and metal content. Net curtain fabrics developed can be used to strengthen the walls and windows, in order to prevent the emission of electromagnetic energy containing secret information, in respect to the counter-intelligence. These net curtain fabrics can also be used in our house and office buildings for protection against electromagnetic radiation from the base stations of cellular phones, TV and radio broadcasting antennas, wireless network etc.

Acknowledgements

I am thankful to Mr. Bayram Surmeli, as well as to many colleagues of *Cihan Textile Company* for their support in undertaking this work. Sincere thanks are also owed to the *National Research Institute of Electronics and Cryptology of Turkey (UEKAE)* for providing their test facilities to evaluate the electromagnetic shielding effectiveness of the fabric samples. I also wish to thank Dr. Omer Galip SARACOGLU from the *Electrical and Electronic Eng. Dept. at Erciyes University* for our valuable discussions.

BIBLIOGRAPHY

- [1] Martinkova, L. *Materiale țesute și tricotate rezistente la flacără și antielectrostatice, obținute prin utilizarea unor noi tehnici de tricotare*. În: *Industria Textilă*, 2008, vol. 59, issue 3, p. 73
- [2] Nicula, Ghe., Belu, N., Necula, E. *Cercetări privind realizarea materialelor textile destinate prevenirii poluării*. În: *Industria Textilă*, 2003, vol. 59, issue 3, p. 113
- [3] *Brevet pentru un nou material de protecție*. În: *Industria Textilă*, 2009, vol. 60, issue 3, p. 180
- [4] Roh, J.-S., Chi, Y.-S., Kang, T. J., Nam, S.-W. *Electromagnetic shielding effectiveness of multifunctional metal composite fabrics*. În: *Textile Ressearch Journal*, 2008, vol. 78, issue 9, p. 825
- [5] Su, C.-I., Chern, J.-T. *Effect of stainless steel-containing fabrics on electromagnetic shielding effectiveness* În: *Textile Ressearch Journal*, 2004, vol. 74, issue 1, p. 51
- [6] Lai, K., Sun, R.-J., Chen, M.-Y., Wu, H., Zha, A.-X. *Electromagnetic shielding effectiveness of fabrics with metalized polyester filaments*. În: *Textile Ressearch Journal*, 2007, vol. 77, issue 4, p. 242
- [7] Koprowska, J., Pietranik, M., and Staski, W. *New Type of textiles with shielding properties*. În: *Fibres & Textiles in Eastern Europe*, 2004, vol. 12, issue 3, p. 39
- [8] Aniolczyk, H., Koprowska, J., Mamrot, P., Lichawska, J. *Application of Electrically conductive Textiles as Electromagnetic Shields in Physiotherapy*. În: *Fibres & Textiles in Eastern Europe*, 2004, vol. 12, issue 4, p. 47
- [9] Cheng, K. B., Lee, M. L., Ramakrishna, S., Ueng, T. H. *Electromagnetic shielding effectiveness of stainless steel/polyester woven fabrics*. În: *Textile Ressearch Journal*, 2001, vol. 71, issue 1, p. 42
- [10] Cheng, K. B. *Production and electromagnetic shielding effectiveness of the knitted stainless steel/polyester fabrics*. În: *Journal Text. Eng.*, 2000, vol. 46, issue 2, p. 42
- [11] Cheng, K. B., Ramakrishna, S., Lee, K. C. *Electromagnetic shielding effectiveness of copper/glass fiber knitted fabric reinforced polypropylene composites*. În: *Composites. Part A: Appl. Sci. Manufact.*, 2000, vol. 31, p. 1 039
- [12] Kim, T., Chung, D. D. L. *Mats and Fabrics for electromagnetic interference shielding*. În: *Journal of Materials Engineering and Performance*, 2006, vol. 15, issue 3, p. 295
- [13] *IEEE Standard method for measuring the effectiveness of electromagnetic shielding enclosures*. IEEE Standard 299-1997

Author:

HÜSEYİN GAZİ ORTLEK
 Department of Textile Engineering
 Erciyes University
 38039, Kayseri – Turkey
 e-mail: ortlekh@erciyes.edu.tr



Characterization on pore size of honeycomb-patterned micro-porous PET fibers using image processing techniques

FAMING WANG

SHANYUAN WANG

REZUMAT – ABSTRACT – INHALTSANGABE

Caracterizarea mărimii porilor la fibrele PET microporoase cu structură tip fagure, prin utilizarea tehnicilor de prelucrare a imaginii

Lucrarea prezintă o metodă de caracterizare a structurii porilor de suprafață ai fibrelor PET cu structură tip fagure, prin utilizarea microscopiei electronice cu scanare (SEM) și a tehnicilor de prelucrare a imaginii. Ei se constituie în pori cu caneluri lineare și pori tip elipsă. Distribuția porilor de suprafață și numărul de micropori variază de la o fibră la alta, ceea ce poate determina diferențe semnificative ale proprietăților firelor filate. Se propune o clătire suficientă, cu apă curată, a fibrelor, anterior proceselor de deshidratare și fixare, în vederea eliminării efectului de supraîncărcare/înfundare a porilor.

Cuvinte-cheie: morfologie de suprafață, pori cu canelură lineară, pori tip elipsă, tehnică de prelucrare a imaginii

Characterization on pore size of honeycomb-patterned micro-porous PET fibers using image processing techniques

This paper presents a method to characterize the pore structure of the fibre surface for the honeycomb-patterned PET fibers, by using a scanning electron microscopy (SEM) and image processing techniques. They consist of linear channel pores (LCP) and ellipse pores (EP). The surface pore distribution and micropore numbers varied from each fiber to another, which can make significant differences on the property of the spun yarns. It is proposed that the fiber should be sufficiently rinsed with clean water before dewatering and setting processes, to eliminate the pore-clogging effect.

Key-words: surface morphology, linear channel pore, ellipse pore, image processing technique

Die Charakterisierung der Porengröße bei den mikroporösen PET-Faser mit Wabenstruktur, durch Benutzung von Bildbearbeitungstechniken

Die Arbeit stellt vor eine Charakterisierungsmethode der Struktur der Oberflächenporen der PET-Faser mit Wabenstruktur, durch Benutzung von elektronischen Mikroskopie mit Bildaufnahme (SEM) und Bildbearbeitungstechniken. Sie sind Poren mit linearen Rillen (LCP) und ellipsenartige Poren (EP) bestehen. Die Verteilung der Oberflächenporen und die Anzahl der Mikroporen schwankt in Abhängigkeit der Faser, was zu wesentlichen Unterschiede der Spinnfasereigenschaften führen kann. In diesem Sinne wird vor den Prozessen für Entfeuchtung (Trocknung) und Fixierung, eine ausreichende Spülung mit reinem Wasser der Faser für die Absonderung des überporositäteffektes (Porenanhäufung), vorgeschlagen.

Schlüsselwörter: Oberflächenmorphologie, Porengröße, Poren mit linearen Rille, ellipsenartige Poren, Bildbearbeitungstechniken

Sportswear, in particular, needs to absorb water and moisture after intense exercise. Synthetic fiber without such function is not suitable for sportswear because of stiffness and stickiness. For this reason, the development of a functional synthetic fiber with water transport and quick dry properties was a major objective over a long period. At present, two approaches can be used to make these functional fabrics. One method to produce such fabrics is using profiled fibers, which can be achieved by using spinning boards with specially designed nozzles. The profiled fibers, such as tetra-channel fiber *Coolmax*, by DuPont (Kajiwara et al., 2000), are mainly used in the market worldwide to produce moisture absorption and quick dry fabrics. The air trapped inside the hollow channel fiber is deemed as a kind of thermal insulating material, which reduces the weight of textiles and keeps the human body warm (Jackson et al., 1994; Dave et al., 1987; Hu et al., 2005). The second approach is using the micro-porous fibre, such as porous hollow fiber *Wellkey*, by Teijin (Wang et al., 2009). Hundreds of thousands of micro pores run through both inside of the fiber and on the surface, which can be treated as a major way to transport water and transfer the moisture vapor.

Previous studies devoted to developing methods of measuring pore characteristics can be found in many porous media fields. The pore structure analysis was

reported by using various micro porous techniques, such as the scanning tunneling microscopy – *STM* (Vignal et al., 1999), scanning electron microscopy – *SEM* (Oshida et al., 1995), transmission electron microscopy – *TEM* (Oshida et al., 1995; Yoshizawa et al., 1998) and other normal optical microscopy (Oshida et al., 1996). Fatt introduced the model of porous media in the rock science (Fatt, 1996). Lot of works were down also in the same rock field (Bakke et al., 1996; Blunt et al., 1991; Delerue et al., 2002, 1999; Hidajat et al., 2002). The pore size distribution and modeling were studied also in nonwoven and membrane fields by using image processing techniques (Zeng et al., 2000; Dimassi et al., 2008). However, the image processing technique applied to such a honeycomb-patterned micro-porous fiber has not yet been reported.

The objective of this study is to use the SEM and image processing technique to measure the pore size of the honeycomb-patterned micro-porous polyester fiber. Four parameters are proposed in this paper to characterize the fiber pore size property. Furthermore, the frequency histogram pictures for the four parameters are also presented and analyzed. Finally, some conclusions and suggestions are projected.

METHODOLOGY

The fibers were observed under a JSM-5610 scanning electron microscopy (JEOL, Japan). It was observed

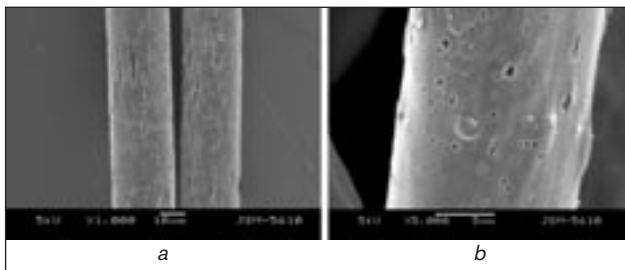


Fig. 1. Linear channel pores (LCP) and ellipse pores (EP):
a – LCPs on the fiber surface; b – EPs on the fiber surface

that there are mainly two kinds of pores on the fiber surface. One type of pores have long channels, which are so called linear channel pores (LCP); another type of pores have an ellipse shape, which are called ellipse pores (EP), as seen in figure 1. These two types of pores greatly increased the fiber specific area, so the water transport property of fiber assemblies is highly enhanced.

It was assumed that each pore on the fiber surface is flat and has a certain depth. Hence, the external shape of these two types of pores can be marked in yellow color by the Paint drawing tool (Microsoft). The JEOL SmileView software (JEOL, Japan) was then used to measure the size of the yellow marked pores. The major diameter D_m , minor diameter D_{mi} of the pore, the ratio of the major and minor pore diameter R , and the pore surface area S_p were used to characterize the size properties of pores on the fiber surface. For LCP, the shape is deemed as diamond-patterned, and then the pore surface area can be calculated by:

$$S_{LCP} = ab \quad (1)$$

where:

S_{LCP} is the pore surface area, μm^2 ;

a – the major diameter of the pore, μm ;

b – the minor diameter of the pore, μm .

For the EP, the surface area SEP of a pore on the fiber surface can be expressed as

$$S_{LCP} = \pi ab/4 \quad (2)$$

The SEM images after the size measurements are presented in figure 2.

RESULTS AND DISCUSSION

The results of maximum, average, and minimum values for the four parameters of the LCP and EP are listed in

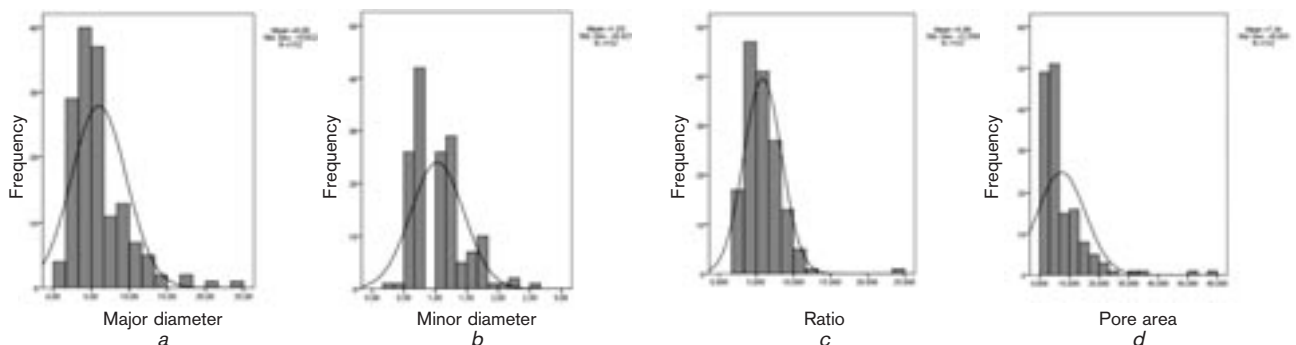


Fig. 3. The frequency histogram pictures of D_m , D_{mi} , R , S_p of LCPs:
a – the major diameter; b – the minor diameter; c – the ratio of major/minor diameter; d – the pore surface area

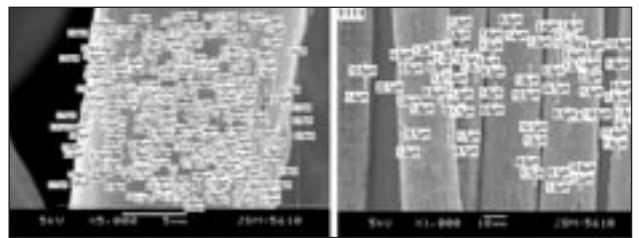


Fig. 2. The pore sizes on the fiber surface measured by JEOL SmileView software

table 1. It was found that the ratio R for LCP is about 3 times higher than that of the EP. For the pore surface area, the averaged value for the LCP is about 62 times that of the EP. Hence, EP on the fiber surface should be amplified to 5,000 times, under a SEM, in order to get an enough clear image.

Three hundred and four measurements were obtained for the LCPs. The frequency histogram pictures were drawn by using the SPSS software, as shown in figure 3. It was found that the major diameter of the LCP has a large distribution, i.e. varied from 1 to 24.70 μm . However, most of the values of the D_m are ranged from 1.67 to 6.67 μm . The minor diameter D_{mi} has a good centralization, about 85% of values ranged from 0.5 to 1.3 μm . For the pore area S_p , it has a standard deviation of 8.093, which showed that values varied a lot. This was mainly due to the larger distribution of the D_m values. The major/minor diameter ratio R was found above 1.67, which proved that the LCPs have long and narrow channels on the fiber surface.

Similarly, three hundred and ten measurements were obtained for the EPs on the fiber surface.

The frequency histogram pictures for the major diameter, minor diameter, ratio of major/minor diameter and the surface area were also drawn, as seen in figure 4.

It can be easily found that the standard deviations of D_m , D_{mi} , R , S_p for EP were 0.335, 0.260, 1.046 and 0.144 respectively, which are much smaller than the values of the LCPs. Hence, EPs have good centralization on those four parameters compared with the LCPs. The majority of D_m values for the EP were ranged from 0.25 to 0.67 μm . For the minor diameter D_{mi} , the main averaged range was from 0.10 to 0.37 μm . Comparing the pore size areas of the EPs with those of the LCPs, EPs have only 1/80 to 1/58 of the LCPs pore area. Thus, EPs are much smaller than the LCPs, which have close to circular shapes on the fiber surface, other than the linear channels for the LCPs.

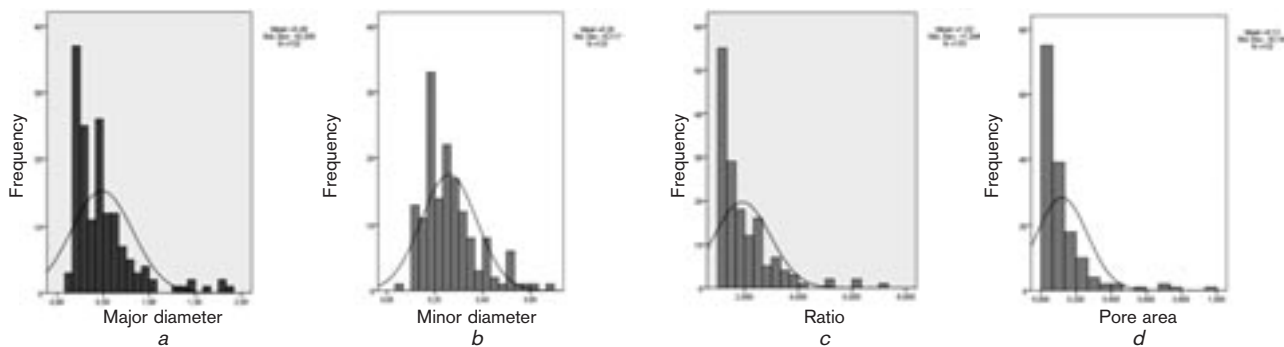


Fig. 4. The histogram pictures of D_m , D_{mi} , R , S_p of ECPs:
 a – the major diameter; b – the minor diameter; c – the ratio of major/minor diameter; d – the pore surface area

Table 1

Parameters	Values for LCP			Values for EP		
	Max.	Mean	Min.	Max.	Mean	Min.
D_m , μm	24.70	5.99	1.00	1.84	0.49	0.14
D_{mi} , μm	2.60	1.03	0.20	0.68	0.26	0.04
R	24.50	5.82	1.67	7.25	1.88	1.00
S_p , μm^2	56.81	6.18	0.60	0.98	0.099	0.0075

Since the pore size of the EP was relatively small, it is suggested that the fibers should be rinsed sufficiently to prevent the pore clogging during the whole further finishing process.

CONCLUSIONS

This paper presents a method for the pore size measuring of the honeycomb-patterned microporous

PET fiber. The pore size was measured and analyzed by a JEOL 5610 SEM and the SmileView image processing software. It was found that the micro pores could be classified into two types, LCP and EP. For the LCP, the averaged major and minor diameters were 5.99 μm and 1.03 μm , respectively. EPs have a good centralization on the fiber surface, as compared to the LCPs, of which the averaged major and minor diameters were 0.49 μm and, respectively, 0.26 μm . It was also found that the pore size distribution varied a lot for each fiber, which may cause the yarn strength varied from each other. Further studies should be paying more attention to the effect of the pore distribution on the yarn strength.

ACKNOWLEDGEMENTS

The test was conducted in the key Lab of Textile Manufacture and Technology, Zhejiang Sci-Tech University.

BIBLIOGRAPHY

- [1] Bakke, S., Oren, P. *3-d pore-scale modeling of heterogeneous sandstone reservoir rocks and quantitative analysis of the architecture, geometry and spatial continuity of the pore network*. European 3-D Reservoir Modeling Conference, Stanvanger, 1996, p. 35
- [2] Blunt, M., King, P. *Relative permeabilities from two- and three-dimensional pore-scale network modeling*. In: Transport in Porous media, 1991, vol. 6, p. 407
- [3] Blunt, M., Sher, H. *Pore network modeling of wet*. In: *Physical Review E*, 1995, vol. 52, p. 63
- [4] Dave, J., Kumar, R., Srivastava, H. C. *Studies on modification of polyester fabrics*. Vol. 1. *Alkaline hydrolysis*. In: Journal of Applied Polymer Science, 1987, vol. 33, issue 2, p. 455
- [5] Delerue, J., Perrier, E. *DXsoil a library for 3D image analysis in soil science*. In: Computer & Geoscience, 2002, vol. 28, p. 1 041
- [6] Delerue, J., Perrier, E., Yu, Z. et al. *New algorithms in 3D image analysis and their application to the measurement of a spatialized pore size distribution in soils*. In: Physics and Chemistry of the Earth. Part A: *Solid Earth and Geodesy*, 1999, vol. 24, issue 7, p. 639
- [7] Dimassi, M., Koehl, L., Zeng, X. et al. *Pore network modeling using image processing techniques*. In: International Journal of Clothing Science and Technology, 2008, vol. 20, issue 3, p. 137
- [8] Fatt, I. *The network model of porous media I. Capillary pressure characterization*. In: AIME Petroleum Transaction, 1956, vol. 270, p. 144
- [9] Hidajat, R., Singh, M., Nohanty, K. *Transport properties of porous media reconstructed from thin sections*. In: SPE Journal, 2002, p. 40
- [10] Hu, J., Li, Y. *Moisture Management Tester: A method to Characterize Fabric Liquid Moisture Management Properties*. In: Textile Research Journal, 2005, vol. 75, issue 1, p. 57
- [11] Jackson, David M., Matthews, Billie J. *High wicking liquid absorbent composite*. United States Patent US5350370, 1994
- [12] Kajiwara, K., Nori, R., Okamoto, M. *New Fibers from Japan*. In: Journal of the Textile Institute, 2000, Part 3, p. 55
- [13] Oshida, K., Erinaga, M., Inagaki, M. et al. *Pore analysis of isotropic graphite using image processing of optical micrographs*. In: Tanso, 1996, vol. 173, p. 142
- [14] Oshida, K., Kogiso, K., Matsubayashi, K. et al. *Application of image processing to high resolution SEM pictures of mesosphere pith-based carbon fibers and quantitative analysis of the structure*. In: Tanso, 1995, vol. 169, p. 207
- [15] Oshida, K., Kogiso, K., Matsubayashi, K. et al. *Analysis of pore structure of activated carbon fibers using high-resolution transmission electron microscopy and image processing*. In: Journal of Material Research, 1995, vol. 10, p. 2 507
- [16] Vignal, V., Morawski, M., Konno, H. et al. *Quantitative assessment of pores in oxidized carbon sphere using STM*. In: Journal of Material Research, 1999, vol. 14, p. 1 102
- [17] Wang, F., Zhou, X., Wang, S. *Development processes and property measurements of moisture absorption and quick dry fabrics*. In: Fibers & Textiles in Eastern Europe, 2009, vol. 17, issue 2, p. 46

- [18] Yoshizawa, N., Yamada, Y., Shiraishi, N. *TEM lattice images and their evaluation by image analysis for activated carbons with disordered micro-texture*. In: Journal of Material Sciences, 1998, vol. 33, p. 199
- [19] Zeng, X., Vasseur, C., Fayala, F. *Modeling micro geometric structures of porous media with a predominant axis for predicting diffusion flow in capillary*. In Applied Mathematical Modeling, 2000, vol. 24, p. 969

Authors:

Dr. eng. FAMING WANG
Thermal Environment Laboratory, EAT
Department of Design Sciences
Faculty of Engineering, Lund University
Lund SE-221 00, Sweden
e-mail: faming.wang@design.lth.se

Conf. dr. eng. SHANYUAN WANG
College of Textiles
Donghua University
Songjiang District
2999 North Remin Road
Shanghai 201620, China

NOTE ECONOMICE

CREȘTERI PE PIAȚA TEXTILELOR TEHNICE DIN S.U.A.

În anul 2009, din cauza recesiunii globale, vânzările de textile, din S.U.A., au scăzut cu 6,3%, iar exporturile cu 23%. Acest domeniu cuprinde cca 7 000 de companii, cu 1 500 de furnizori de fibre, fire și materiale și distribuitori de echipamente și servicii și 5 500 de fabricanți de produse finite. Valoarea acestor produse textile a fost în 2009 de 27,8 miliarde de dolari, iar în 2010 se estimează a fi de 26,8 miliarde de dolari. Datorită faptului că cererile armatei se mențin considerabile, din cauza conflictelor din Afganistan și Irak, acest sector a înregistrat o creștere de 10% – în anii 2008–2009, prin cele 190 000 de corturi necesare anual și cele 575 000 de seturi de echipamente individuale de protecție, destinate atât armatei, cât și forțelor de aplicare a legii. Prin amendamentul Berry se solicită fabricarea, în S.U.A., a 100 de produse pentru acest sector. Recentă rectificare Kissell a extins această solicitare și în cadrul sectorului de securitate internă și de pază a coastei.

În industria geosinteticelelor din S.U.A., în care activează peste 50 de companii și care se ridică la o producție anuală de 800 de milioane m² de material, s-a înregistrat o creștere de 5–6%, în 2008, rămânând constantă și în 2009. Pentru piața structurilor tehnice textile, IFAI prognozează o scădere cu 5–10%.

Piața materialelor destinate industriei constructoare de mașini a scăzut cu 35%, în ultimii doi ani, fiind afectată în mod direct de scăderea vânzărilor la mașini. Piața articolelor pentru timp liber și recreere înregistrează un declin de 40% în sectorul construcțiilor de ambarcațiuni și de 15–20% în cel al umbrarelor și baldachinelor rezidențiale.

Potrivit previziunilor IFAI, materialele geosintetice, militare și de protecție, dar și cele medicale, de grafică digitală, textilele inteligente și cele ecologice din S.U.A. vor înregistra, în următorii ani, procente de piață în creștere, prin intermediul a trei materiale de bază – tricoturi din urzeală, materiale compozite și textile neșesute.

*Smarttextiles and nanotechnology,
decembrie 2009, p. 12*



Mathematical modelling and the technological process optimization for the bio-scouring of the cotton textile materials

ALINA POPESCU
AURELIA GRIGORIU
CARMEN ZAHARIA

RODICA MUREȘAN
AUGUSTIN MUREȘAN

REZUMAT – ABSTRACT – INHALTSANGABE

Modelarea matematică și optimizarea procesului tehnologic de biocurățare a materialelor textile din bumbac

Din multitudinea de posibilități de reducere a poluării apelor reziduale rezultate din procesele tehnologice de finisare, în lucrare s-a abordat prelucrarea materialelor textile din bumbac 100%, cu pectinaza alcalină monocomponentă BioPrep 3000L, ca alternativă la tratamentul alcalin la cald, care este mare consumator de energie și are un impact negativ asupra mediului, prin cantitatea mare de alcalii, tenside, secheștranzii de ioni și agenți reducători utilizați. Sunt prezentate modelarea matematică și optimizarea procesului tehnologic de biocurățare a materialelor textile din bumbac, utilizând un program factorial central compozițional rotabil de ordinul 2⁴.

Cuvinte-cheie: biocurățare, pectinază, bumbac, modelare matematică, optimizare

Mathematical modeling and the technological process optimization for the bio-scouring of the cotton textile materials

Among the multitude of possibilities extant for the pollution decrease of wastewaters resulted from finishing technological processes, 100% cotton textile materials processing was addressed, with mono-component alkaline pectinase BioPrep 3000L, as an alternative to the alkaline boiling, which is a big energy consumer and has a negative impact over the environment, by its high quantity of alkalies, surfactants, ion sequestrants and reducing agents used. In this article, the mathematical modeling and the optimization of the technological process for the cotton textile material bio-scouring were presented, by the rotatable central composition design enabled by the factorial programme order 2⁴.

Key-words: bio-scouring, pectinase, cotton, mathematical modeling, optimization

Die mathematische Modellierung und die Optimierung des technologischen Prozesses für Bioreinigung der Baumwolltextilmaterialien

Aus der Vielfalt von Möglichkeiten für Reduzierung der Umweltverschmutzung durch Abwässer aus technologischen Veredelungsprozessen, wurde die Bearbeitung der Textilmaterialien aus 100% Baumwolle mit monokomponenter alkaliner Pektinase BioPrep 3000L verwendet, als Alternative zur alkaliner Wärmebehandlung, welches energieaufwendig ist und einen negativen Impact auf die Umwelt hat, durch die grosse Menge an Alkali, Tensiden, ionische Komplexbildner und reduzierende Agenten. Es wird die mathematische Modellierung und die Optimierung des technologischen Prozesses für Bioreinigung der Baumwolltextilmaterialien vorgestellt, mit Hilfe eines zentralen, faktoriellen drehbar-zusammensetzendes Programm des Grades 2⁴.

Schlüsselwörter: Bioreinigung, Pektinase, Baumwolle, mathematische Modellierung, Optimierung

Traditionally, cotton preliminary treatment, meant to remove the non-cellulose impurities (waxes, pectines, hemicellulose, and lignin) of the auxiliary substances used in the manufacturing flow (spinning, winding, weaving) or certain accidental impurities, is carried out by a boiling process. This takes place at a temperature round 95–100°C, in a concentrated sodium hydroxide or other alkaline agent, such as sodium carbonate, potassium hydroxide or their mixtures, at a strongly alkaline pH (i.e. pH = 12–13), in the presence of surfactants, complexing agents and reducing agents [1].

The alkaline boiling is efficient from the point of view of the non-cellulose impurities removal; cotton wettability is improved; lignin is expanded in the alkaline solution and is removed at the subsequent oxidative bleaching. But, the process has the following disadvantages: the strongly alkaline chemical process affects the cellulose and determines the modification of the physical-mechanical and physical-chemical fibre characteristics; the treatment generates wastewaters with a very high alkalinity and, implicitly, with a negative impact over the environment; the process is carried out at high energy consumption (high treating temperature and duration); and, it needs large quantities of water for repeated rinsing conducted for the removal of caustic soda residual content [2].

At global level, preoccupations were intensely focused on the substitution of the alkaline boiling process by the enzymes cleaning process. Depending on the nature of non-cellulose impurities, the action of certain enzymes was investigated over cotton impurities, such as: acid

and alkaline pectinase [3–11], cellulase [12–15], protease [16–19], lipase [17, 19] and xylanase [15].

Among the multitude of possibilities for pollution reduction of wastewaters resulted from finishing technological processes, in this paper, there was approached the preliminary treatment of the textile materials made of 100% cotton with mono-component alkaline pectinase BioPrep 3000L. This enzyme is a bacterial pectate-lyase obtained from a genetically modified *Bacillus* species, which is more efficient than the conventional multi-component acid pectinase from fungi. The characterization of this enzyme is, according to the provisions of the Enzymology Commission, E.C. 4.2.2.2, fact that classifies it as being a lyase.

In accordance with the normatives, the enzymes that destroy pectines are named pectinases. The advantage in using pectinases is that these enzymes attack only the pectin substrate, without decomposing the cellulose material. By pectines destruction, the other natural impurities of the cellulose materials are concomitantly removed: waxes, mineral substances, pigments and proteins, which are usually combined with pectines.

In this article, the mathematical modeling and the optimization of the bio-scouring technological process was presented for the cotton textile materials, through the rotatable central compositional design enabled by factorial programme order 2⁴. So as to conceive a programme optimization for the biotechnology related to the preliminary treatment of cotton textile materials, woven fabrics were used made of 100% cotton (Crivina article), 122.5 g/m² in mass, which were enzymatically treated with BioPrep 3000 L pectinase.

Table 1

CODIFICATION OF THE INDEPENDENT VARIABLES				
Variable/Value	Real variable	Coded variable	Basic actual value	Variation step
Concentration of pectinase BioPrep 3000L, g/L	Z_1	x_1	0.102	0.04
pH	Z_2	x_2	8.5	0.5
Temperature, °C	Z_3	x_3	55	5
Duration of enzymatic hydrolysis, minutes	Z_4	x_4	40	10

MATHEMATICAL MODELING OF THE BIO-SCOURING PROCESS FOR THE COTTON TEXTILE MATERIALS

The modeling, simulation and optimization of the treating processes shall follow a certain algorithm, which needs the following stages:

- I – set of an optimization criterion or the target function, Y_i , for the technological process under study;
- II – select the independent or decision-enabling variables, x_i ;
- III – set the various types of restrictions the decision-enabling variables are subjected to;
- IV – work the mathematical model (find the target function) for the process under study regarding textile treatment/finishing, as well as same model simplification under reasonable limits;
- V – testing and interpretation of the mathematic modeling, respectively the assessment of the extent to which it represents the process under real conditions;
- VI – select the method to further determine the optimal solution or the optimum;
- VII – find the optimal solution and the maximum or minimum value of the target function or the mathematical model proposed.

ACTIVE EXPERIMENTAL PLANNING CENTRAL COMPOSITIONALLY ROTATABLE OF 2⁴ ORDER

The empirical model shape which lays at the basis of the central compositionally rotatable planning corresponds to the following relation:

$$Y = b_0 + \sum_{i=1}^n b_i X_i + \sum_{j,i=1}^n b_{ji} X_i X_j \quad (1)$$

in which:

- Y – represented the response function or the dependent variable or the target function;
- X_i, X_j – the coded variables of the process studied;
- b_0, b_i, b_j, b_{ji} – the model coefficients.

The significance of the coefficients was tested by the application of the t test (Student), followed by finding and interpretation of the target function optimum carried out by conventional optimization methods [20].

To work out the present mathematical model, the experiments planning was performed in conformity with the

rotatable central composition programme of 2⁴ order [21–23], considering four independent variables (x_i): x_1 – concentration of the pectinolytic enzyme – BioPrep 3000L, g/L; x_2 – pH; x_3 – temperature, °C; x_4 – the duration of the enzymatic hydrolysis reaction, minutes.

The basic values and the variation step for each independent variable used within the working experimental programme are presented in table 1.

The optimization criteria or the target functions, taken as dependent variables (Y_i , %), were considered the following: Y_1 – content of pectines, %; Y_2 – content of waxes, %; Y_3 – average polymerization degree; Y_4 – water absorption by capillarity, %; Y_5 – whiteness degree.

The empirical mathematical model (functional relation) between the target function, Y_i (dependent variable) and independent variables (X_1, X_2, X_3, X_4), takes the form of a regression equation:

$$Y = b_0 + b_1 X_1 + b_2 X_2 + b_3 X_3 + b_4 X_4 + b_{12} X_1 X_2 + b_{13} X_1 X_3 + b_{14} X_1 X_4 + b_{23} X_2 X_3 + b_{24} X_2 X_4 + b_{34} X_3 X_4 + b_{11} X_1^2 + b_{22} X_2^2 + b_{33} X_3^2 + b_{44} X_4^2 \quad (2)$$

The coefficients of the target function above were determined by the least squares method using the following matrix relation [21]:

$$b = (X^T \cdot X)^{-1} \cdot X^T \cdot Y \quad (3)$$

in which:

b is column matrix of the regression coefficients, b_i ;

X – coded variable matrix x_i ;

Y – column matrix of the experimental values for target function Y_i .

The values of the coefficients for all the five suggested target functions, Y_i , are schematically presented in table 2. The meaning of the target function coefficients was tested by t test (Student), removing the non-significant ones, the remaining significant coefficients corresponding to the mathematical model in equations (4) – (8).

In accordance with coefficients significance found, the expressions of the target functions are:

For Y_1 :

$$Y_1 = 0.3973 - 0.0202X_1 + 0.0141X_2 - 0.0195X_4 + 0.0181X_2X_4 + 0.0833X_2^1 - 0.0079X_2^2 - 0.0454X_3^2 - 0.0204X_4^2 \quad (4)$$

For Y_2 :

$$Y_2 = 0.574 - 0.0425X_1X_3 + 0.0225X_1X_4 - 0.055X_2X_3 - 0.0172X_2^2 - 0.0247X_4^2 \quad (5)$$

For Y_3 :

$$Y_3 = 1.2144 + 0.0275X_2X_3 - 0.0205X_3X_4 + 0.0621X_1^2 + 0.0375X_2^2 + 0.0488X_3^2 \quad (6)$$

Table 2

TARGET FUNCTION COEFFICIENTS, Y_i					
Coefficient	Y_1	Y_2	$Y_3 \cdot 1.0 e - 003^*$	Y_4	Y_5
b_0	0.3973	0.5740	1.2144	92.2187	0.4398
b_1	-0.0202	-0.0063	-0.0057	0.1462	-0.0273
b_2	0.0141	0.0035	0.0015	-0.1362	-0.1349
b_3	0.0067	0.0047	0.0010	0.0615	-0.1369
b_4	-0.0195	-0.0030	-0.0118	-0.4873	-0.0439
b_{12}	0.0056	0.0000	0.0006	1.5469	-0.0113
b_{13}	-0.0069	-0.0425	0.0029	-1.3181	0.3462
b_{14}	0.0056	0.0225	-0.0144	-0.5844	0.0713
b_{23}	0.0056	-0.0550	0.0275	2.6806	1.8150
b_{24}	0.0181	-0.0125	-0.0158	0.8744	-1.1550
b_{34}	0.0056	-0.0100	-0.0205	3.5294	-0.6300
b_{11}	0.0833	-0.0097	0.0622	0.4873	-0.3043
b_{22}	-0.0079	-0.0172	0.0375	0.8360	0.0607
b_{33}	-0.0454	-0.0059	0.0488	0.6448	-0.4056
b_{44}	-0.0204	-0.0247	-0.0071	1.2110	0.4707

For Y_4 :

$$Y_4 = 92.2187 + 1.5469X_1X_2 - 1.3181X_1X_3 + 2.6806X_2X_3 + 0.8744X_2X_4 + 3.5294X_3X_4 + 0.836X_2^2 + 0.6448X_3^2 + 1.2110X_4^2 \quad (7)$$

For Y_5 :

$$Y_5 = 80.4398 + 1.8150X_2X_3 - 1.550X_2X_4 - 0.630X_3X_4 - 0.4056X_3^2 + 0.4707X_4^2 \quad (8)$$

In table 3, the final coefficients for the equations of target functions Y_1 - Y_5 are presented. Thus, there were achieved the mathematical equations, which describe the dependencies between the proposed independent variables of the cotton bio-scouring process (enzyme concentration, pH, temperature and enzymatic hydrolysis duration) and the optimization criterion or, as considered, the dependent variable (content of pectines, content of waxes, average polymerization degree, content of water adsorbed by capillarity, whiteness degree).

Appropriateness of the mathematical model proposed was checked by computing the Fisher test value, F :

$$F = \frac{(n-1) \sum_{i=1}^n (Y_{ei} - \bar{Y}_e)^2}{(k-1) \sum_{i=1}^k (Y_{eki} - \bar{Y}_{ek})^2} \quad (9)$$

in which:

Y_{ei} represented experimental values of the dependent variable;

Table 4

VERIFICATION OF THE MATHEMATICAL MODEL SUITABILITY, FISHER - F TEST					
Function,	Sum $(Y_{ei} - \bar{Y}_e)^2$, $N = 1, \dots, 31$	Sum $(Y_{eki} - \bar{Y}_{ek})^2$, $k = 1, \dots, 7$	F_{calc}	F_{tub}	$F_{calc} < F_{tub}$
Y_1	0.9642	0.0228	211.4474	245.95	adequate
Y_2	0.2658	0.0221	60.1357		adequate
Y_3	519547	35811.71	72.5387		adequate
Y_4	1034.195	56.8812	90.9083		adequate
Y_5	447.5645	26.2748	85.1699		adequate

Table 3

FINAL COEFFICIENTS FOR THE EQUATIONS OF THE TARGET FUNCTIONS					
Coefficient	Y_1	Y_2	$Y_3 \cdot 1.0 e + 003^*$	Y_4	Y_5
b_0	0.3973	0.5740	1.2144*	92.2187	80.4398
b_1	-0.0202	0	-0.0057	0	0
b_2	0.0141	0	0.0015	0	0
b_3	0	0	0.0010	0	0
b_4	-0.0195	0	-0.0118	0	0
b_{12}	0	0	0.0006	1.5469	0
b_{13}	0	-0.0425	0.0029	-1.3181	0
b_{14}	0	0.0225	-0.0144	0	0
b_{23}	0	-0.0550	0.0275	2.6806	1.8150
b_{24}	0.0181	0	-0.0158	0.8744	-1.1550
b_{34}	0	0	-0.0205	3.5294	-0.6300
b_{11}	0.0833	0	0.0622	0	0
b_{22}	-0.0079	-0.0172	0.0375	0.8360	0
b_{33}	-0.0454	0	0.0488	0.6448	-0.4056
b_{44}	-0.0204	-0.0247	-0.0071	1.2110	0.4707

- \bar{Y}_e – average value of the dependent variable;
- Y_{eki} – experimental values of the dependent variable in the center of the programme;
- \bar{Y}_{ek} – average value of the experimental values in the center of the programme;
- n – total number of experiments within the experimental matrix;
- k – number of experiments in the center of the programme.

Suitability of the five proposed mathematical models, as compared to the experimental values ($n = 31$ and $k = 7$), is presented in table 4.

RESULTS AND DISCUSSION

The mathematical models proposed were graphically represented, by Matlab programme, keeping constant the basic value of two or three variables. The emphasis on the effects the significant factor interactions have over the target function, Y_i , proposed was drawn by marking out the response surfaces and the constant level curves. The values of the five target functions were computed and graphically market out by:

- simultaneous variation of the four independent variables, $Y_i = Y_i(x_1, x_2, x_3, x_4)$; three independent variables remained in the domain center ($x_i = 0$), and the fourth variable took values in the experimental domain, the pursue being the variation of the dependent variable values;
- two of the independent variables kept at their basic value ($x_i = 0$; $x_j = 0$), the other ones having values in the so considered suitable experimental domain.

The analysis of the model for the pectines content – Y_1

By simultaneous variation of the four independent variables, the pectines content is under a continuous decreasing up to the central area of the experimental domain, after which it has a growing trend (fig. 1).

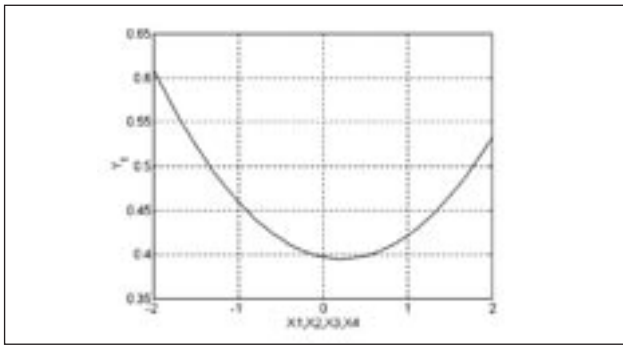


Fig. 1. Influence of the independent variables over pectines content

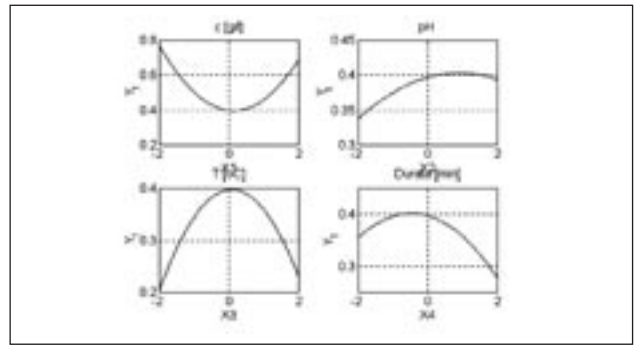


Fig. 2. Influence of one independent variable over pectines content

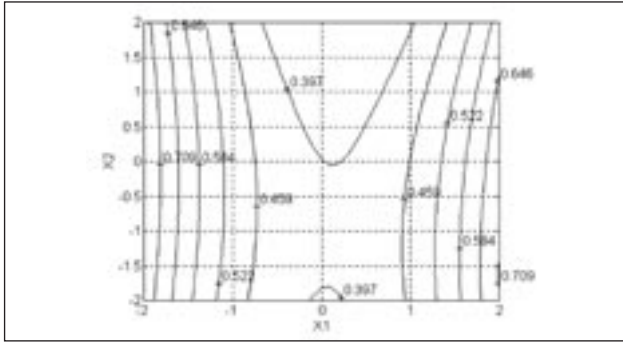


Fig. 3. Influence of independent variables x_1 and x_2 over pectines content (curves of the constant level)

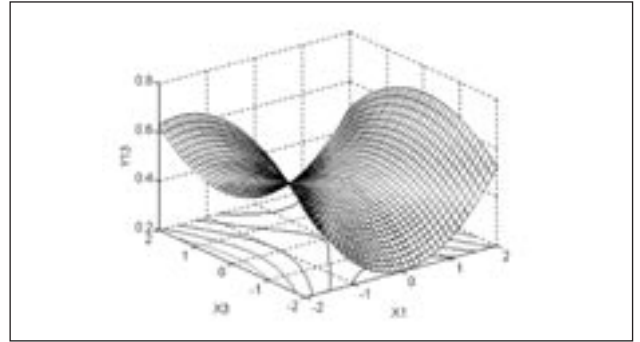


Fig. 4. Influence of independent variables x_1 and x_3 over pectines content (response surface areas)

In case three independent variables are kept constant within the experimental domain center and just one of the independent variables is changed, the following tracks are to be noticed (fig. 2):

- once with increasing the enzymatic product concentration, the pectines content decreases from 0.77, for $x_1 = -2$, to 0.4 in the center of the experimental domain and increases again around the value of 0.68, for $x_1 = +2$;
- in the case the pH increases, the pectines content grows continuously up to a maximum value situated around 0.4%, for $x_2 = +1$, from now on showing a slight decreasing trend;
- by temperature increase, the content of pectic substances in the materials increases up to a maximum value situated in the center of the experimental domain, followed by a decrease; the lowest values of the content in pectic substances are obtained for $x_3 = -2$;
- by duration increase, first, there is a slight increasing of the content in pectic substances, in the first interval of the experimental domain, followed, as noticed, by a pronounced decrease.

In case x_1 and x_2 vary, the other variables being maintained in the center of the experimental domain, there can be noticed that the significant influence is performed by variable x_1 (fig. 3). For variable x_1 , the content of pectines continuously decreases towards the center of the experimental domain, as for x_2 the influence is low. Nevertheless, the lowest values obtained are situated in the central area, ranged around 0.397 % obtained for x_2 very close to -2 , and x_2 in the interval 0 and $+2$. Further on, by a content increase of the enzymatic product, the content of pectic substances also increases.

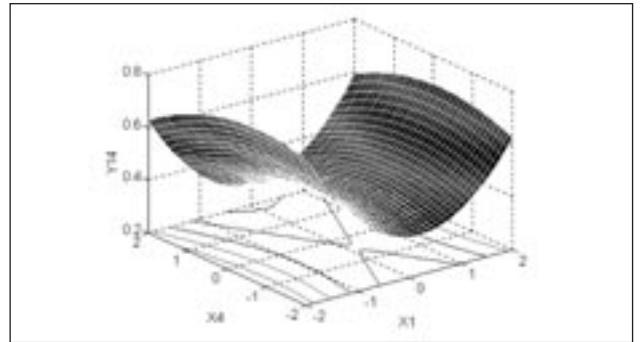


Fig. 5. Influence of independent variables x_1 and x_4 over pectines content (response surface areas)

For the independent variables x_1 and x_3 , the content of pectic substances varies for both variables (fig. 4a). As regards the influence of the independent variable x_1 , the content of pectines continuously decreases towards the center of the experimental domain, thus being obtained a minimum value, to then increase again. For x_3 , the maximum values of the pectic substances content are obtained in the central area of the experimental domain.

In the case of parameters variation for x_1 and x_4 , the significant influence for the domain under analysis is represented by the enzymatic product concentration, while the influence of the hydrolysis duration is low (fig. 5). By concentration increase of the enzymatic product meant for treatment, the content of pectines decreases towards the central area of the experimental domain, thus being obtained a minimum value, after which it increases again.

The influence of variables x_2 (pH) and x_3 (temperature) is presented in figure 6. Minimum values are obtained

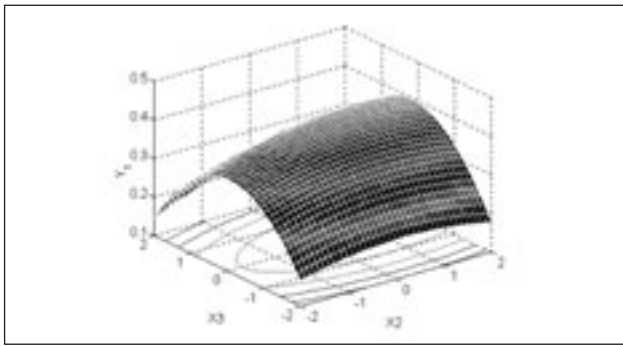


Fig. 6. Influence of independent variables x_2 and x_3 over pectines content (response surface areas)

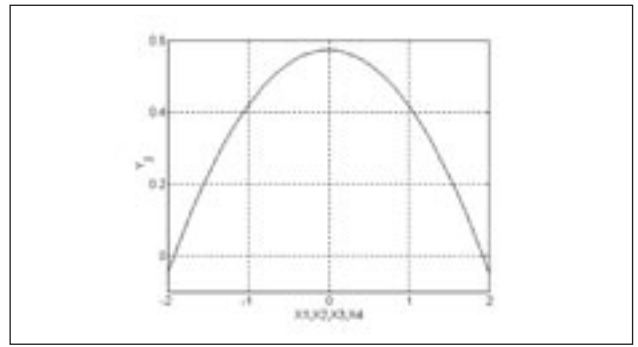


Fig. 7. Influence of the independent variables over waxes content

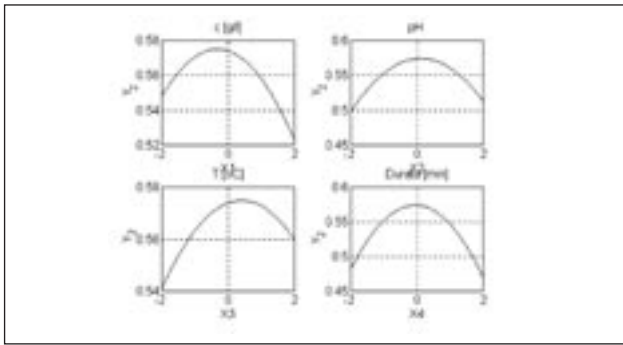


Fig. 8. Influence of one independent variable over waxes content

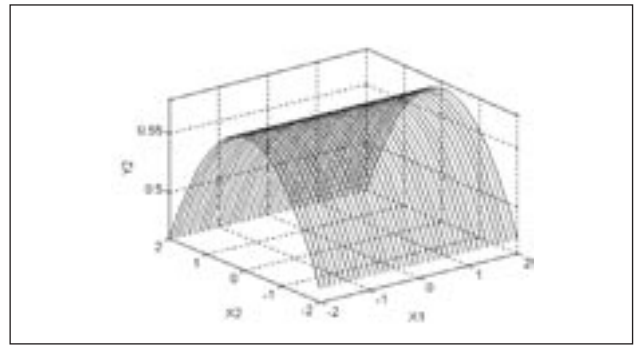


Fig. 9. Influence of independent variables x_1 and x_3 over waxes content (response surface areas)

at the extremity of the experimental domain, namely $x_2 = -2$ to -1.5 , and $1.8-2$, as for $x_3 = -2$ to -1.8 and 1.8 to 2 . The values increase towards the center of the experimental domain, where the maximum value is to be found.

In the case of pH variation (x_2) and hydrolysis duration (x_4), the lowest values of the pectines content (0.181%) can be obtained for x_2 , ranged between -2 and -1.5 , and for $x_4 = +1.75$ to $+2$.

In the case of variation for temperature (x_3) and duration (x_4), significant influence takes only variable x_4 , there being obtained the minimum values of pectines content (0.18%), for $x_4 = -2$ and $x_4 = +2$.

The analysis of the model for the waxes content – Y_2

By simultaneous variation of all the independent parameters on the experimental domain, there can be noticed that the content of waxes has an increase to the maximum value around the center of the experimental domain, after which there is a decreasing tendency towards zero at the domain extremity (fig. 7).

In case a single independent variable is varied, the other ones being maintained in the center of the experimental domain, the following things are to be noticed (fig. 8):

- for the independent variable x_1 , the content of waxes increases close to the central area of the domain, after which it continuously decreases;
- for the x_2 variable, the content of waxes increases until the middle of the experimental domain, after which it continuously decreases;

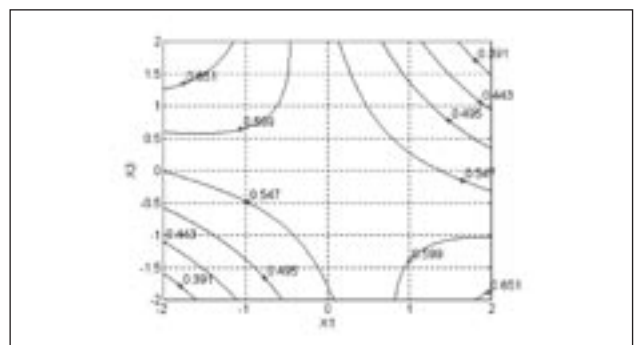


Fig. 10. Influence of independent variables x_1 and x_3 over waxes content (curves of the constant level)

- for the x_3 variable, the content of waxes has a minimum value at $x_3 = -2$, after which it continuously increases until around the value of $x_3 = 0.5$, and then it has a continuous decreasing trend;
- regarding the enzymatic hydrolysis duration, low values of the content in waxes are obtained, both at minimum values ($x_4 = -2$), and at maximum ones ($x_4 = +2$).

In case x_1 și x_2 parameters (fig. 9) are varied, a higher influence over the content of waxes is expressed by the pH value. Maximum values are obtained close to the central area of the experimental domain, the minimum values decreasing towards extremities.

In case x_1 and x_3 parameters are varied, minimum values are obtained for the content of waxes (0.391%), either for $x_1 = -2 - -1.5$ and $x_3 = -2 - -1.6$, and for $x_1 = 1.6 - +2$ and $x_3 = 1.5 - +2$, respectively (fig. 10). In the case of x_1 and x_4 variables, a higher influence has variable x_1 , the content of waxes decreasing once with the increase of the enzymatic product concentration

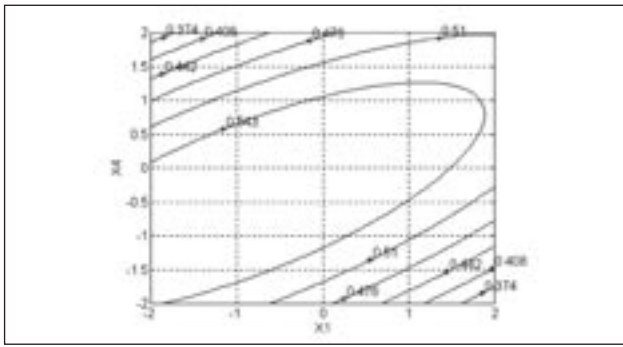


Fig. 11. Influence of independent variables x_1 and x_4 over waxes content (curves of the constant level)

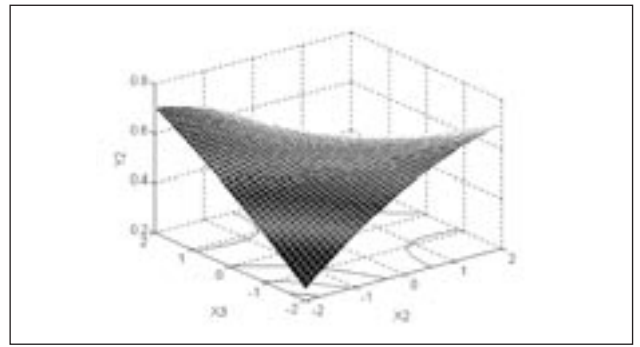


Fig. 12. Influence of independent variables x_2 and x_3 over waxes content (response surface areas)

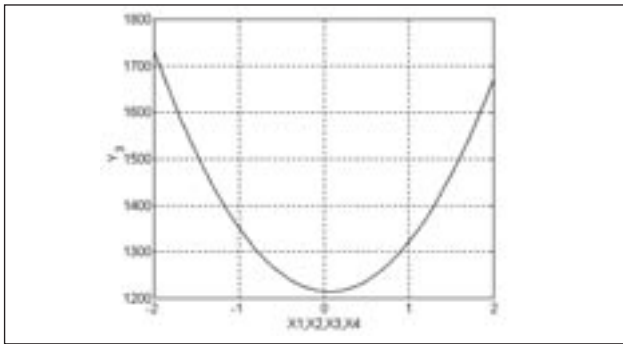


Fig. 13. Influence of the independent variables over the PD

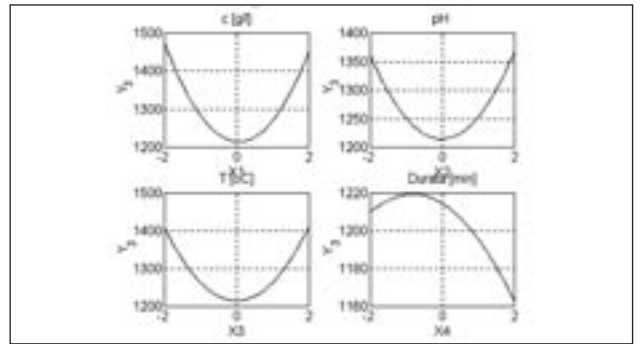


Fig. 14. Influence of one independent variable over the PD

(fig. 10). The lowest values of waxes content (0.374%) can be obtained either by using increased concentrations of the enzymatic product and short hydrolysis durations ($x_1 = +1.7 - +2$, $x_4 = -1.75 - -2$), or low concentrations and long durations ($x_1 = -1.75 - -2$, $x_4 = +1.8 - +2$).

In the case of x_2 and x_3 variables, the content of waxes is influenced by their variation (fig. 12). Minimum values of the content of waxes (0,311%) can be obtained either for the minimum values of the variables ($x_2 = -2 - -1.75$; $x_3 = -2 - -1.5$), or for their maximum values ($x_2 = +1.8 - +2$ and $x_3 = +1.75 - +2$).

In the case of x_2 and x_4 parameters variation, according to the analysis of the constant level curves, one can notice that the minimum values of the content of waxes decrease towards the extremities of the experimental domain. In turn, according to the analysis on the influence expressed by variables x_3 and x_4 , one can notice that only duration has a significant influence, minimum values being obtained in short treatment durations, as well as in long ones ($x_4 = -2$ and $x_4 = +2$).

The analysis of the model for the average polymerization degree (PD) – Y_3

By simultaneous variation of the four parameters, the average polymerization degree (PD) presents a continuous decreasing until the central area of the experimental domain, after which it increases again (fig. 13). In case the variation takes place for a single independent parameter, for x_1 , x_2 and x_3 , the shape of the curve is almost identical, namely presenting a minimum value decrease in the central area of the domain, after which it has a continuous increase up to around the 1 350–1 440 values (fig. 14).

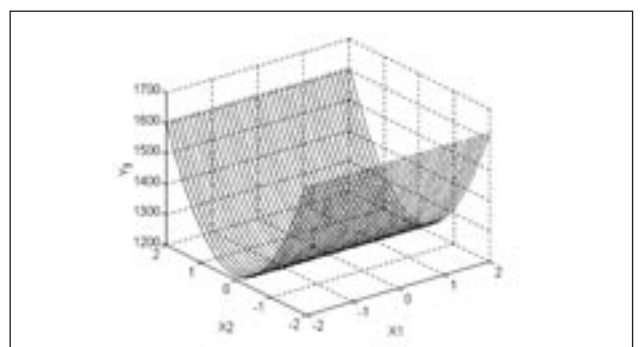


Fig. 15. Influence of independent variables x_1 and x_2 over the PD (response surface areas)

In case the variation takes place for parameters x_1 and x_2 (fig. 15) or x_1 and x_3 (fig. 16) the average polymerization degree (PD) presents a minimum value in the central area of the experimental domain, the maximum values ranging at the four extremities of the experimental domain.

In the case of x_1 and x_4 parameters, the influence of the enzymatic product concentration is significant, as compared to the enzymatic hydrolysis duration (fig. 17). Once the enzymatic product concentration increases, the average polymerization degree (PD) decreases, reaching a minimum value in the central area of the experimental area, after which it increases again.

The influence of x_2 and x_3 parameters lead to the obtaining of a maximum value for the average polymerization degree (1 613), either by using low values of the pH and temperature, or when taking values ranging at the experimental domain maximum (fig. 18).

For x_2 and x_4 (fig. 19), the average polymerization degree (PD) presents a decrease once with the pH

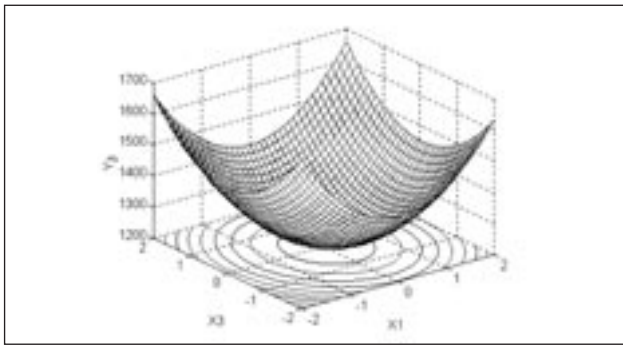


Fig. 16. Influence of independent variables x_1 and x_3 over the PD (response surface areas)

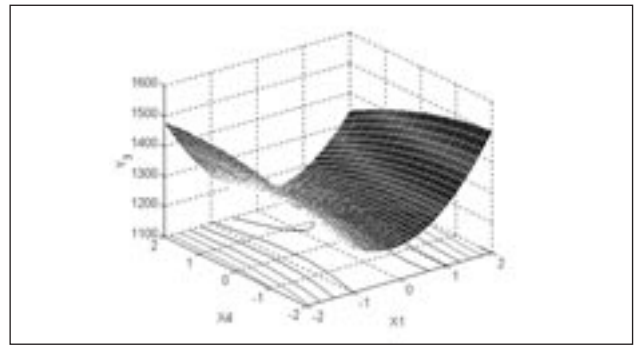


Fig. 17. Influence of independent variables x_1 and x_4 over the PD (response surface areas)

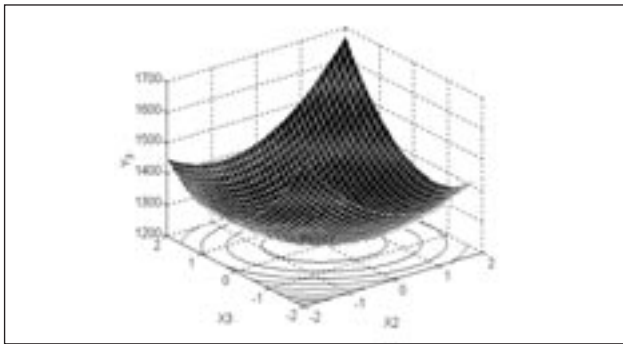


Fig. 18. Influence of independent variables x_2 and x_3 over the PD (response surface areas)

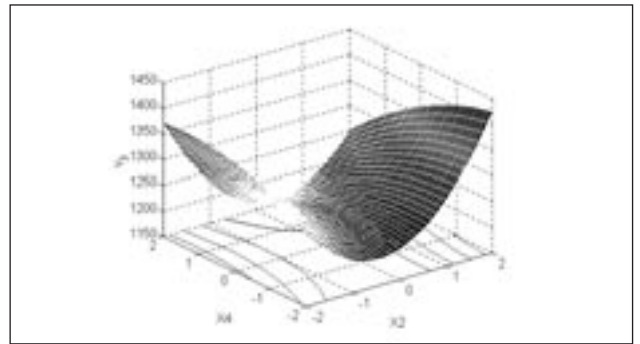


Fig. 19. Influence of independent variables x_2 and x_4 over the PD (response surface areas)

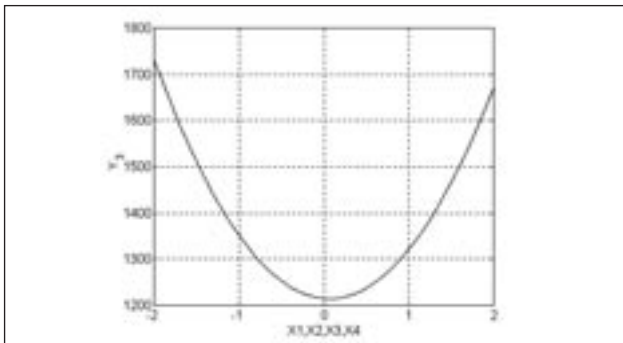


Fig. 20. Influence of the independent variables over water absorption

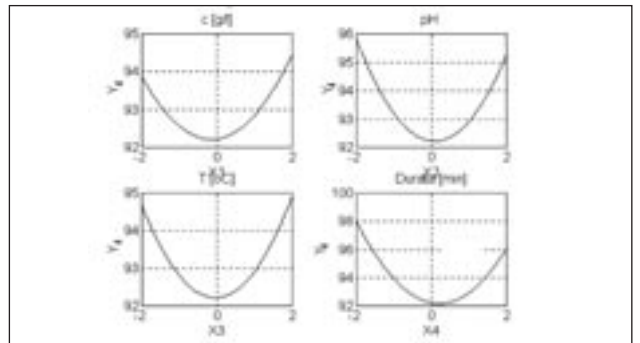


Fig. 21. Influence of one independent variable over water absorption by capillarity

increase, a minimum value being obtained at 1 193, after which it increases again. The maximum value of the average polymerization degree (1 393) is obtained at a pH ranging on the analyzed domain $x_2 = +1.7 - +2$ and a shorter hydrolysis duration ($x_4 = -0.5 - -2$). In case of temperature x_3 and duration x_4 variation, only parameter x_4 takes the significant influence.

The analysis of the model for water absorption by capillarity – Y_4

The curve shape of capillarity water absorption by concomitant variation of the four independent parameters decreases from the left extremity of the experimental domain ($x_i = -2$) and presents a minimum value in the central area, after which it increases again for the maximum values of the variables ($x_i = +2$) (fig. 20). The values obtained at the two extremities are akin. In case variation takes place for a single independent parameter, the curves obtained for all the dependent

variables present the same variation direction, with a minimum value in the central area of the experimental domain ranging around the 92% value (fig. 21).

In the case of x_1 and x_2 parameters, the maximum values of this (independent) parameter can be obtained either by using small concentrations of the enzymatic product and a high pH, or high concentrations and a small pH (fig. 22).

In the case of x_1 and x_3 parameters variation as well, water absorption by capillarity is influenced by both variables (fig. 23), there being obtained high values of water absorption either by using small concentrations of the enzymatic product and a high temperature, or a low temperature and high concentrations.

In the case of variation for x_1 and x_4 parameters (fig. 24) or for parameters x_2 and x_3 (fig. 25), the minimum values of water absorption by capillarity are obtained in the central area of the experimental domain. The maximum values can be obtained as follows:

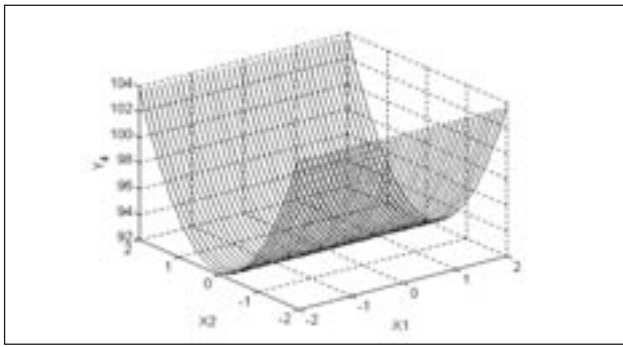


Fig. 22. Influence of independent variables x_1 and x_2 over water absorption by capillarity (response surface areas)

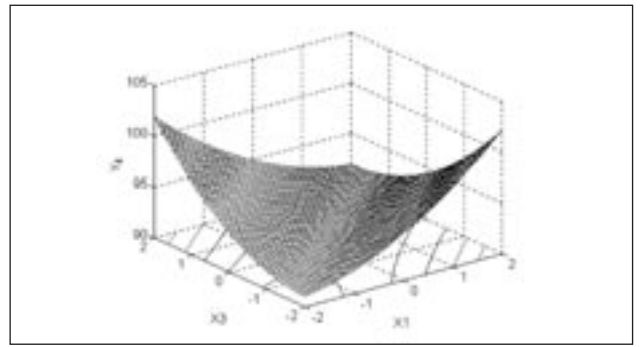


Fig. 23. Influence of independent variables x_1 and x_3 over water absorption by capillarity (response surface areas)

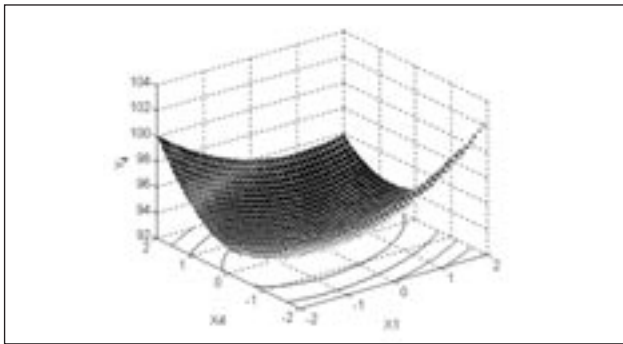


Fig. 24. Influence of independent variables x_1 and x_4 over water absorption by capillarity (response surface areas)

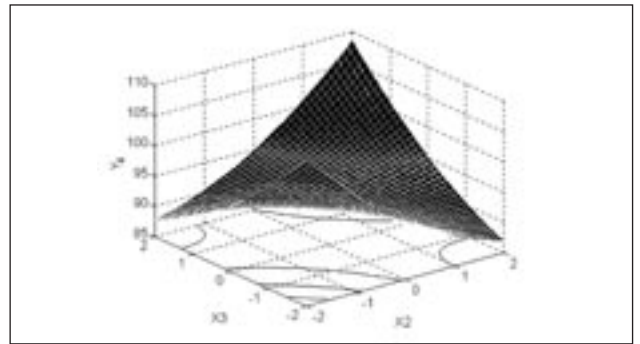


Fig. 25. Influence of independent variables x_2 and x_3 over water absorption by capillarity (response surface areas)

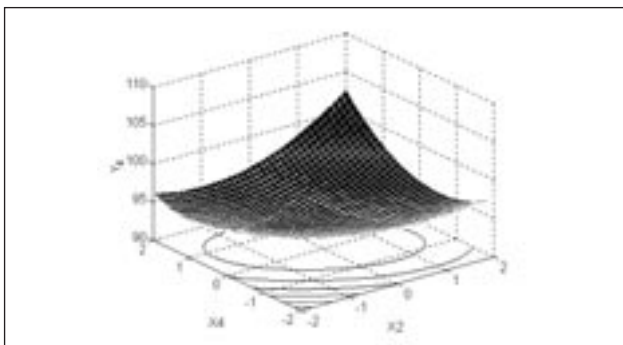


Fig. 26. Influence of independent variables x_2 and x_4 over water absorption by capillarity (response surface areas)

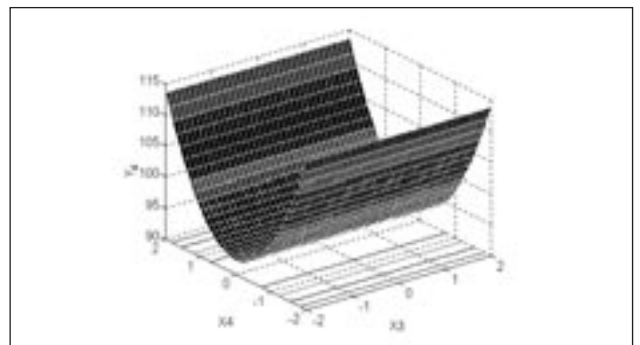


Fig. 27. Influence of independent variables x_3 and x_4 over water absorption by capillarity (response surface areas)

- low enzyme concentrations and high hydrolysis duration or high enzyme concentrations and short durations (in the case of variation for x_1 and x_4 parameters);
- either low, or high pH and temperature (in the case of variation for x_2 and x_3 parameters).

By variation of x_2 and x_4 parameters, the maximum water absorption by capillarity (103%) is obtained for the minimum or for the maximum values of these variables (fig. 26). According to the analysis on the influence of x_3 and x_4 parameters, one can notice that only duration has a significant influence (fig. 27).

The analysis of the model for the whiteness degree – Y_5

By simultaneous variation of all the independent parameters on the experimental domain, there can be noticed that the whiteness degree presents a conti-

nuous decreasing up to value $x_i = +1$, after which it shows a slight increasing trend (fig. 28).

In case variation takes place for a single independent parameter, the other ones being maintained in the central part of the experimental domain, following things can be noticed (fig. 29):

- for the independent parameter x_1 , the whiteness degree increases up to around 80%, for $x_1 = 0$, until the center of the experimental domain, after which it continuously decreases up to around 79.25%, for $x_1 = +2$;
- for parameter x_2 , the whiteness degree continuously decreases from 80.95%, for $x_2 = -2$, up to around 80.4%, for $x_2 = +2$;
- for parameter x_3 , the whiteness degree shows a maximum value (80.6%) at $x_3 = -0.5$, after which it continuously decreases up to around 78%, for $x_3 = +2$;
- regarding the hydrolysis duration, the whiteness degree decreases, presenting a minimum value

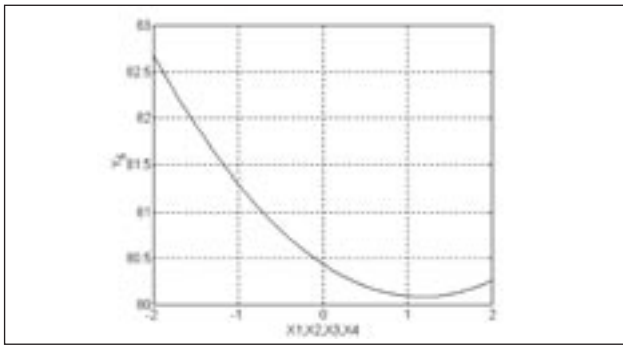


Fig. 28. Influence of the independent variables over whiteness degree

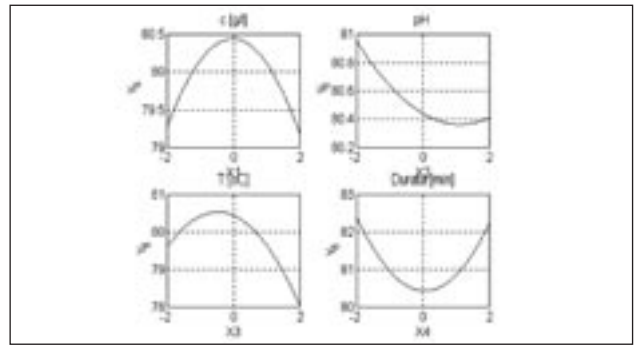


Fig. 29. Influence of one independent variable over whiteness degree

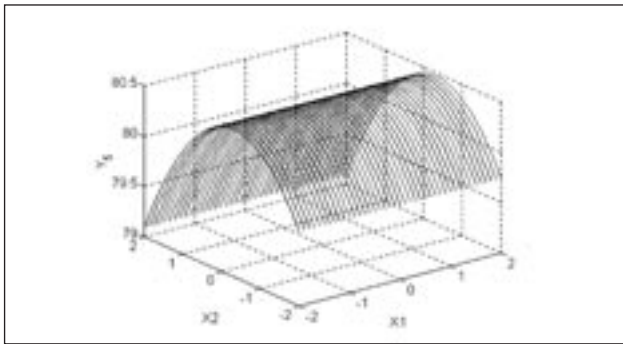


Fig. 30. Influence of independent variables x_1 and x_2 over whiteness degree (response surface areas)

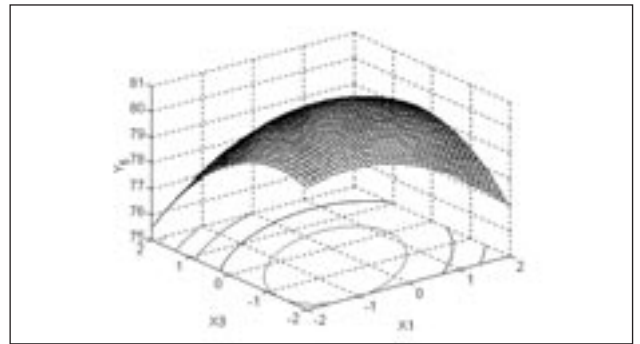


Fig. 31. Influence of independent variables x_1 and x_3 over whiteness degree (response surface areas)

(80.4%) for $x_4 = 0$, after which it increases again up to around 82%, for $x_4 = +2$.

The curves obtained in the case of parameters x_1 and x_2 show that the concentration of the enzymatic product has a higher influence (fig. 30). The whiteness degree increases towards the central area of the experimental domain.

The influence of x_1 and x_3 parameters shows that the maximum value of the whiteness degree is ranging within the chosen domain. The two parameters maximum value is situated around $x_1, x_3 = -0.5$ (fig. 31).

For the independent parameters x_1 and x_4 , the whiteness degree varies, depending on both parameters (fig. 32). As far as the influence of independent parameter x_1 is concerned, the whiteness degree increases towards the center of the experimental domain, there being obtained a maximum value, after which it decreases again. As regards x_4 , the maximum values of the whiteness degree are obtained at the two extremities. By the analysis of constant level curves (fig. 32), one can notice that the same value (82%) can be obtained either at a shorter or longer duration, for a constant value of the enzymatic product concentration.

By the graphic representation of the curves obtained through parameters x_2 and x_3 variation, there can be noticed that the maximum values of the whiteness degree are obtained by pairs of values situated in the left side or in the right side of the experimental domain (fig. 33).

In the case of parameters x_2 and x_4 variation (fig. 35), the maximum values of the whiteness degree can be obtained at a low pH and longer duration or at a high pH and short treating duration.

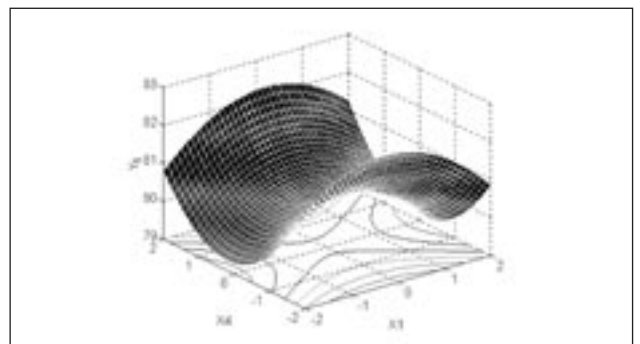


Fig. 32. Influence of independent variables x_1 and x_4 over water absorption by capillarity (response surface areas)

From the graphical analysis of parameters x_3 and x_4 variation, there results the fact that only the hydrolysis duration has a significant influence over the whiteness degree.

THE OPTIMIZATION OF THE PROPOSED MATHEMATICAL MODELS Y_1 - Y_5

To find the optimum values for the five target functions, the conventional method was used for optimization; this consists in finding the stationary points (x_1^* , x_2^* , x_3^* and x_4^*), as well as the nature of the stationary point, namely the maximum point or the minimum point.

Finding of the stationary points consists in solving a system of four equations with 4 items unknown, obtained after the 1st order derivatives of the target function are set equal to zero in relation to each variable. The stationary point is identified by determination of higher order derivatives (if $n = 2k = \text{even}$ and the value of $2k$ order derivatives determinate is negative, we have got a maximum point; yet, if this value

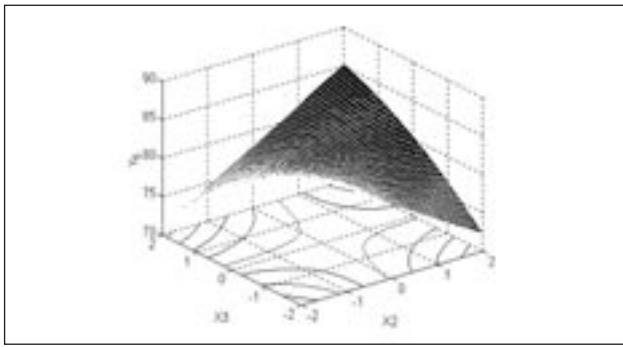


Fig. 33. Influence of independent variables x_2 and x_3 over whiteness degree (response surface areas)

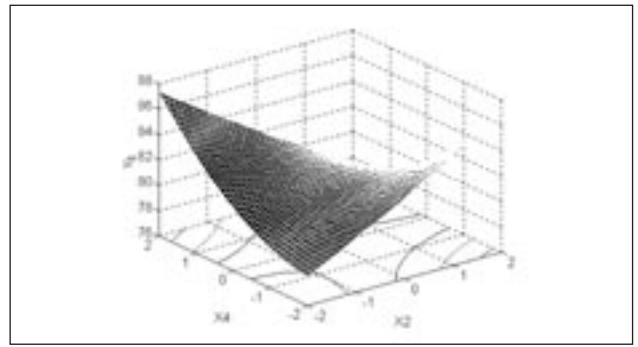


Fig. 34. Influence of independent variables x_2 and x_4 over whiteness degree (response surface areas)

is positive, we have got a minimum point; if $n = 2k + 1 = \text{odd}$, there is an inflexion point, the function having no minimum or maximum).

In the case of Y_1 function (content of pectines), the stationary point found by the application of the conventional method is $x_1^* = +0.1212$, $x_2^* = +1.5556$, $x_3^* = 0$ and $x_4^* = -0.5794$, this corresponding to a value of the target function, $Y_1 = 0.387028$. This stationary point is an inflexion point. The Y_1 function has no distinct maximum or minimum point; yet, it shows an outmost local maximum point, $x_1^* = -2$ (0.004 g/L BioPrep 3000 L), $x_2^* = 0$ (pH = 8.5), $x_3^* = 0$ (55°C) and $x_4^* = 0$ (40 minutes), corresponding to the 0.7 709 % value Y_1 .

In the case of Y_2 function (content of waxes), the stationary point found by the application of the conventional method is $x_1^* = 0$, $x_2 = 0$, $x_3^* = 0$ and $x_4^* = 0$, this corresponding to a value of the target function, namely $Y_2 = 0.574$. This stationary point is an inflexion point. The Y_2 function has no distinct maximum or minimum point; yet, it shows an outmost local maximum point, namely $x_1^* = -1$ (0.053 g/L BioPrep 3000 L), $x_2^* = -1$ (pH = 8.0), $x_3^* = +1$ (60°C) and $x_4^* = -1$ (30 minutes), corresponding to the 0.8543 % value Y_2 .

In the case of Y_3 function (average polymerization degree), the stationary point found by the application of the conventional method is $x_1^* = 0$, $x_2 = 0$, $x_3^* = 0$ and $x_4^* = 0$, this corresponding to a value of the target function, $Y_3 = 1214.4$. This stationary point is an inflexion point. The Y_3 function shows an outmost local maximum point, $x_1^* = -1$ (0.053 g/L BioPrep 3000 L), $x_2^* = +1$ (pH = 9.0), $x_3^* = +1$ (60°C) and $x_4^* = -1$ (30 minutes), corresponding to a real value of 1410.1 (Y_3).

In the case of Y_4 function (water absorption by capillarity), the stationary point found by the application of the conventional method is $x_1^* = 0$, $x_2 = 0$, $x_3^* = 0$ and $x_4^* = 0$, this corresponding to a value of the target function, $Y_4 = 92.2187$. The Y_4 function has no distinct maximum or minimum point; yet, it shows an outmost local maximum point, $x_1^* = -1$ (0.053 g/L BioPrep 3000 L), $x_2^* = -1$ (pH = 8.0), $x_3^* = -1$ (50°C) and $x_4^* = -1$ (30 minutes), corresponding to 100 % value Y_4 .

In the case of Y_5 function (whiteness degree), the stationary point found by the application of the conventional method is $x_1^* = 0$, $x_2 = 0$, $x_3^* = 0$ and $x_4^* = 0$, this

corresponding to a value of the target function, $Y_5 = 80.4398$. The Y_5 function has an outmost local maximum point, $x_1^* = -1$ (0.053 g/L BioPrep 3000 L), $x_2^* = -1$ (pH = 8.0), $x_3^* = -1$ (50°C) and $x_4^* = -1$ (30 minutes), corresponding to 82.8449% value Y_5 .

CONCLUSIONS

The rotatable central composition design enabled by factorial programme order 2^4 has led to the following general conclusions:

- The variation mode of the independent variables chosen for the bio-scouring of the cotton fibres: x_1 – pectinolytic enzyme concentration BioPrep 3000L, g/L; x_2 – pH; x_3 – temperature, °C and x_4 – duration of the enzymatic hydrolysis reaction, minutes – corresponds to the values set by the application of the active empirical planning possible through the rotatable central composition design of the 2^4 order;
- Mathematical equations were found for the five suggested target functions: Y_1 – content of pectines; Y_2 – content of waxes; Y_3 – average polymerization degree; Y_4 – water absorption by capillarity and Y_5 – whiteness degree – the mathematical models being validated by the application of the t test (Student) and by models suitability check with Fisher test; the expressions of the mathematical models are appropriate, corresponding to the experimental data; thus, the optimum values were found for the target functions, which are outmost local maximum points;
- In case the 4 independent variables are varied (pectinolytic enzyme concentration BioPrep 3000L, pH, temperature and duration of enzymatic hydrolysis reaction), by the interpretation of the mathematical models found for the 5 target functions, the following conclusions result:
 - a reduced content of pectines Y_1 remnant on the woven fabric and a high whiteness degree Y_5 in the central area of the experimental domain are obtained, but also optimum values of these characteristics, at a concentration of the enzymatic product ranging between 0.05–0.15 g/L, together with the variation of the independent parameters, with the following variants: low pH – low tempe-

rature – high hydrolysis duration or high pH – high temperature – low hydrolysis duration;
 – as regards the content of waxes Y_2 , the average polymerization degree Y_3 and water absorption by capillarity Y_4 , optimum values are obtained at the extremities of the experimental domain; the optimal combination of the independent variables that leads to optimum values of these characteristics is low concentration of the enzymatic product – low pH – low temperature – high hydrolysis duration or high concentration of the enzymatic product – high

pH – high temperature – low hydrolysis duration; case in which, there should be considered that, once with the increase in pH and of the enzymatic product concentration, the average polymerization degree decreases, reason for which the application of the first combination of values is preferred for the technologic parameters;

- Graphics created by Matlab programme, which is marking out the response surfaces and constant level curves, can be considered work nomograms, in the case alkaline pectinases are industrially applied for preliminary cotton treatment.

BIBLIOGRAPHY

- [1] Grindea, M., Grigoriu, A., Hanganu, A., Pușcaș, E. L. *Tehnologia Chimică Textilă*. Editura Tehnică, București, 1981
- [2] *Diminuarea efectelor finisării textile asupra mediului*. In: Industria Textilă, 2009, vol. 60. issue 6, p. 342
- [3] Li, Y., Hardin, I.R. *Enzymatic Scouring of Cotton: Effects on Structure and Properties*. In: Text. Chem. Color., 1997, vol. 29, issue 8, p. 71
- [4] Eters, J. N. *Alkaline pectinase: A new Approach to Environmentally Responsible Cotton Preparation*. Enzymes Business, Novo Nordisk, 1999
- [5] Nicolov, A. *Bio-preparation – The enzymatic way for scouring*. 1st Annual Workshop Cost Action 847, *Textile Quality and Biotechnology*, Madeira, 2001
- [6] Bach, E., Schollmeyer, E. *Vergleich des alkalischen Abkochprozesses mit der enzymatischen Entfernung der Begleitsubstanzen der Baumwolle*. In: Text. Prax. Int., 1993, issue 3, p. 220
- [7] Rössner, U. *Enzyme in der Baumwoll-vorbehandlung*. In: Textilveredlung, 1995, vol. 30, issue 3, 4, p. 82
- [8] Sawada, K., Tokino, S., Ueda, M., Wang, X.Y. *Bioscouring of cotton with pectinase enzyme*. In: J. Soc. Dyers Col., 1998, vol. 114, issue 11, p. 333
- [9] Thiagarajan, P., Selvakumar, N. *Cotton, pectinolytic enzymes and enzymatic scouring of cotton*. In: Colourage, 2008, issue 9, p. 51
- [10] Tzanov, T., Calafell, M., Gübitz, G.M., Cavaco-Paulo, A. *Bio-preparation of cotton fabrics*. In: *Enzyme and microbial technology*, 2001 vol. 29, issue 4, p. 357
- [11] Calafell, M., Garriga, P. *Effect of some process parameters in the enzymatic scouring of cotton using an acid pectinase*. In: *Enzyme Microbiology Technology*, 2004, vol. 34, p. 326
- [12] Cavaco-Paulo, A., Almeida, L., Bishop, L. *Cellulase activities and finishing effects*. In: Text. Chem. Color., 1996, issue 28, p. 28
- [13] Li, Y., Hardin, I.R. *Treating Cotton with Cellulases and Pectinases: Effects on Cuticle and Fiber Properties*. In: Text. Res. J., 1998, vol. 68, issue 9, p. 671
- [14] Csiszar, E., Szakacs, G., Rusznak, I. *Combining Traditional Cotton Scouring with Cellulase Enzymatic Treatment*. In: Text. Res. J., 1998 vol. 68, issue 3, p. 163
- [15] Wang, Q., Fan, X., Hua, Z., Gao, W., Chen, J. *Influence of combined enzymatic treatment on one-bath scouring of cotton knitted fabrics*. In: *Biocatal. & Biotransf.*, 2007, vol. 25, issue 1, p. 9
- [16] Hsieh, Y.L., Cram, L. *Proteases as Scouring Agents for Cotton*. In: Text. Res. J., 1999, vol. 69, issue 8, p. 590
- [17] Buchert, J., Pere, J., Pualakka, A., Nousiainen, P. *Scouring of cotton with pectinases proteases and lipases*. In: *Tex. Chem. Color. & Amer. Dyes. Rep.*, 2000, vol. 32, p. 48
- [18] Lin, C.H., Hsieh, Y.L. *Direct scouring of greige cotton fabrics with proteases*. In: Text. Res. J., 2001, vol. 71, p. 425
- [19] Sangwatanaroj, U., Choonukulpong, K., Ueda, M. *Cotton scouring with pectinase and lipase/ protease/ cellulase*. In: *AATCC Review*, 2003, issue 3, p. 17
- [20] Curievici, I. *Optimizări în industria chimică*. Editura Didactică și Pedagogică, București, 1980
- [21] Macoveanu, M., Nicu, V., Curievici, I. *Bazele tehnologiei chimice. Metodologia elaborării modelelor matematice ale proceselor din industria chimică*. Editura Rotaprint, Universitatea Tehnică Gheorghe Asachi, Iași, 1991

Authors/Autori:

Dr. ing./Dr. eng. ALINA POPESCU
 Institutul Național de Cercetare-Dezvoltare pentru Textile și Pielărie
 Str. Lucrețiu Pătrășcanu nr. 16, 030508 București/
The National Research and Development Institute for Textiles and Leather
 16 Lucrețiu Pătrășcanu Street, 030508 Bucharest
 e-mail: certex@ns.certex.ro

Prof. dr. ing./Prof. dr. eng. AURELIA GRIGORIU
 Conf. dr. chim./Conf. dr. chem. RODICA MUREȘAN
 Prof. dr. ing/ Prof. dr. eng. AUGUSTIN MUREȘAN
 Universitatea Tehnică Gheorghe Asachi
 Facultatea de Textile, Pielărie și Management Industrial
 Bd. D. Mangeron nr. 53-55, 700050 Iași/
Gheorghe Asachi Technical University
The Faculty of Textiles, Leather and Industrial Management
 53-55 D. Mangeron Bvd., 700050 Iași
 e-mail: augrigor@tex.tuiasi.ro, amuresan@tex.tuiasi.ro

Conf. dr. ing./Conf. dr. eng. CARMEN ZAHARIA
 Universitatea Tehnică Gheorghe Asachi
 Facultatea de Inginerie Chimică și Protecția Mediului
 Bd. D. Mangeron nr. 71A, 700050 Iași/
Gheorghe Asachi Technical University
The Faculty of Chemical Engineering and Environment Protection
 71 A D. Mangeron Bvd., 700050 Iași
 e-mail: czah@ch.tuiasi.ro

Relația structură-proprietăți pentru țesături antistatice, destinate echipamentelor de protecție

LUCICA CIOARĂ
IOAN CIOARĂ

DOINA TOMA

ABSTRACT – INHALTSANGABE

Structure-properties relationship of the antistatic woven fabrics for protective equipment application

The paper presents the results of researches conducted for the structure-properties relationship of the antistatic woven fabrics made of conductive yarns only in the weft direction. Thus, the choice was for a Rhovyl 95% and Bekinox 5% fibers weft yarn, and the weaving variants have been designed as simple and compound. An optimal utilization was tried for the beneficial properties of raw materials entering the fabric composition, as well as a compensation of the disadvantageous characteristics. Structure optimization was achieved by a correct dimensioning of critical characteristics, so that each component should contribute to the accomplishment of woven fabric quality indices. In order to perform this analysis on different woven fabric variants, the main properties providing the fabrics the use value were tested, respectively the antistatic properties, but also the comfort and durability ones.

Key-words: woven fabrics, protective equipment, functionality, weave, properties, surface resistivity, mechanical characteristics

Die Beziehung Struktur-Eigenschaften für antistatische Gewebe bestimmt der Protektionsanzüge

In der Arbeit werden die Ergebnisse der Forschungen betreff der Beziehung Struktur-Eigenschaften vorgestellt, realisiert aus Gewebe mit antistatischen Eigenschaften, welche durch Anwendung von leitfähigen Garne erhalten werden, ausgesetzt nur in Richtung des Schusses. Es wurde der Schussgarn gebildet aus 95% Rhovyl + 5% Bekinox Faser ausgewählt. Die Gewebevarianten wurden als einfache und zusammengesetzte Strukturen entworfen, durch den Versuch eine optimale Anwendung der vorteilhaften Rohstoffeigenschaften der Gewebeszusammensetzung sowie eine Begleichung der unvorteilhaften Eigenschaften, zu erzielen. Die Strukturoptimierung wurde durch korrekte Eigenschaftsdimensionierung erhalten, so dass jede Komponente zur Einhaltung der Leistungsindizes der Gewebequalität beitragen soll. Um diese Analyse auf verschiedenen Gewebevarianten durchzuführen, wurden diejenigen prioritäre Eigenschaften getestet, welche den Geweben Anwendungswert verleihen. Es wurden die antistatischen Eigenschaften bewertet, welche die grösste Bedeutung haben, sowie die Eigenschaften für Komfort und Nachhaltigkeit.

Schlüsselwörter: Gewebe, Protektionsanzüge, Funktionalität, Struktur, Eigenschaften, Obeflächenwiderstand, mechanische Charakteristiken

Tematica privind proiectarea, realizarea și optimizarea materialelor textile destinate confecționării echipamentelor de protecție, care să asigure securitatea muncii și calitatea vieții, este una de actualitate, dar și de perspectivă. Caracteristicile structurale ale țesăturilor din care se confecționează echipamentele de protecție trebuie să fie astfel proiectate, încât să ofere, pe de o parte, confort fiziologic, iar pe de altă parte protecție împotriva factorilor de risc care pot amenința siguranța sau chiar viața purtătorului [1–4]. Proiectarea unei astfel de țesături trebuie realizată în urma analizei cerințelor și proprietăților pe care aceasta trebuie să le îndeplinească în procesul de exploatare.

Echipamentele de protecție contra riscurilor create de electricitatea statică sunt necesare pentru desfășurarea în siguranță a unor activități specifice din domeniile minier, petrolier, electronic (camere curate), pirotehnic, militar etc. [5].

Prevenirea încărcării electrostatice a echipamentelor de protecție confecționate din țesături poate fi obținută prin [5–7]:

- folosirea țesăturilor realizate în totalitate din fire conductive – o soluție inadecvată, din cauza costurilor ridicate;
- placarea sau pulverizarea de vapori de metal sau argint pe suprafața țesăturii – un tratament costisitor, care necesită instalații speciale;
- folosirea unor țesături cu rețele de fire conductive, distribuite pe direcția urzelii sau/și a bătăturii, având rolul de a descărca sarcinile acumulate în timpul exploatării;
- tratarea țesăturilor cu produse antistatice – o soluție posibilă, dar care presupune reînnoirea tratamentului

la fiecare spălare, iar omogenitatea tratamentului nu poate fi garantată.

Adoptarea practică a uneia sau a alteia dintre aceste soluții trebuie justificată atât prin raportul *preț-calitate*, cât și prin raportul *preț-utilitate*. Alegerea se face în funcție de riscurile de contaminare și pericolele determinate de acestea, precum și în funcție de frecvența de schimbare a echipamentelor. Soluția considerată cea mai avantajoasă pentru realizarea țesăturilor cu proprietăți antistatice este cea a utilizării firelor conductive distribuite uniform în structură, deoarece efectul de antistatizare este stabil în comparație cu celelalte metode și, de asemenea, acesta nu depinde de umiditatea aerului. Rațiunea pentru care se face această apreciere este aceea că fibrele de inox se caracterizează nu numai prin proprietăți conductive bune, dar și printr-o foarte bună rezistență la spălare. Proprietățile antistatice ale echipamentului de protecție, definite prin standardul EN 1149, trebuie să se mențină constante până la 200 de cicluri de spălare [8, 9].

PARTEA EXPERIMENTALĂ

În lucrare sunt prezentate rezultatele cercetărilor privind structura și proprietățile unor țesături cu caracteristici antistatice, cu conținut de fibre metalice, destinate confecționării de echipamente de protecție. Proprietățile antistatice ale unei țesături sunt apreciate în funcție de rezistivitatea de suprafață a acestora și, din acest punct de vedere, ele pot fi clasificate în:

- materiale conductive – cu o rezistivitate mai mică de $10^{55} \Omega$;
- materiale antistatice – cu o rezistivitate cuprinsă între 10^5 și $10^{12} \Omega$;

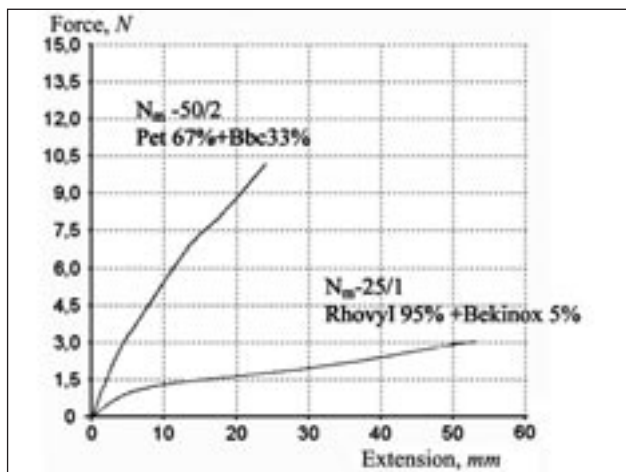


Fig. 1. Diagramele efort-alungire

- materiale izolatoare – cu o rezistivitate mai mare de $10^{12} \Omega$;
 - materiale cu proprietăți de scut pentru undele electromagnetice – cu o rezistivitate mai mică de $10^3 \Omega$.
- Pentru țesăturile la care antistatizarea se realizează cu fibre metalice, chiar și un procent relativ mic al acestora, de 2–4%, asigură obținerea valorilor recomandate ale rezistivității de suprafață.

În proiectarea țesăturilor din cadrul programului experimental s-a avut în vedere atât asigurarea proprietăților antistatice – prin distribuția omogenă a fibrelor metalice, cât și a tuturor celorlalte proprietăți ale țesăturii, care conferă o bună funcționalitate a echipamentelor de protecție. S-au utilizat țesături care au pe direcția bătăturii fire N_m 25/1, cu conținut de fibre metalice, respectiv 95% fibre Rhovyl și 5% fibre Bekinox. Toate variantele au fost realizate cu fire de urzeală N_m 50/2, din 67% PET și 33% bumbac.

Caracteristicile mecanice ale firelor folosite la realizarea țesăturilor sunt prezentate în tabelul 1, iar în diagramele efort-alungire ale celor două fire în figura 1.

Alungirea și forța de rupere nu furnizează suficiente informații pentru aprecierea comportării acestora în timpul prelucrării și utilizării și, din acest motiv, trebuie analizate diagramele efort-alungire ale firelor (fig. 1), precum și o serie de indicatori calculați cu ajutorul lor (tabelul 1). Caracteristicile mecanice prezentate în tabelul 1 pun în evidență faptul că cele două fire au o comportare diferită la solicitările de întindere.

Firul N_m 50/2, din 67% fibre PET și 33% fibre de bumbac, are o forță la rupere mai mare și o alungire la rupere mai mică decât firul N_m 25/1, din 95% fibre Rhovyl și 5% fibre Bekinox. Factorul lucrului mecanic, care este $> 0,5$ pentru ambele fire, indică o bună capacitate de deformare a acestora și, prin urmare, o rezistență adecvată la solicitările din timpul prelucrării și utilizării. Limita de proporționalitate efort-alungire este înregistrată, pentru firul N_m 50/2 (PET 67% – bumbac 33%), la valori cu mult mai mari față de firul N_m 25/1 (Rhovyl 95% – Bekinox 5%). Alura curbelor efort-alungire ale celor două fire este semnificativ diferențiată. Pe diagrama firului N_m 25/1 se observă o zonă mare de fluaj. Firul va avea deformații mari la modificări relativ mici ale efortului. Se poate anticipa că, în țesătură, cele două fire vor genera caracteristici tensionale diferite [10, 11].

Tabelul 1

Parametrul	Fir de urzeală PET 67% + + bumbac 33%	Fir de bătătură Rhovyl 95% + + Bekinox 5%
Finețea firului N_m , m/g	50/2	25/1
Diametrul firelor, mm	0,255	0,266
Forța de rupere, N	10,5	3,168
Alungirea la rupere, % (distanța dintre cleme = = 250 mm)	9,6	21,2
Lucrul mecanic de rupere, J	0,1570	0,1249
Factorul de lucru mecanic	$> 0,5$	$> 0,5$
Limita de proporționalitate, N/mm	3,75 6,8	1,16 2,55

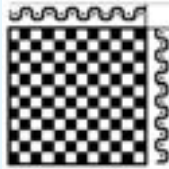
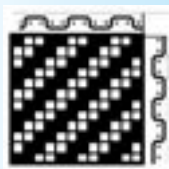
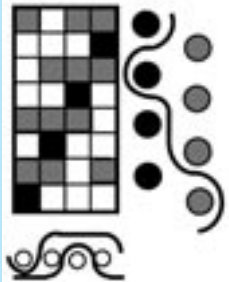
Programul experimental de cercetare cuprinde două variante de țesături simple și o variantă de țesătură compusă. Pentru toate variantele de țesături, firele cu fibre de inox au fost inserate în structură ca fire de bătătură. Țesăturile au fost realizate pe o mașină de țesut cu proiectil.

Varianțele de țesături simple au fost proiectate conform practicii obișnuite din proiectarea țesăturilor, folosind un model geometric al structurii țesăturii [1]. Modelul geometric al țesăturii a fost elaborat pentru o țesătură cu legătură pânză. Prima variantă din programul experimental V-I este cu legătură pânză și este varianta pentru care s-au calculat desimile geometrice minime și desimile tehnologice maxime, corespunzătoare celor nouă faze de structură, conform modelului geometric al țesăturii (tabelul 2). Desimile tehnologice ale firelor de urzeală și de bătătură, pentru varianta de țesătură V-I, au fost astfel alese încât, pe de o parte, țesăturile să corespundă destinației pentru care au fost proiectate, iar pe de altă parte să nu existe, din punct de vedere tehnologic, probleme majore de prelucrare la țesere. S-a optat pentru o structură echilibrată, în care desimea firelor pe cele două direcții să fie aceeași, și care să se realizeze în faze de structură orientate în jurul fazei 5. Intervalul de variație a desimilor tehnologice admis prin proiectare este prezentat în tabelul 2.

Cea de-a doua variantă de țesătură are aceleași caracteristici ca și cele ale variantei V-I, cu deosebirea că legătura este diagonal D2/2. Legăturile adoptate pentru variantele de țesături simple, V-I și V-II, respectiv pânză

Tabelul 2

Nr. fazei de structură	Înălțimile de undă, mm		Desimile geometrice minime, mm		Desimile tehnologice maxime, fire/10 cm	
	h_u	h_b	$l_{u \min}$	$l_{b \min}$	$P_{u \max. \text{ fire/10 cm}}$	$P_{b \max. \text{ fire/10 cm}}$
1	0	0,5208	0,5208	0,266	192	376
2	0,0651	0,4557	0,5169	0,266	193	376
a (2,13)	0,0732	0,4478	0,5158	0,266	194	376
3	0,1302	0,3906	0,5045	0,3448	198	290
4	0,1953	0,3255	0,4830	0,4068	207	245
5	0,2604	0,2604	0,4520	0,4520	221	221
6	0,3255	0,1953	0,4068	0,4830	245	207
7	0,3906	0,1302	0,3448	0,5045	290	198
b (7,98)	0,4536	0,0667	0,255	0,5167	392	194
8	0,4557	0,0651	0,255	0,5169	392	193
9	0,5208	0	0,255	0,5208	392	192

CARACTERISTICILE DE STRUCTURĂ ALE ȚESĂTURILOR				
		V-I	V-II	V-III
Materia primă	Urzeală	Bumbac 33% + PET 67%		
	Bătătură	Rhovyl 95% + Bekinox 5%		B_1 – bumbac 33% + PES 67% B_2 – Rhovyl 95% + Bekinox 5%
Finețea firelor, $T_{tex} (N_m)$	Urzeală	20 x 2 (50/2)		
	Bătătură	40 (25/1)		$B_1 = 20 \times 2 (50/2)$ $B_2 = 40 (25/1)$
Desimea firelor, fire/10 cm	Urzeală	230	224	220
	Bătătură	225	225	230
Contractia firelor, %	Urzeală	4,15	1,77	4,85
	Bătătură	8,34	7,1	5,2
Masa țesăturii, g/m ²		192	192	284
Procentul de fibră metalică din masa țesăturii, %		2,5	2,4	1,65
Legătura		Pânză 	D 2/2 	Semidublă de bătătură 

și diagonal D2/2, au același grad de echilibrare, iar bătătura care conține fibre de inox este orientată echilibrat pe fața și dosul țesăturii. Diferența dintre cele două legături este dată de mărimea segmentului de legare și, deci, de fermitatea legării.

Pentru varianta a treia, V-III, s-a ales o structură compusă. Pe o structură de referință echivalentă cu V-I s-a proiectat o țesătură cu legătură dublă de bătătură, bătătura B_1 din 33% bumbac și 67% PET și bătătura B_2 din 95% Rhovyl și 5% Bekinox. În acest fel, se urmărește compensarea caracteristicilor mecanice defavorabile ale bătăturii B_2 cu cele ale bătăturii B_1 . De asemenea, prin tipul de legătură, bătătura care conține fibre metalice va fi orientată numai către una din fețele țesăturii.

Pentru a analiza modul de distribuție a firelor de bătătură cu fibre metalice în structura țesăturii, lângă desenul legăturii sunt reprezentate secțiuni pe direcția urzelii, respectiv a bătăturii (tabelul 3). La țesăturile simple, V-I și V-II, se observă că bătătura apare, în egală măsură, pe fața și dosul acestora, iar la varianta V-III o bătătură este orientată pe fața țesăturii și cealaltă numai pe dosul acesteia.

În tabelul 3 sunt prezentate caracteristicile de structură pentru cele trei variante de țesături realizate. S-a calculat, pentru fiecare variantă, procentul de fibră metalică din masa țesăturii.

Optimizarea structurii, din punct de vedere al funcționalității, impune dimensionarea corectă a caracteristicilor, astfel încât fiecare componentă să contribuie la atingerea indicilor de performanță/calitate a țesăturii. Această optimizare presupune cunoașterea relației dintre structura și proprietățile țesăturii. Pentru a efectua această analiză pe variantele de țesături realizate, au

fost testate principalele proprietăți care conferă valoare de utilizare țesăturilor. Indicatorii prin care se apreciază proprietățile fizico-mecanice ale variantelor de țesături sunt prezentați în tabelul 4.

REZULTATE ȘI DISCUȚII

Analiza valorilor experimentale obținute în urma testelor de laborator permite formularea unor interpretări care sunt prezentate în continuare.

Analiza proprietăților electrostatice

Țesăturile cu proprietăți antistatice superioare sunt considerate cele care au rezistivitatea cuprinsă între 10^5 și $10^9 \Omega$.

Valorile rezistivității de suprafață, cu ordinul de mărime 10^2 , 10^3 , 10^4 , măsurate pe cele trei variante, se încadrează în limitele recomandate pentru țesăturile la care sarcina electrică se disipează prin conductivitate.

Țesăturile simple, V-I și V-II, cu un conținut de fibră metalică de 2,5%, au valori similare ale rezistivității, datorită faptului că toate caracteristicile sunt foarte apropiate, iar legăturile au același grad de echilibrare.

Varianta V-III, cu un conținut de fibră metalică de 1,65%, se caracterizează printr-o rezistivitate de suprafață bună, cu toate că procentul de fibră metalică este mai mic. Diferența dintre valorile rezistivității de pe fața, respectiv dosul țesăturii, pune în evidență faptul că, prin legătura compusă, bătătura cu fibre de inox este orientată numai către una din fețele țesăturii (fig. 2). Țesătura are proprietăți antistatice și prezintă avantajul dispunerii firelor cu conținut de fibre metalice pe fața sau dosul țesăturii. Ca urmare, poate fi eliminat factorul de disconfort datorat fibrelor metalice, atunci când se confecționează echipamente de protecție.

PROPRIETĂȚILE FIZICO-MECANICE ALE ȚESĂTURILOR				
Caracteristica		V-I	V-II	V-III
Rezistivitatea de suprafață, Ω	Față	$1,27 \times 10^3$	$1,74 \times 10^3$	$1,04 \times 10^4$
	Dos	$1,90 \times 10^3$	$2,22 \times 10^3$	$2,50 \times 10^2$
Rezistența la frecare – testul Martindale, nr. de cicluri până la rupere		> 230	> 175	> 422
Rezistența la rupere, N	Urzeală	1 190	1 070	1 073
	Bătătură	466	416	1 311
Alungirea la rupere, %	Urzeală	18,00	12,19	15,56
	Bătătură	36,67	34,31	18,30
Rezistența la sfâșiere, N	Urzeală	88,1	94,9	93,9
	Bătătură	54,4	68,85	155,6
Permeabilitatea la aer, mm/s		617,2	684,7	396,8

Analiza permeabilității la aer

În ceea ce privește permeabilitatea la aer, valorile înregistrate pentru țesăturile analizate asigură funcția de confort fiziologic impusă unui echipament de protecție [1].

Țesăturile realizate ca structuri simple, V-I și V-II, au o permeabilitate mai mare, fiind mai puțin compacte. Țesăturile sunt mai permeabile și datorită faptului că firele simple de pe direcția bătăturii sunt mai voluminoase și permit trecerea aerului.

Varianta de țesătură V-III, cu bătătură dublă, are o permeabilitate cu 60-65% mai mică decât primele două variante de țesături. Valoarea permeabilității de 400 mm/secundă se încadrează în limitele recomandate țesăturilor destinate îmbrăcămintei.

Analiza comportării la întindere

Pe direcția urzelii, toate variantele de țesături au aproximativ aceeași forță de rupere, deoarece sunt realizate din aceeași urzeală. Varianta V-I, cu cea mai mare fermitate de legare a firelor de urzeală, are cea mai mare sarcină de rupere.

Alungirea la rupere pe direcția urzelii diferă de la o variantă la alta, din cauza tipului de legătură și a desimii în bătătură. Aceste caracteristici determină frecvența de undulare a firelor de urzeală.

Varianta V-I, cu legătură pânză, și varianta V-III, cu legătură dublă de bătătură, au alungirea comparabilă, deoarece contracția firelor de urzeală este aproximativ aceeași (varianta V-I are contracția firelor de urzeală 4,15%, iar varianta V-III, 4,85%). Curbele efort-alungire din figura 3 pun în evidență faptul că frecvența de undulare a firelor de urzeală influențează alungirea la rupere pe direcția urzelii.

Pe direcția bătăturii, caracteristicile de structură pentru țesăturile analizate se deosebesc semnificativ și, în consecință, se diferențiază și valorile forței și ale alungirii la rupere.

Valorile mici ale sarcinii la rupere pe direcția bătăturii, pentru variantele de țesătură VI și VII, se explică prin folosirea în bătătură a firelor simple de Rhovyl și Bekinox. Desimea în bătătură este comparabilă cu cea din urzeală, în timp ce sarcina de rupere în bătătură este 35–45% din sarcina de rupere pe direcția urzelii. Din cauza valorilor mici ale sarcinii de rupere, se poate considera că acestea nu îndeplinesc condițiile de du-

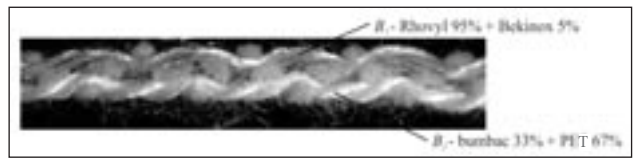


Fig. 2. Aspectul microscopic al secțiunii transversale a țesăturii VIII

rabilitate și de siguranță impuse unui echipament de protecție.

Varianta V-III cu bătătură dublă are două sisteme de bătătură. Una dintre bătături este alcătuită dintr-un fir răsucit Nm 50/2, din 67% PET și 33% bumbac, iar cea de-a doua bătătură este fir formată dintr-un simplu Nm 25/1, din 95% Rhovyl și 5% Bekinox. Forța de rupere pe direcția bătăturii, la această țesătură, este de trei ori mai mare decât la primele două variante și este comparabilă cu cea de pe direcția urzelii.

Alungirea la rupere pe direcția bătăturii este influențată semnificativ de caracteristicile materiei prime, gradul de undulare a firelor fiind mai puțin important. Firele de bătătură Nm 25/1, din 95% Rhovyl și 5% Bekinox, conferă variantelor V-I și V-II o alungire la rupere mare (34,31%, respectiv 36,67%), care poate fi considerată un dezavantaj, dacă deformația care apare în timpul utilizării țesăturii este remanentă.

Utilizarea pe direcția bătăturii a celei de-a doua bătături, care are alte caracteristici tensionale (sarcină mare și alungire mai mică), are rolul de a corecta dezavantajele date de firele din fibre Rhovyl. Pe diagrama din figura 4 se observă diferența de comportament la tracțiune dintre cele trei variante de țesături. Modificarea comportamentului la întindere pe direcția bătăturii evidențiază faptul că utilizarea legăturii semiduble reprezintă o modalitate de optimizare a relației structură-proprietăți.

Analiza comportării la sfâșiere

Comportarea la sfâșiere pe direcția urzelii este aceeași pentru toate variantele de țesături. Pe direcția bătăturii este evident faptul că cea mai mare rezistență o prezintă țesătura compusă, datorită faptului că are două sisteme de bătătură.

Analiza comportării la frecare

Comportarea la frecare a țesăturilor interesează, în primul rând, sub aspectul definirii durabilității țesăturii, dar și al eficienței în asigurarea proprietăților antistatice. S-a considerat că, pentru aprecierea comportării la frecare a țesăturilor, este suficientă determinarea numărului de cicluri până la ruperea epruvetei.

Pentru toate cele trei variante de țesături, amestecul de patru componente, cu proprietăți distincte, reprezintă un factor care accelerează fenomenul ciclic de distrugere prin frecare a țesăturilor.

Variantele de țesături simple cu legătură diagonal, V-II, au cea mai mică rezistență la frecare. Aceasta se explică prin faptul că structura are compactitate mică, fibrele fiind cu ușurință scoase din fir și din țesătură.

Varianta V-I, cu legătură pânză, are caracteristici de structură similare cu cele ale variantei V-II, dar datorită tipului de legătură are compactitate mare și, în consecință, o rezistență la uzură semnificativ crescută – numărul de cicluri de solicitare până la rupere, pentru varianta V-II, cu legătură diagonal, reprezintă 24% din

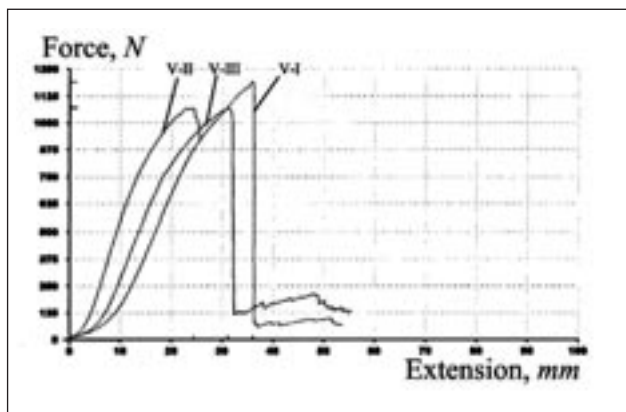


Fig. 3. Diagrame efort-alungire pe direcția urzelii

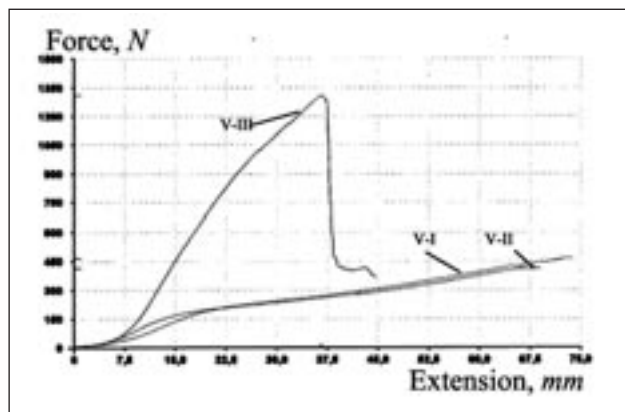


Fig. 4. Diagrame efort-alungire pe direcția bătăturii

numărul de cicluri corespunzătoare variantei V-I, cu legătură pânză.

Țesătura compusă V-III are, de asemenea, o rezistență mare la frecare, țesătura fiind constituită din trei sisteme de fire. Solicitarea a fost efectuată în condițiile cele mai defavorabile, respectiv pe partea cu fibră conductivă, care se presupune că va fi și cea mai solicitată în timpul utilizării. La varianta V-III, firele din fibre Rhovyl sunt cele care se rup primele, la 250 de cicluri, și se consideră că structura este distrusă prin frecare. Această constatare este importantă pentru stabilirea valorii de utilizare și pentru estimarea performanțelor țesăturii pe perioada de folosire.

CONCLUZII

Pentru țesăturile destinate echipamentelor de protecție multifuncționale, se impune stabilirea – pe baza unor criterii științifice obiective – a funcțiilor pe care trebuie să le îndeplinească țesătura și a nivelului de importanță a acestora. Prin testarea principalelor proprietăți fizice și mecanice poate fi apreciat nivelul de funcționalitate a țesăturii.

Proprietățile antistatice au cea mai mare importanță pentru categoria de țesături analizate. Din acest punct de vedere, se apreciază că toate variantele de țesături corespund cerințelor impuse. Pentru țesăturile care au o rezistivitate de suprafață peste limita impusă de standarde, se recomandă utilizarea acestora sub formă de componente ale echipamentului de protecție.

Varianta V-I are proprietăți funcționale corespunzătoare și se recomandă utilizarea acesteia pentru confecționarea echipamentelor de protecție ușoare.

Utilizarea a două bătăturii în structura țesăturii, la varianta VIII, urmărește compensarea caracteristicilor mecanice defavorabile ale bătăturii B_2 , Nm 25/1, din 95% fibre Rhovyl și 5% fibre Bekinox, cu cele ale bătăturii B_1 , Nm 50/2, din 67% fibre PET și 33% fibre de bumbac. Modificarea comportamentului la întindere a țesăturii pe direcția bătăturii, prin utilizarea legăturii duble de bătătură, se consideră ca fiind o optimizare a relației structură-proprietăți.

Orientarea fibrelor conductive către una din fețele țesăturii elimină dezavantajele legate de caracteristica de disconfort, generată de acestea.

BIBLIOGRAFIE

- [1] Mitu, S., Hâncu, S. P., Matenciu, C. C., Bârlădeanu, E. *Limitele indicilor sanogenetici pentru ansambluri cu noi particularități structurale*. În: Industria Textilă, 2008, vol. 59, nr. 1, p. 14
- [2] Peng Cui, Fumei Wang. *The clothing layers' influence on its warming performance*. În: Industria Textilă, 2009, vol. 60, nr. 3, p. 115
- [3] Cioară, L. *Caracteristicile de structură – resurse pentru designul țesăturilor*. În: Industria Textilă, 2009, vol. 60, nr. 4, p. 215
- [4] Guldemet Basal, Diren Mecit, Deniz Duran, Sevcin Ilgaz. *Comfort properties of double layered knitted and woven fabrics*. În: Industria Textilă, 2009, vol. 60, nr. 6, p. 299
- [5] Fuchs, H., Haase, J. *Overview of new protective clothing types against thermal and electrical risk*. În: Technical Textiles, noiembrie 1998, p. 211
- [6] Lin, J.H., Lou, C.W. *Electrical properties of laminates made from a new fabric with PP/stainless steel commingled yarns*. În: Textile Research Journal, 2003, vol. 73, nr. 4
- [7] Gilles Bonnot. *L'électricité statique éliminée*. În: TUT, 1996, nr. 4, p. 55
- [8] Lieven Tack. *Des solutions de sécurité pour les vêtements de protection*. În: TUT, 2007 nr. 65, p. 32
- [9] Pinar, A., Michalak, L. *Influence of structural parameters of wale and knitted fabrics on their electrostatic properties*. În: Fibres & Textiles in Eastem Europe, 2007, nr. 5, p. 69
- [10] *Manualul inginerului textilist*. Vol. 1. Editura AGIR, București, 2002, p. 53
- [11] Chinciu, D. *Bazele proiectării țesăturilor*. Editura Tehnică, BIT 1996

Autori/Authors:

Conf. univ. dr. ing./Conf. dr. eng. LUCICA CIOARĂ
Prof. dr. ing./Prof. dr. eng. IOAN CIOARĂ
Universitatea Tehnică Gheorghe Asachi
Facultatea de Textile-Pielărie și Management Industrial
Bd. D. Mangeron nr. 53, 700050 Iași/
Gheorghe Asachi Technical University
61 D. Mangeron Blvd., 700050 Iași
e-mail: lcioara@tex.tuiasi.ro

Cerc. șt. gr. III ing./Senior researcher eng. DOINA TOMA
Institutul Național de Cercetare-Dezvoltare
pentru Textile și Pielărie
Str. Lucrețiu Pătrășcanu nr. 16, 030508 București/
Research-Development National Institute
for Textiles & Leather
16 Lucrețiu Pătrășcanu Street, 030508
e-mail: certex@ns.certex.ro

REZUMAT – ABSTRACT – INHALTSANGABE

Nanopulbere compozită pentru textile antibacteriene

Interesul față de dezvoltarea tehnologiilor de obținere a unor textile antibacteriene pentru aplicații medicale a crescut mult în ultima perioadă datorită numărului mare de infecții cauzate de germenii patogeni comuni, cât și de germenii mutați rezistenți la antibiotice. Lucrarea prezintă rezultatele cercetărilor privind obținerea și caracterizarea unor noi agenți antibacterieni pe bază de nanopulberi compozite de tip Ag/TiO₂. Aceștia au fost obținuți prin reducerea chimică in situ a ionilor de Ag⁺ aflați într-o suspensie apoasă de nanoparticule de TiO₂. Produsele obținute au fost caracterizate din punct de vedere chimic, fizic și antibacterian. Rezultatele au dovedit obținerea unor amestecuri de nanopulberi uniform dispersate și cu activitate antibacteriană față de un spectru larg de germeni patogeni.

Cuvinte cheie: nanopulberi, argint-dioxid de titan, textile antibacteriene

Composite nanopowder for antibacterial textiles

The interest in the development of technologies of production of some antibacterial textiles for medical applications has grown much lately due to the high number of infections caused both by common pathogenic germs and the mutant germs resistant to antibiotics. The paper presents the research results on the obtaining and characterization of new antibacterial agents based on composite nanopowders of Ag/TiO₂ type. They were obtained by in situ chemical reduction of Ag⁺ ions being in an aqueous suspension of TiO₂ nanoparticles. The obtained products were characterized from the chemical, physical and antibacterial point of view. The results proved the obtaining of some nanopowders mixtures dispersed uniformly with antibacterial activity against a broad spectrum of pathogen germs.

Key-words: nanopowders, silver-titanium dioxide, antibacterial textiles

Nanopulververbundstoffe für antibakterielle Textilien

Die Interesse in der Entwicklung der Produktionstechnologien für Textilien mit antibakteriellen Eigenschaften für medizinische Zwecke ist in letzter Zeit stark gestiegen, wegen der grossen Anzahl der Infektionen verursacht von allgemeinen Krankheitserreger, als auch von mutanten Krankheitserreger, welche gegenüber Antibiotika widerstandsfähig sind. Die Arbeit stellt die Forschungsergebnisse vor, der Produktion und Charakterisierung einiger neuen antibakteriellen Substanzen, auf Nanopulververbundbasis des Types Ag/TiO₂. Diese wurden durch die chemische Reduzierung „in situ“ der Ag-Ionen erhalten, welche sich in einer wässrigen Suspension aus TiO₂ Nanopartikel befinden. Die erhaltenen Produkte wurden aus chemischen, physischen und antibakteriellen Standpunkt charakterisiert. Die Ergebnisse haben die Produktion einiger Mischungen aus gleichförmig verteilten Nanopulvern bewiesen mit antibakterieller Aktivität gegenüber einem breiten Spektrum von Krankheitserreger.

Schlüsselwörter: Nanopulver, Titansilberdioxid, antibakterielle Textilien

At present, the researches on the processing of textiles to antibacterial functionalization represent an active field of interdisciplinary scientific investigations due to a large diversity of infection sources from the environment [1–15].

Moreover, the need for antibacterial products for hospitals is very large to prevent infections contracted from medical equipment used in hospitals (nosocomial infections). A brief look at the data reported on this type of infections has a major negative impact on health and quality of patients' life and very high treatment costs from the budget of any country, due to resistance to antibiotics of mutant germs from hospitals and arise complications.

Speaking only of industrialized countries, they represent 25% of all infectious diseases. 10% of Europe's population is hospitalized and 5% contracts a nosocomial infection. In USA from 2 000 000 patients affected by these types of infections, 90 000 die. The treatment of a bacterial infection due to catheters costs USD 2 836 [16].

From the data published recently by the Health Protection Agency (HPA) is revealed that, every year in England, about 7 000 hospitalized patients had bacterial infections with meticulo-resistant Staphylococcus aureus (MRSA) and more than 50 000 of those aged over 65 had infections with Clostridium difficile.

A report of the Romanian Ministry of Health showed that during 2003–2007 nosocomial infections were contracted by 55 253 patients. During 2001–2006, of approximately 20 000 infections, 21.6% were with

MRSA. Also during this time period, the rate of growth for all types of nosocomial infections at children was of 30%. Also, as a result of this study was concluded that places like healthcare units, hospitals and wards with chronically patients and individuals have the greatest risk to infections with MRSA.

A major priority for preventing the transmission of infections from medical staff to patients is the creation of some textiles of antimicrobial barrier type.

The antimicrobial treatment of textiles is achieved through two main methods: the antibacterial agent is mixed directly with the polymer or fiber during the spinning or the textile is treated at the end of processing just like the dyeing.

Since the most of the synthesis antibacterial organic agents have been shown to be harmful to health or are not biodegradable, it is necessary to reduce the industrial quantities used from these compounds and to redirect to new ecological inorganic compounds. In this aim are recommended biocides mixed with metallic oxides, hydroxides or their mixtures (oxides of Al, Ca, Ce, Mg, Sr, Sn, Ti and Zn) in the form of reactive nanocrystallites with sizes of about 20 nm and specific surfaces of about 15 m²/g dispersed in an aqueous or non-aqueous fluid medium. The optimal weight content of biocide is selected in the range of 0.01–5%, of nanoparticles is in the range of 0.1–10%, and of fluid medium is in the range of 85–99% [17].

Titanium dioxide (TiO₂), which is a n-type semiconductor and a very active photo-catalyst, was very much

studied for applications in various fields: air purification, waste water treatment (removal of dyes) and to obtain products with superhydrophilic, anti reflex, self-cleaning or antibacterial properties. For applications for environmental cleaning, the most active is considered to be the nanometric powder in anatase crystalline form, which has the forbidden band at 3.2 eV and absorbs photons in the UV light at wavelengths below 388 nm. The presence of oxygen and water adsorbed superficial forms active oxygen species as HO⁻ radicals and O₂⁻ ions that are highly reactive and have a decisive role in these photocatalytic reactions.

Unfortunately, despite of these very promising properties, TiO₂ applications are still limited to the UV field that occupies approximately 4–5% of the solar spectrum. In the closed environment where the light is only available in lighting lamp exist only photons in the visible domain and a very small quantity of UV light (approximately 1 μW/cm²).

If the active photocatalytic effect could be extended in the visible light region (400–700 nm) by inducing a batho-chromium movement (for example, a decrease of the forbidden band or introduction of a state of intra-forbidden band, which would lead to a higher absorption of visible light) practical applications of TiO₂ could be much wider and the light energy could be used with much greater efficiency. In this respect, in literature have been reported improvements of photocatalytic activity of TiO₂ in the visible light by doping with non-metals or metals or their compounds [18, 19].

In the field of water's photocatalytic decomposition, these methods have been studied and developed. To purify the environment that requires large consumptions of energy and materials, these methods are not feasible. At industrial level the production costs of the photocatalysts must remain low for any type of application [20].

For antibacterial applications it is necessary to be created materials to work in all conditions, including in darkness. Because of the antibacterial action of Ag is well known and takes place in any lighting conditions, a series of works were targeted for improvement of the photocatalytic activity of TiO₂ nanoparticles by the addition of Ag nanoparticles [21–23].

This paper presents a new nanocomposite material based on TiO₂ doped with Ag nanoparticles, and the methods of its production and characterization. Depending on the use, the material can be obtained either in the form of aqueous slime, either in the form of powder.

EXPERIMENTAL PART

Materials used

In the experiments, there were used the following raw materials:

- deionized water with conductivity of 18.2 MΩ · cm at 25°C;
- nanopowder of TiO₂ in anatase cristallization form (TiO₂Np), TiO₂ ≥ 99.5%, LOBA;
- silver nitrate p.a., crystallized, AgNO₃ ≥ 99.9%, Fluka;
- tri-sodiumcitrate, C₆H₅Na₃O₇ · 2H₂O, 99–101%, Merck;

- poly [1-vinyl-2-pyrrolidone] (C₆H₉NO)_x, PVP, Sigma-Aldrich;
- sodium borohydride, NaBH₄ ≥ 96 %, Merck.

Work methodology

The obtaining method of composite powders of Ag/TiO₂ type, symbolized AgNp/TiO₂Np, consists in an in situ chemical deposition of silver nanoparticles symbolized AgNp on TiO₂ nanoparticles symbolized TiO₂Np, in optimal conditions relating to concentration, temperature, pH, lighting conditions, working atmosphere, food rate and stirring of the reactive agents.

In the first step, the TiO₂Np were dispersed in an ultra sound bath. Than, an AgNO₃ aqueous solution as source of Ag⁺ ions was added.

The obtaining of AgNp started with a soft reduction at warm of Ag⁺ ions in presence of PVP using a tri-sodium citrate solution. After that, the suspension was cooled and the reduction reaction was finalized by adding of a NaBH₄ solution.

Aqueous colloidal suspensions were prepared with a weight content of 1%, 5% and 10% TiO₂Np and 0.005%, 0.0075% and 0.01% AgNp.

To obtain AgNp/TiO₂Np in form of concentrated slimes, the suspension was centrifuged to the desired wet content.

To obtain the material in form of powders, the centrifuged slimes were dried in vacuum at 70°C.

Characterizations

The final products were characterized as follows:

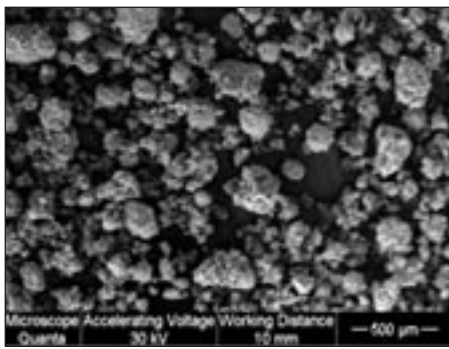
- *chemical composition*. TiO₂Np content by gravimetrically method and AgNp content by atomic absorption spectroscopy;
- *crystalline structure and crystallite dimensions* by X-ray diffraction;
- *powders reflectance and suspensions absorbance in UV-Vis* by spectrophotometry;
- *mean diameter and grain size distribution of nanoparticles* by dynamic light scattering (DLS);
- *shape and dimensions of nanoparticles* by transmission (TEM) and scanning electronic microscopy (SEM).

The antibacterial activity tests were performed using the microdilutions method, according to the normative in force, against common and aggressive germs: *Staphylococcus aureus* ATCC 25923, *Escherichia coli* ATCC 25922, *Enterobacter cloacae* ATCC 13047, *Acinetobacter baumannii* ATCC 17978, *Candida albicans* ATCC 10231, *Pseudomonas aeruginosa* ATCC 27853 and *meticilino-resistant Staphylococcus aureus*, MRSA.

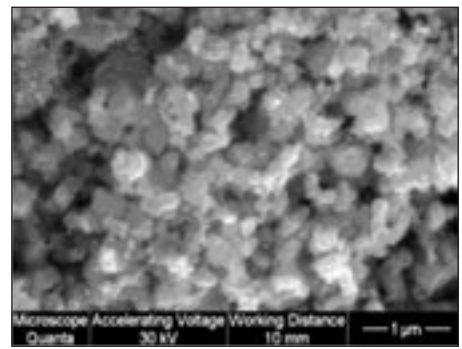
RESULTS AND DISCUSSIONS

The tests for chemical analysis showed the obtaining of some products with designed concentrations.

Since the characteristics of the samples prepared by the method described above are similar, further we will present only the results obtained for the colloidal suspension with a content of 5% TiO₂Np and 0.0075% AgNp. The weight concentration of AgNp of the powder obtained from this suspension by centrifugation and drying in vacuum at 70°C was of 0.149%.



a



b

Fig. 1. SEM images of:
a – nondispersed TiO_2Np powders; b – dispersed TiO_2Np powders

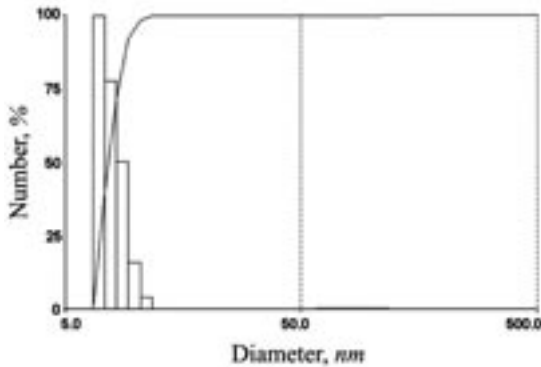


Fig. 2. Grain size distribution of TiO_2Np powders

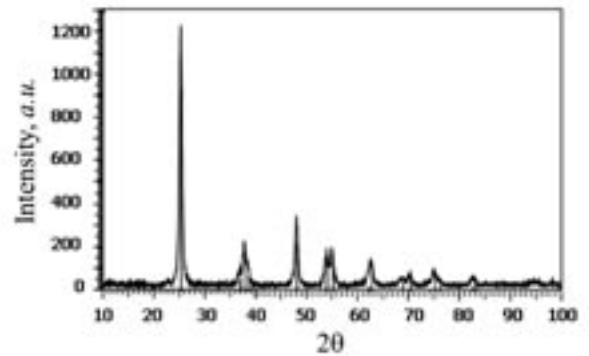


Fig. 3. X-ray diffraction pattern of $\text{AgNp}/\text{TiO}_2\text{Np}$ nanopowders

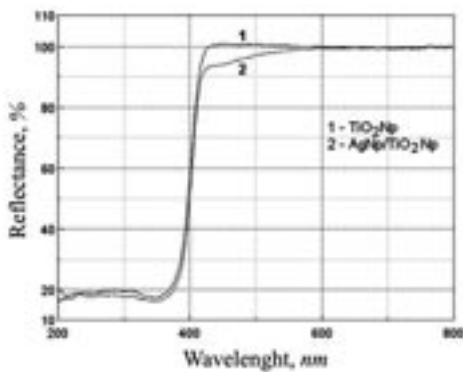


Fig. 4. Reflectance spectra in UV-Vis of:
1 – TiO_2Np powders; 2 – $\text{AgNp}/\text{TiO}_2\text{Np}$ powders

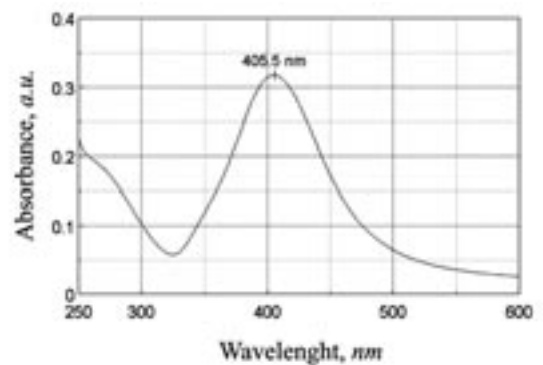


Fig. 5. Absorbance spectrum in UV-Vis of AgNp colloidal solutions

In figures 1–7 is presented the physical characteristics of this material during processing and in final. The test results of chemical and physical characterization confirm the obtaining of nanocomposite powders consisting of TiO_2Np with an average diameter of 7.8 nm (fig. 2), with crystallographic structure of anatase (fig. 3) and AgNp with an average diameter of 11.4 nm (fig. 4–7). In synthesis process, AgNp were stabilized electro-steric (fig. 8).

The electro-steric stabilization achieves a double protection: an electrostatic one with citrate ions, and a steric one with PVP. The protection of AgNp with citrate anions is achieved by forming of an electric double layer and is provided by the interaction of coulombian rejection, which occurs when two particles loaded with the same charge are approaching one another. The steric protection is conferred by attaching

of PVP molecules to the nanoparticles surface. Since either citrate anions or polymer molecules of PVP cannot give separately to AgNp a convenient stability, it can be considered that this type of protection is the result of synergistic action of these two substances.

The achievement of the characteristics of the $\text{AgNp}/\text{TiO}_2\text{Np}$ composite nanopowders above presented creates the premises of achieving of bioactive AgNp acting in any lighting conditions.

Thus, the antibacterial tests performed on $\text{AgNp}/\text{TiO}_2\text{Np}$ slimes shows that the minimum inhibitory concentration (MIC) reported on AgNp concentration is of 14.9 ppm.

The biocidal action of AgNp begins with bacterial cell membrane destruction, which is actually its respiratory organ [23]. AgNp from the nanocomposite mixture are nucleophile and tend to conjugate with compounds

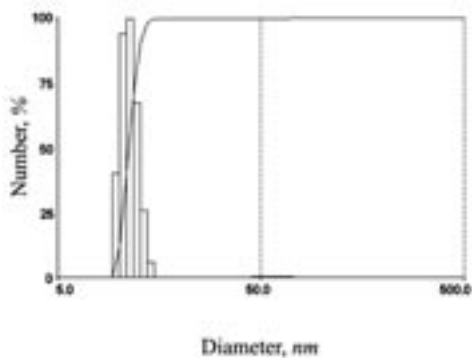


Fig. 6. Grain size distribution of AgNp extracted from AgNp/TiO₂Np composite powders

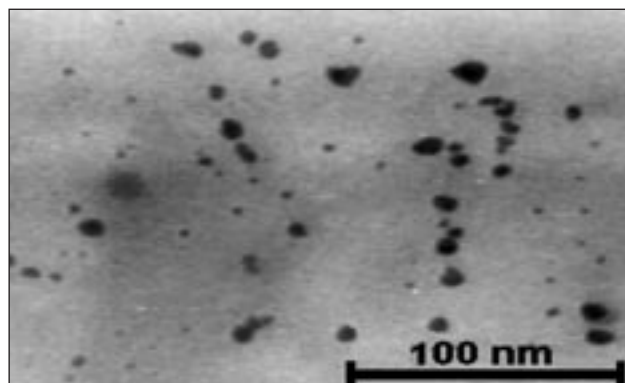
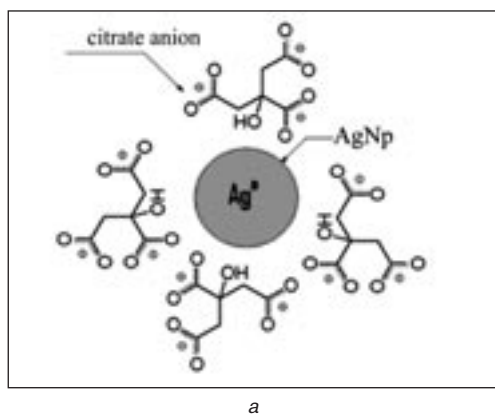
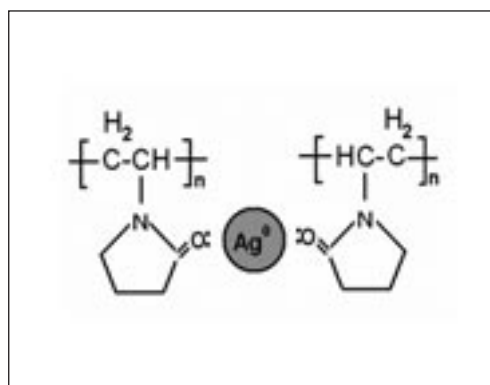


Fig. 7. TEM image of AgNp extracted from AgNp/TiO₂Np composite powders



a



b

Fig. 8. Stabilization of:
a – AgNp with citrate anions; b – with PVP

having positive charge of bacterial cell membrane. In the same time, the membrane shows redox systems that can promote oxidation of Ag⁰ to Ag⁺ ions, which in turn blocks the S-H-bonds of proteins, enzymes and coenzymes components thereof. Membrane perforation, cellular respiration suppression and invasion of AgNp and of Ag⁺ ions in cytoplasm are followed after a certain time period by distortion of DNA, stopping of multiplication, and finally bacteria dies.

The photocatalytic effects by which are manifested the destruction activity of micro-organisms of TiO₂Np are oxidative and are governed by a mechanism with free radicals for which degradation speeds are close to a large number of organic compounds. The photocatalytic activity of TiO₂ is very much influenced by crystallinity, presence and size of pores, density of OH⁻ groups, surface acidity, number and nature of active centers available within the network and on the crystal surface. Thus, the nanopowders with high crystallinity presented the best photocatalytic activity, while the amorphous nanopowders were not photoreactive. The structural defects due to oxygen vacancies affect both the adsorption of water on the surface of the crystal and the rate of dissociation of water into protons and hydroxyl groups. Dissociation of water requires the presence of acidic sites (represented by weak coordinate titanium cations and that link initially the water molecules) and basic sites (oxygen bridges exposed on crystal surface and that accept protons) close and in pair. OH⁻ groups participate directly in the reaction mechanism by capturing of photo-generated gaps and the catalyst surface enriching in HO⁻ radicals having a

high reactivity. This process is important not only for the production of free radicals, but also to avoid electrons-holes recombination. A high content of OH⁻ groups can be achieved by TiO₂Np impregnation with water or by synthesis of non stoichiometric TiO_xNp (0 < x < 2). Specific surface influences less these photocatalytic reactions. A large specific surface area is favorable for photo degradation due to its ability to absorb organic molecules, including the microorganisms. In the same time, it is unfavorable due to the presence of a large number of defects in crystallization, which in turn facilitates the electron-hole recombination.

Particle size is another important parameter for efficiency of the photocatalytic reactions because it conditions the electron-hole recombination. The nanoparticles of semiconductors can have physical and chemical properties different from the bulk material. Small variations in diameter can lead to significant changes of volume and ratio of diameter and specific surface, which is the index of efficiency of nanoparticles.

The results of the experiments showed that the TiO₂ nanometer powders present an optimal rate of oxidation of organic substances to the values of average diameter around 10 nm. In the laboratory experiment, the treatment of waste water with TiO₂ in the presence of UV radiations of high energy led to the total removal of the micro-organisms. It was also found that micro-organisms respond differently to this type of treatment, both from the point of view of minimum inhibitory concentration (MIC) and the duration of exposure. The bacterial cell membrane acts as a barrier in the

destruction process. The cell death occurs when the DNA is also affected.

In an illumination with UV radiation of low intensity, the TiO₂Np surface does not show a significant antimicrobial activity. AgNp improve this feature by extending of the activity domain and increasing of the destructive power against many pathogen germs.

Since the bacterial cell is endowed with the capacity to regenerate and self defend, the designing of biocidal materials based on TiO₂Np, which work by exposure to UV radiations of low intensity, is a challenge in terms of their composition and structure.

CONCLUSIONS

The researches presented in this paper had the aim to improve the bio-activity of TiO₂Np by extending of the photocatalytic activity field outside the UV field.

In this aim, the works have been targeted towards TiO₂Np doping with AgNp whose biological activity is

manifested at very small concentrations (of ppm order) and in any lighting conditions.

The paper presents the obtaining method of a nano-composite powder of AgNp/TiO₂Np type by a chemical deposition of AgNp on TiO₂Np with crystallographic structure of anatase.

The material was characterized from chemical, physical and antimicrobial point of view. The method allows the obtaining of some AgNp/TiO₂Np nanopowders with adjustable chemical composition in a concentration range that ensures product stability and antimicrobial activity in any lighting conditions. The method is efficient, has low production costs and can be extended at small scale production.

The material can be prepared both in the powdery state and in the form of aqueous suspensions and it is applicable for the antimicrobial treatment of textiles with medical applications.

BIBLIOGRAFIE

- [1] Yeon Ki, H., Kim, J. H., Kwon, S. C., Jeong, S. H. *A study on multifunctional wool textiles treated with nano-sized silver*. In: Journal of Material Science, 2007, vol. 42, p. 8 020
- [2] Onose, G., Chendreau, C., Neacșu, A., Grigorian V., Strâmbu V. ș.a. *Textile inteligente pentru monitorizarea noninvazivă a semnalelor fiziologice*. In: Industria Textilă, 2009, vol. 60. issue 3, p. 124
- [3] Hwang, K. Y. *Method for producing nanosilver on large scale, method for manufacturing nanosilver-adsorbed fiber, and antibacterial fiber thereby*. US Patent Application Publication, No. 0278534 A1, Dec. 14, 2006, USA
- [4] Soane, D. S., Offord, D. A., Linford, M. R., Millward, D. B., Ware, W., Erskine, L., Green, E., Lau, R. *Nanoparticle-based permanent treatments for textiles*. US Patent Application Publication, No. 0013369 A1, Jan. 16, 2003, USA
- [5] Qian, L., Hinestroza, J. P. *Application of nanotechnology for high performance textiles*. In: Journal of Textile and Apparel. Technology and management, 2004, vol. 4, issue 1, p. 1
- [6] Gupta, P., Bajpai, M., Bajpai, K. *Investigation of antibacterial properties of silver nanoparticle-loaded poly(acrylamide-co-itaconic acid)-grafted cotton fabric*. In: The Journal of Cotton Science, 2008, vol. 12, p. 280
- [7] Lee, H. J., Yeo, S. Y., Jeong, S. H. *Antibacterial effect of nanosized silver colloidal solution on textile fabrics*. In: Journal of Material Science, 2003, vol. 38, p. 2 199
- [8] Jeong, S. H., Hwang, Y. H., Yi, S. C. *Antibacterial properties of padded PP/PE nonwovens incorporating nano-silver colloids*. In: Journal of Material Science, 2005, vol. 40, p. 5 413
- [9] Duran, N., Marcato, P. D., Souza G. I. H., Alves, O. L., Esposito, E. *Antibacterial effect of silver nanoparticles produced by fungal process on textile fabrics and their effluent treatment*. In: Journal of Biomedical Nanotechnology, 2007, issue 3, p. 203
- [10] Lee, M. S., Nam, S. I. *Colloidal solution of metal nanoparticles, metal-polymer nanocomposites and method for preparation thereof*. EU Patent No. WO No. 087749 A1, 7 Nov. 2002, EU
- [11] Dong, Q., Su, H., Zhang, D. *In situ depositing silver nanoclusters on silk fibrion fibers supports by a novel biotemplate redox technique at room temperature*. In: Journal of Physical Chemistry, B, 2005, vol. 109, p. 17 429
- [12] Sun, G., Li, D. *Dyeing textiles using nanoparticles*. US Patent, No. 7, 048,771 B2, May 23, 2006, USA
- [13] Liang, D., Hsiao, B. S., Chu, B. *Functional electrospun nanofiber scaffolds for biomedical applications*. In: Advanced Drug Delivery Reviews, 2007, vol. 59, p. 1 392
- [14] Maneerung, T., Tokura, S., Rujiravanit, R. *Impregnation of silver nanoparticles into bacterial cellulose for antimicrobial wound dressing*. In: Carbohidrate Polymers, 2008, issue 72, p. 43
- [15] Jeong, S. H., Yeo, S. Y., Yi, S. C. *The effect of filler particle size on the antibacterial properties of compounded polymer/silver fibers*. In: Journal of Materials Science, 2005, vol. 40, p. 5 407
- [16] Lin, T. L., Lu, M. F., Sheu, M. S., Su, S. H., Tang, L. *A remedy for medical device-related infections*. In: Medical Device Technology, issue 1, Oct. 2001, p. 4
- [17] Carnes, C. L., Klabunde, K. J. *Decontaminating systems containing reactive nanoparticles and biocides*. US Patent Application Publication, No. 0067159 A1, Apr. 8, 2004, USA
- [18] Carp, O., Huisman, C. L., Reller, A. *Photoinduced reactivity of titanium dioxide*. In: Progress in Solid State Chemistry, 2004, vol. 32, p. 33
- [19] Fujishima, A., Zhang, X., Tryk, D. A. *TiO₂ photocatalyst and related surface phenomena*. In: Surface Science Reports, 2008, vol. 63, p. 515
- [20] Wakefield, G. *Nanomaterials: costs and opportunities*. In: Nanotoday, 2008, vol. 3, issue 3-4, p. 48
- [21] Liu, S. X., Qu, Z. P., Han, X. W., Sun, L. C. *A mechanism for enhanced photocatalytic activity of silver-loaded titanium dioxide*. In: Catalysis Today, 2004, vol. 93-95, p. 877
- [22] Liu, Y., Wang, X., Yang, F., Yang, X. *Excelent antimicrobial properties of mesoporous anatase TiO₂ and Ag/TiO₂ composite films*. In: Microporous and Mesoporous Materials, 2008, vol. 114, p. 439
- [23] Gavriliu, S., Ardelean, I., Lungu, M., Moisescu, C., Gavriliu, L. *The influence of chemical colloidal silver solutions upon bacterial cell respiration and multiplication*. Conference Proceedings of 3rd International Conference on Biomaterials and Medical Devices BIOMMEDD'2008, Bucharest, Romania, 13-16 Nov., 2008, p. 313

Authors/Autori:

Dr. chem./Dr. chimist ȘTEFANIA GAVRILIU

Dr. eng./Dr. ing. MAGDALENA LUNGU

Dr. eng./Dr. ing. ELENA ENESCU

National Institute for Research and Development
in Electrical Engineering ICPE-CA

313 Splaiul Unirii Street, 030138 Bucharest, Romania/
Institutul Național de Cercetare-Dezvoltare

în Ingineria Electrică ICPE-CA

Splaiul Unirii nr. 313, 030138 București

e-mail: stefgrav@icpe-ca.ro

Dr./Medical dr. LIANA GAVRILIU

"Carol Davila" University of Medicine
and Pharmacy

37 Dionisie Lupu Street

020021 Bucharest, Romania/
Universitatea de Medicină și Farmacie

"Carol Davila"

Str. Dionisie Lupu nr. 37

020021 București

e-mail: lianagavriliu@yahoo.com

Noi materiale biocompozite bazate pe celuloză regenerată, utilizate la confecționarea branțurilor destinate diabeticilor

CIPRIAN MURARIU
MARTA HARNAGEA
FLORENTINA HARNAGEA

ROMEN BUTNARU
ALINA MURARIU

ABSTRACT – INHALTSANGABE

New bio-composite materials based on regenerated cellulose used in making insoles for the diabetic foot

The paper presents new polymeric bio-composite materials based on regenerated cellulose as well as compounds with a bio-active potential and applications in the footwear industry, namely for the diabetic foot. By incorporation into such composites of some therapeutic drug substances – chloramphenicol, sulphathiazole and nystatin – these can be used in obtaining insoles covers for the medical footwear. After the bio-active compound inclusion into the cellulosic matrix, the composite thus achieved meant for the manufacture of footwear parts was tested according to the European standard EN 12770:1999, aiming to determine water absorption-desorption – critical feature for the insole covers having an orthopedic functional role. Thus, beside the therapeutic role achieved by including drug substances into the matrix, a hydrophilic character is also gathered, which is of primary importance for this type of product.

Key-words: cellulose composites, prophylaxis, diabetic foot, absorption, desorption, insoles

Neue Bioverbundwerkstoffe aus regenerierter Zellulose für die Herstellung von Einlagen für Diabetiker

Die Arbeit stellt vor neue polymerische Bioverbundwerkstoffe aus regenerierter Zellulose und Bindungen mit bioaktiven Potential, mit Anwendungen in der Schuhindustrie für den diabetischen Fuss. Durch die Einbindung einiger medizinischen Substanzen – Chloranphenicol, Sulphathiazol, Nystatin – in diesen Verbundwerkstoffen, können sie bei der Herstellung von Einlagendecken für medizinische Schuhware angewendet werden. Nach der Einschliessung der bioaktiven Bindungen in der zellulosischen Matrix wurde das so erhaltene Verbundwerkstoff, bestimmt für die Produktion von Schuhware, gemäss dem Europäischen Standard EN 12770:1999 für Wasserabsorption, getestet. Die Wasserabsorption hat eine definierende Qualität im Falle der Einlagendecken mit ortopedischer Funktionsrolle. Die Ergebnisse der Absorptionsteste haben das kategorisch bessere Verhalten der Bioverbundwerkstoffe hervorgehoben, im Vergleich mit den klassischen Produkten vom Markt. Neben der therapeutischen Rolle, erhalten durch die Eingliederung der medizinischen Stoffbindungen in der Matrix, wird auch ein hydrophiles Charakter erhalten, welches besonders notwendig für dieses Produkttyp ist.

Schlüsselwörter: zellulosische Verbundwerkstoffe, Profilaxie, Diabetikerfuss, Absorption, Desorption, Einlagen

COMPOZITE CELULOZICE – DEFINIȚIE, STRUCTURĂ

Compozitul este un material în care doi sau mai mulți constituenți separați se unesc pentru a forma un compus cu proprietăți mai bune. Materialele compozite sunt, la ora actuală, cele mai răspândite materiale din lume și fac parte din viața fiecăruia dintre noi. De exemplu, țesutul osos, betonul, hârtia, lemnul etc. sunt materiale compozite. În cele mai multe cazuri, materialele compozite sunt definite prin două noțiuni, și anume matricea și armătura. Practic, cele două elemente formează materialul compozit. Ele sunt obligatoriu diferite și joacă în structura compozitului roluri complementare. În cazul biocompozitelor se aplică aceeași regulă de structurare, doar că, în locul armăturii, apare compusul bioactiv, nefiind absolut necesar ca, în obținerea unui material compozit, să fie îmbunătățite doar proprietățile reologice [1, 2].

În plus, biocompozitele pot avea mai mult de doi constituenți, în funcție de tipul materialului studiat. Așadar, structura poate fi descrisă astfel: matrice celulozică, compus bioactiv înglobat în matrice și un element cu rol ranforsant, care poate fi o țesătură din bumbac, o spumă poliuretanică, o țesătură din fibre de carbon etc. Structura materialului compozit pe bază de celuloză regenerată și agent bioactiv este o structură de tip sandwich, caracteristică materialelor compozite (fig. 1). Avantajele utilizării unui astfel de material sunt evidente. În cazul persoanelor suferinde de diabet, la nivelul picioarelor se poate instala neuropatia diabetică, rezultată din afectarea sistemului nervos periferic, care duce la scăderea sensibilității dureroase, tactile, termice și vibratorii în anumite părți ale corpului și, uneori, poate să afecteze capacitatea de mișcare și forța musculară. Cel

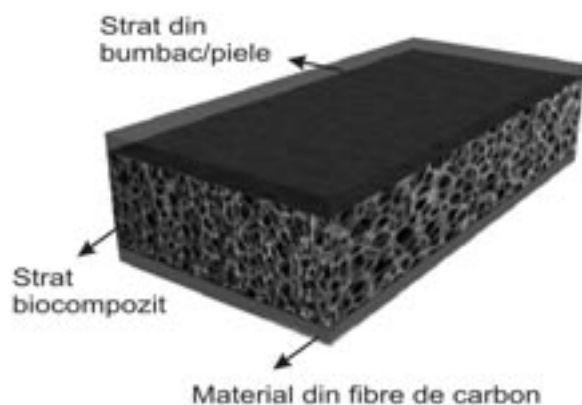


Fig. 1. Structura materialului compozit pe bază de celuloză regenerată și agent bioactiv

mai frecvent, sunt afectate picioarele (laba piciorului și gamba) și poate contribui la apariția unor probleme serioase, cum ar fi ulcerarea, infecțiile sau deformările osoase și articulare. Este cea mai frecventă formă de neuropatie diabetică. Drept urmare, agravarea ulcerărilor și calozităților este foarte probabilă, mai ales dacă verificarea suprafeței tegumentului la nivelul membrelor inferioare nu se face zilnic, așa cum este indicat. Situațiile de acest gen se pot agrava, atât de tare, încât pot determina amputarea piciorului (figurile 2, 3).

Ulcerările diabetice constituie una dintre cele mai importante probleme la nivel mondial. În prezent, în Europa sunt peste 60 de milioane de pacienți care suferă de diabet, cu o incidență de ulcerării la nivelul piciorului de aproximativ 20–25%, raportată pe întreaga durată de viață a pacienților. În prezent, la nivel european se înregistrează aproximativ 100 000 de amputări anuale

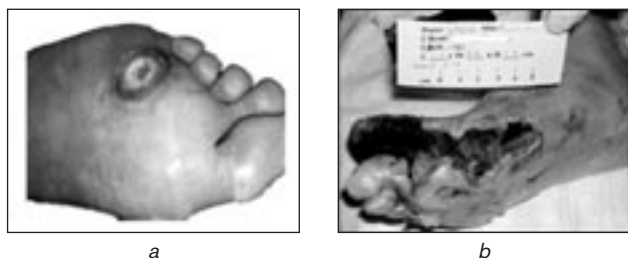


Fig. 2. Agravarea ulcerărilor netratate la diabetici

ale membrelor, din cauza cronicizării ulcerărilor diabetice. Costul exact al tratamentului convențional al acestor afecțiuni este greu de determinat, dar se apropie de milioane de dolari. Așadar, diabeticii și, prin urmare, ulcerățiile la nivelul piciorului reprezintă o problemă în creștere, care trebuie tratată cu seriozitate [3].

Prezența în acoperișul de brant a unui material biocompozit permite eliberarea la nivelul piciorului, în spațiul subvestimentar, a unor compuși cu rol profilactic sau curativ. Prin urmare, se asigură un mediu care nu favorizează dezvoltarea microorganismelor, eliminând riscul apariției micozelor și al ciupercilor, iar în cazul unor răniri accidentale sau cauzate de utilizarea unor produse de încălțăminte neadecvate, previn inflamarea zonei. Această etapă este favorizată în cazul bolnavilor de diabet și de viteză lentă de vindecare, din cauza fluxului crescut de glucide din sânge și, nu în ultimul rând, de climatul subvestimentar din interiorul încălțăminteii – umiditate crescută, cauzată de transpirație, lipsa luminii și temperatura crescută.

Prezența biocompozitului la nivelul acoperișului de brant permite tratarea locală, elimină disconfortul aplicării diverselor unguenți, nu obligă bolnavul la perioade de repaus și, deoarece este aplicat local, se elimină tranzitul hepatic existent în cazul tratamentelor cu antibiotice administrate pe cale orală și, mult mai important, prin funcția de interschimbabilitate a acestor acoperișuri de brant, întregul sistem capătă un rol profilactic. Pentru obținerea acoperișurilor de brant din materiale biocompozite este necesară parcurgerea mai multor etape.

Obținerea materialului celulozic

Pentru obținerea celulozei s-a utilizat procedeul clasic până la etapa de structurare a viscozei, etapă în care s-a adăugat un procentaj de sare Glauber, reluându-se apoi procesul clasic. După obținerea celulozei, aceasta este supusă unui tratament de albire, iar prin introducerea în apă se urmărește dizolvarea sării și realizarea unui material cu structură poroasă. Cantitatea de sare este principalul factor care influențează densitatea matricei celulozice.

Includerea compusului bioactiv

După uscarea materialului celulozic, așa cum este descrisă în etapa experimentală a lucrării, se trece la includerea compusului bioactiv (în cazul de față, a compușilor de sulfatiazol, nistatin și cloramfenicol), prin solubilizarea acestuia într-un solvent organic biocompatibil, iar apoi matricea celulozică se introduce în soluția astfel obținută, fiind urmată de procesul de includere fizică.

Îmbunătățirea proprietăților reologice

Pentru a fi utilizat ca acoperiș de brant, biocompozitul obținut are nevoie de ranforsare, așa încât să reziste la solicitările din timpul procesului de purtare și fabricație. Cea mai simplă metodă de structurare este caracteristică materialelor compozite și se numește structură de tip sandwich. Așadar, matricea celulozică – având compusul biologic deja înglobat – se interpune între două straturi ranforsante: unul din meșină porcină sau din țesătură de bumbac cu legătură pânză, care să permită transferul facil dintre biocompozit și suprafața plantară a piciorului, și unul din țesătură de fibre de carbon, cu rol de creștere a rezistenței subansamblului [3].

Într-o altă lucrare [3], s-a studiat capacitatea de fixare a unor compuși bioactivi (cloramfenicol, sulfatiazol și nistatin) pe un material compozit, obținut din celuloză regenerată (spongi), și s-a ajuns la concluzia că fixarea acestor compuși bioactivi este influențată de structura chimică a compusului și de concentrația acestuia în soluția de tratare.

Imaginea macroscopică a acestor tipuri de compozite, după tratarea cu agent bioactiv, este prezentată în figura 3.

În lucrare este analizată capacitatea de absorbție a apei pentru o serie de materiale compozite folosite la fabricarea acoperișurilor de brant.

PARTEA EXPERIMENTALĂ

La realizarea experimentărilor, pe lângă materialul compozit obținut conform tehnologiei prezentate în lucrarea menționată anterior, s-au utilizat un număr de 5 materiale compozite clasice.

Materialul biocompozit folosit la fabricarea acoperișurilor de brant, cu rol medical ortopedic, trebuie să prezinte o serie de proprietăți, care să răspundă în mod optim la o serie de teste specifice acestui fabricat. O proprietate foarte importantă pe care acoperișurile de brant trebuie să o îndeplinească, mai ales în cazul utilizării acestora pentru tratarea sau profilaxia anumitor afecțiuni de la nivelul piciorului, o reprezintă capacitatea de absorbție de apă [4].



Fig. 3. Aspectul macroscopic al materialului compozit bioactiv



Fig. 4. Acoperiș de branț din celuloză presată, cu rol absorbant

Pentru a determina parametrii menționați, s-a apelat la metodologia recomandată de standardele în vigoare, și anume SR EN 12746:2000 și EN 12770:1999.

Înainte de a prezenta modalitatea de lucru, este necesară definirea termenului de absorbție a apei, care reprezintă creșterea masei pe unitatea de suprafață a epruvetei, din cauza absorbției de apă în timpul unuia sau a mai multor intervale de timp menționate.

Aparatura utilizată

Pentru determinări gravimetrice, s-a utilizat o balanță de laborator cu precizie de 0,01 g, pentru debitarea epruvetelor s-a utilizat un cuțit de formă pătrată cu dimensiunile de 50 ± 1 mm x 50 ± 1 mm, ștanță hidraulică, hârtie de filtru și apă distilată. Cu ajutorul cuțitului și a ștanței s-au debitat epruvete de formă pătrată, cu dimensiunile de 50 ± 1 mm x 50 ± 1 mm, care apoi au fost cântărite. Următoarea etapă a fost imersarea în apă a epruvetelor timp de 6 ore. După extragerea probelor din apă s-a eliminat excesul de apă pe o hârtie de filtru și s-au refăcut determinările gravimetrice utilizând o balanță cu precizie de 0,01 g. Întregul proces s-a desfășurat în condiții atmosferice standard, la o temperatură de $20 \pm 2^\circ\text{C}$.

Interpretarea analitică a rezultatelor obținute

Pentru determinarea absorbției W_A , se utilizează ecuația:

$$W_A = \frac{M_F - M_0}{A} \quad [\text{g/m}^2] \quad (1)$$

în care:

M_0 reprezintă masa inițială a epruvetei, în stare uscată, g;

M_F – masa finală a epruvetei, în stare umedă, g;

A – aria epruvetei, m^2 .

Absorbția de apă este exprimată cu o exactitate de 1 g/m^2 .

Tabelul 1

Lotul	Nr. probă	M_0 , g	M_F , g	W_A , g/m^2
Branțuri clasice absorbante	P_1	0,080	1,080	188,8
	P_2	0,603	1,130	210,8
	P_3	0,613	1,121	203,2
	P_4	0,618	1,107	195,6

Tabelul 2

Lotul	Nr. probă	M_0 , g	M_F , g	W_A , g/m^2
Branțuri clasice parfumate	P_1	1,826	7,016	2 076
	P_2	1,837	7,148	2 124,4
	P_3	1,811	6,966	2 062
	P_4	1,791	6,487	1 878,4

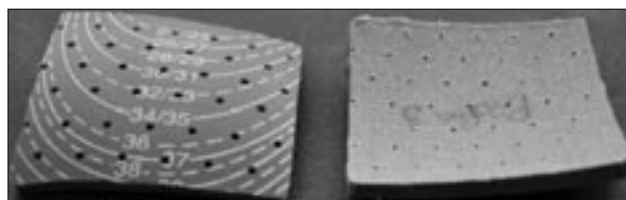


Fig. 5. Acoperiș de branț parfumat

Pentru a pune în evidență proprietățile matricei celulozice, exprimarea rezultatelor s-a realizat prin comparația cu epruvetele debitate din acoperișuri de branț, confecționate din materiale clasice. Rezultatele obținute, pentru fiecare grup testat, sunt prezentate în tabelele 1–6. Testele s-au efectuat utilizând câte patru probe din același tip de material, care au fost notate conform denumirii comerciale.

Acoperiș de branț absorbant

Primul lot testat a fost format dintr-un acoperiș de branț cu proprietăți absorbante, din celuloză presată cu fibre de bumbac, produse de firma Classico din Italia (fig. 4). S-au analizat câte 4 probe din același material.

$$W_{A \text{ mediu}} = 199,6 \text{ g/m}^2 \quad (2)$$

Acoperiș de branț parfumat

Acoperișurile de branț din acest lot sunt produse de firma italiană Classico și sunt structurate dintr-o spumă poliuretanică, impregnată cu o substanță parfumată, peste care este lipită o țesătură din bumbac cu legătură pânză, având un rol estetic (fig. 5).

$$W_{A \text{ mediu}} = 2035,2 \text{ g/m}^2 \quad (3)$$

Acoperiș de branț termoizolant

Produsele din acest lot sunt alcătuite dintr-un strat de spumă poliuretanică și un strat de material neșesut din fibre de lână și poliamidă (fig. 6).

$$W_{A \text{ mediu}} = 3456,1 \text{ g/m}^2 \quad (4)$$

Acoperiș de branț din plută

Acoperișurile de branț din acest lot sunt produse dintr-un strat de plută, acoperit cu o țesătură cu legătură pânză (fig. 7).

$$W_{A \text{ mediu}} = 225,1 \text{ g/m}^2 \quad (5)$$

Tabelul 3

Lotul	Nr. probă	M_0 , g	M_F , g	W_A , g/m^2
Branțuri clasice termoizolante	P_1	1,970	10,497	3 410,8
	P_2	1,954	10,383	3 371,6
	P_3	1,935	11,022	3 634,8
	P_4	1,960	10,478	3 407,2

Tabelul 4

Lotul	Nr. probă	M_0 , g	M_F , g	W_A , g/m^2
Branțuri din plută	P_1	1,492	2,041	219,6
	P_2	1,465	2,041	230,4
	P_3	1,471	2,044	229,2
	P_4	1,467	2,020	21,2

Tabelul 5

Lotul	Nr. probă	M_0 , g	M_F , g	W_A , g/m ²
Branțuri din meșină	P_1	0,967	2,171	481,6
	P_2	1,003	2,219	486,4
	P_3	1,067	2,385	527,2
	P_4	0,963	2,125	464,8



Fig. 6. Acoperiș de branț termoizolant

Tabelul 6

Lotul	Nr. probă	M_0 , g	M_F , g	W_A , g/m ²
Branțuri din compozit	P_1	0,642	12,753	4 844,4
	P_2	0,857	18,940	7 233,2
	P_3	1,072	26,651	10 231,6
	P_4	1,092	25,614	9 808,8



Fig. 7. Acoperiș de branț din plută



Fig. 8. Acoperiș de branț din meșină



Fig. 9. Acoperiș de branț din compozit obținut pe bază de celuloză regenerată și compus bioactiv

Acoperiș de branț din meșină (fig. 8)

$$W_{A \text{ mediu}} = 490 \text{ g/m}^2 \quad (6)$$

Acoperiș de branț din material compozit celulozic

Acest acoperiș este un material biocompozit în care s-au înglobat substanțe bioactive. El este realizat din celuloză regenerată, de porozitate ridicată, întărită cu țesătură din fibre de carbon (fig. 9).

$$W_{A \text{ mediu}} = 8029,5 \text{ g/m}^2 \quad (7)$$

Valorile foarte mari ale absorbției de apă se datorează prezenței în structura materialului compozit a straturilor de celuloză regenerată, de porozitate mare.

Raportul compoziției celuloză/sare determină, de fapt, densitatea spongiilor. Cu cât procentul de celuloză este

mai scăzut, cu atât densitatea spongiilor este mai mică și, prin urmare, capacitatea de absorbție a apei este mai mare. Acest lucru arată că densitatea spongiilor este un factor determinant pentru capacitatea de absorbție a apei. De altfel, ambii parametri sunt foarte importanți în cazul materialelor poroase.

Îmbunătățirea proprietăților mecanice ale spongiilor comerciale se face cu proporții diferite de fibre de bumbac, introduse în soluția de viscoză, pentru a consolida materialul final. Rezultatele sunt prezentate în tabelul 7. Este evident faptul că densitatea spongiilor este dependentă în mod direct de procentajul fibrelor de bumbac din material, în proporție de 20–60%. Cantitatea maximă de bumbac creează o densitate de 0,07 g/cm³, iar cea minimă o densitate de 0,05 g/cm³, ceea

Tabelul 7

Conținutul de fibre din bumbac	Poziția în spongi a fibrelor din bumbac – modul de reticulare	Densitatea spongiilor, g/cm ³	Absorbția de apă		
			IWR, g/g compozit celulozic	PWR, g/g compozit celulozic	PWR/IWR, %
20% neorientat	perpendicular	0,049	25,4	1,45	5,7
	paralel	0,050	23,9	1,84	7,71
	valoare medie	0,050	24,6	1,82	7,38
40% neorientat	perpendicular	0,053	25,4	2,79	10,98
	paralel	0,060	22,8	2,13	9,35
	valoare medie	0,056	24,1	2,47	10,26
40% orientat	perpendicular	0,067	17,5	2,37	13,53
	paralel	0,058	19,5	2,29	11,74
	valoare medie	0,062	18,5	2,34	12,66
60% neorientat	perpendicular	0,066	17,5	2,16	12,33
	paralel	0,069	17	2,21	13,00
	valoare medie	0,067	17,2	2,18	12,70
60% orientat	perpendicular	0,071	16,9	2,29	13,55
	paralel	0,075	16,7	1,92	11,50
	valoare medie	0,073	16,8	2,11	12,53
60% fibre scurte	perpendicular	0,070	16,8	1,92	11,43
	paralel	0,089	17,7	1,95	11,00
	valoare medie	0,079	17,2	1,95	11,32

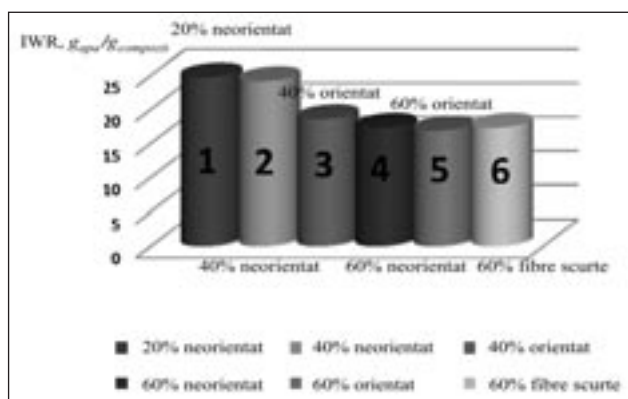


Fig. 10

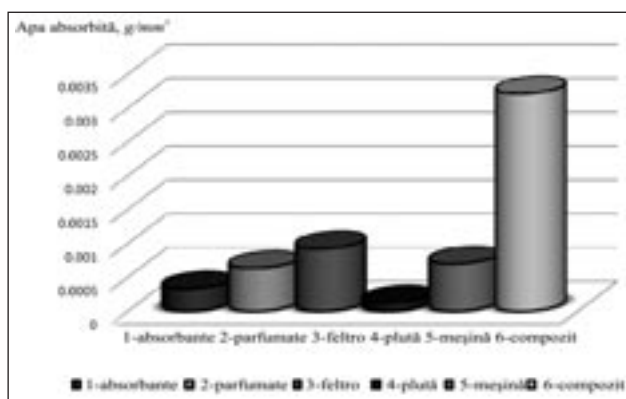
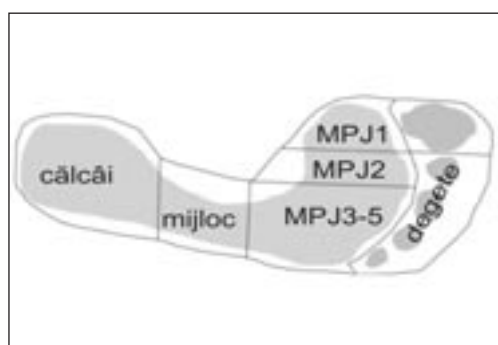
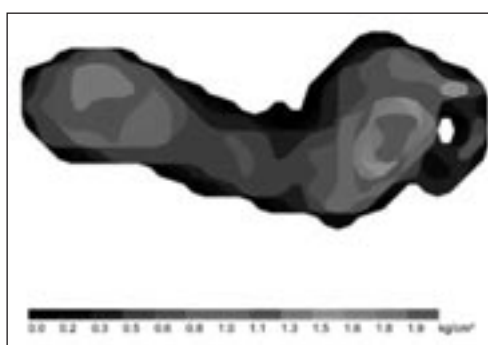


Fig. 12



a



b

Fig. 11

ce demonstrează, de asemenea, o foarte bună capacitate de absorbție a apei. Orientarea fibrelor nu modifică în mod semnificativ densitatea spongilor consolidați cu fibre de bumbac, ci o măresc la o scară neglijabilă.

Pentru a determina rezultatele absorbției de apă în etapa de purtare a produsului, s-a aplicat asupra compozitului celulozic o presiune de 1,9 kg/cm². Aceasta este presiunea maximă exercitată de un adult, cu o greutate corporală de 70–80 kg, aflat în poziția de sprijin ortostatic bilateral, asupra acoperișurilor de branț, și, prin urmare, în acest caz valorile absorbției de apă sunt determinate în stare presată. Valorile absorbției de apă sunt raportate apoi la cele inițiale, ținându-se cont și de procentajul de fibre de bumbac aflat în componența fiecărui lot de probe, dar și de orientarea acestora [5].

Rezultate experimentale privind valorile inițiale ale retenției de apă au fost raportate la cele obținute imediat după presare (tabelul 7). Rezultatele privind absorbția inițială de apă și dependența acesteia de procentajul de fibre de bumbac inclus pentru ranforsarea celulozei regenerate analizate sunt ilustrate grafic în figura 10.

Din tabelul 7 se observă că, deși imersat în stare presată, materialul își menține proprietățile absorbante, cu toate că, așa cum se știe, dimensiunile cavităților interioare se reduc drastic prin presare.

Pentru a exemplifica mai bine modul de exercitare a presiunii la nivelul plantar, la un adult, în poziție de sprijin ortostatic bilateral, s-au realizat hărți ale acestei presiuni (fig. 11). Se observă că variațiile de presiune plantară sunt cuprinse între 0 și 1,9 kg/cm². Testele de absorbție s-au efectuat pentru valoarea maximă, iar

materialul și-a păstrat condițiile absorbante și în aceste condiții.

Pentru a compara capacitatea de absorbție a compozitului pe baza de celuloză cu cea a materialelor clasice a fost necesară exprimarea absorbției în grame de apă absorbită pe mm³ de probă.

Având în vedere faptul că materialul compozit pe bază de celuloză absoarbe apa nu numai în funcție de suprafața probei, ci și de volumul acesteia, pentru o comparație corectă între capacitățile de absorbție ale materialelor compozite testate, s-a introdus un indice care să exprime absorbția apei și pe unitatea de volum, nu numai pe unitatea de suprafață.

În acest scop, s-a utilizat aceeași ecuație, cu raportare la volum (1). Graficul de dependență a absorbției pe unitatea de volum, în funcție de caracteristicile structurale ale materialului, este prezentat în figura 12.

CONCLUZII

Lucrarea prezintă un compozit polimeric cu porozitate ridicată, pe bază de celuloză regenerată și compuși bioactivi, având potențiale aplicații în designul încălțămintei – pentru tratarea piciorului diabetic sau ca element profilactic la nivelul piciorului. Substanțe medicamentoase din clasa antibioticelor, sulfamidelor și antimicoticelor au fost incluse în matricea celulozică nemodificată sau oxidată. Gradul de retenție este dependent de porozitatea și distribuția dimensională a porilor acesteia, dar și de volumul molecular sau de solubilitatea în etanol a compușilor bioactivi.

Raportul compoziției celuloză/sare determină, de fapt, densitatea spongilor. Cu cât procentul de celuloză este mai redus, cu atât densitatea spongilor este mai mică

și, prin urmare, capacitatea de absorbție a apei este mai mare.

În momentul simulării condiției de purtare, în stare presată, la presiune maximă, materialul suferă o pierdere a capacității de absorbție, însă se menține în parametri normali, ceea ce demonstrează bunele

caracteristici ale compozitului.

În ceea ce privește absorbția de apă, compozitul celulozic prezintă un comportament de excepție, demonstrând că este candidatul ideal – ca materie primă – pentru confecționarea acoperișurilor de branț, destinate bolnavilor de diabet.

BIBLIOGRAFIE

- [1] Ciurea, J., Gheorghită, E., Onose, G. *Escarele de decubit – o actualizare a unei probleme vechi și soluții noi*. În: Industria Textilă, 2009, vol. 60, nr. 5, p. 284
- [2] Murariu, C. *Rheological behavior of carbon fiber composites*. 2nd Young Researchers Conference on "FRP Reinforcement" – Dübendorf, Switzerland, 17-18 January 2007
- [3] Murariu, C., Butnaru, R., Ciovică, S., Murariu, A. *Biocompozite polimerice cu aplicații medicale*. În: RSCC, 2008, vol. 8, nr. 3, p. 32
- [4] Ando, H., Takamura, T., Nagai, Y. et al. *Erythrocyte sorbitol level as a predictor of the efficacy of epalrestat treatment for diabetic peripheral polyneuropathy*. In: Journal Diabetes Complications. nov.-dec. 2006, vol. 20, nr. 6, p. 367
- [5] Neu, H. C., Gootz, T. D. *Antimicrobial Chemotherapy: Antimicrobial inhibitors of ribosome function*. Baron's Medical Microbiology (Baron S. et al, eds.), 4th ed. University of Texas Medical Branch, 1996
- [6] Murariu, A., Pielichowski, K., Ciovică, S., Murariu, C., Mocanu, C., Pielichowski, J. *Pressure and water absorption effects on a drug delivery matrix based on cellulose-poly (aspartic acid) composite material*. In: Modern Polymeric Materials for Environmental Application, 2006, vol. 2

Autori/Authors:

Drd. ing./Drd. eng. CIPRIAN MURARIU
Ing./Eng. MARTA HARNAGEA
Prof. dr. ing./Prof. dr. eng. FLORENTINA HARNAGEA
Prof. dr. ing./Prof. dr. eng. ROMEN BUTNARU
Drd. chim./Drd. chem. ALINA MURARIU
Universitatea Tehnică Gheorghe Asachi
Facultatea de Textile, Pielărie și Management Industrial
Bd. D. Mangeron nr. 53, 700050 Iași/
Gheorghe Asachi Technical University
The Faculty of Textiles, Leather and Industrial Management
53 D. Mangeron Bvd., 700050 Iași
e-mail: murake@murake.ro

Referenții articolelor publicate în acest număr al revistei INDUSTRIA TEXTILĂ/ Scientific reviewers for the papers published in this number:

- Cerc. șt. gr. I prof. dr. ing./Senior researcher prof. dr. eng. EFTALEA CĂRPUȘ
Cerc. șt. gr. II dr. ing./Senior researcher dr. eng. CARMEN MIHAI
Cerc. șt. gr. II dr. ing./Senior researcher dr. eng. IULIANA DUMITRESCU
Cerc. șt. gr. III dr. ing./Senior researcher dr. eng. ALINA POPESCU
Cerc. șt. gr. III dr. ing./Senior researcher dr. eng. ALEXANDRA-GABRIELA ENE
Cerc. șt. gr. III drd. ing./Senior researcher drd. eng. RADU POPESCU
Cerc. șt. gr. II ing./Senior researcher eng. MARIA DAN
Cerc. șt. drd. ing./Senior researcher drd. eng. ANA MARIA MOCIOIU

De conținutul articolelor răspund autorii!

Reproducerea integrală sau parțială a textelor sau ilustrațiilor din revista „Industria Textilă” nu se poate face decât cu acordul prealabil scris al autorilor.

Redacția revistei „Industria Textilă” îi roagă pe autorii materialelor trimise spre publicare ca, în conformitate cu tema tratată, în referințele bibliografice să fie introduse articolele apărute în această revistă, în ultimii doi ani.

Revista „INDUSTRIA TEXTILĂ”, Editura CERTEX – Institutul Național de Cercetare-Dezvoltare pentru Textile și Pielărie – București

Redacția, administrația și casieria: București, str. Lucrețiu Pătrășcanu nr. 16, sector 3, Tel.: 021-340.42.00, 021-340.02.50/226, e-mail: certex@ns.certex.ro; Fax: +4021-340.55.15. Abonamentele se primesc la administrația revistei. Instituțiile pot achita abonamentele în contul nostru de virament: RO25RNCB0074029214420001 B.C.R. sector 3, București. Costul unui abonament, în anul 2010, este de 163,5 lei, cu TVA inclus – pentru persoane juridice și 60 lei, cu TVA inclus – pentru persoane fizice.

Lucrare executată la S. P. «BUCUREȘTII NOI», str. Hrisovului nr. 18A, sector 1, București, tel.: 667.64.28; 667.55.70; fax: 668.59.51